Effect of Material and Geometric Parameters on Deformations of a Dynamically loaded Prenotched Plate

By

Rakesh. R. Gummalla

Thesis submitted to the faculty of the

Virginia Polytechnic Institute and State University

in partial fulfillment of the requirements for the degree of

Master of Science

In

Engineering Mechanics

APPROVED:

_____

Prof. Romesh C. Batra, Chairman

_____ _____

Prof. Saad. A. Ragab Prof. S. Thangjitham

April, 1999

Blacksburg. Virginia

Effect of Material and Geometric Parameters on Deformations of a Dynamically loaded Prenotched Plate

By

Rakesh. R. Gummalla

Abstract

We analyze plane strain thermomechanical deformations of a prenotched rectangular plate impacted on one side by a prismatic body of rectangular cross-section and moving parallel to axis of the notch. Both the plate and the projectile are made of the same material. Strain hardening, strain-rate hardening and thermal softening characteristics of the material are modeled by the Johnson-Cook relation. The effect of different material parameters, notch-tip radius, impact speed and the length of the projectile on the maximum tensile principal stress and the initiation and propagation of shear bands at the notch-tip is analyzed. It is found that for high impact speeds or enhanced thermal softening, two shear bands, one at -10^{O} and the other at -128^{O} to it propagate from the notch tip. Otherwise, only one shear band nearly parallel to the notch-ligament initiates at the notch-tip. The notch-tip distortion for high strength materials is quite different from that for low strength materials. The maximum tensile principal stress occurs at a point on the upper surface of the notch-tip and for every set of values of material parameters and impact speeds studied equals about 2.3 times the yield stress of the material in a

quasistatic simple tension or compression test. We assume that the brittle fracture occurs when the maximum tensile principal stress equals twice the yield stress of the material in a quasistatic simple tension test and a shear band initiates when the effective plastic strain at a point equals 0.5. The effect of material and geometric parameters on the time of initiation of each failure mode is computed. It is found that for low impact speeds (< 30 m/s), a material will fail due to the maximum tensile principal stress exceeding its limiting value, and at high impact speeds due to the initiation of a shear band at the notch-tip. Results are also computed for a C-300 steel with material parameters given by Zhou et al. For an impact speed of 50 m/s, the shear band speed and the maximum effective plastic strain-rate before a material point melts are found to be 350 m/s and 5 x 10^7 /s respectively.

Acknowledgements

I would like to express my sincere thanks to Dr. Romesh Batra for his valuable help and guidance all through this work. I want to express my gratitude to my parents for providing me with constant inspiration and moral support without whom this would never have been possible. I will also like to take this opportunity to thank all my friends at Virginia Tech.

Contents

List of Figures.

1 Introduction

Kalthoff (1987) and Kalthoff and Winkler (1987) have experimentally studied the deformations near the notch tip in a prenotched rectangular plate made of a maraging steel and impacted on the notched side by a cylindrical projectile moving parallel to the axis of the notch. They obtained essentially identical results for both single notched and double notched plates. For impact speeds V_O below a critical value V_C, a crack developed at a point on the notch surface and propagated into the plate at about 70^O to the notch-axis. However, for impact speeds greater than V_C a shear band developed at the notch tip and propagated at an angle of at -10^O to -15^O to the notch-axis. They postulated that the maximum effective plastic strain-rate at the notch-tip is proportional to $V_O / \sqrt{r_O}$ where r_O is the radius of the notch-tip. Mason et al. (1994) and Zhou at al. (1996a) also used an experimental set-up similar to that of Kalthoff (e.g. see Fig. 1) and found that no failure ensued at low impact speeds but at high speeds of impact a shear band initiating from the notch-tip propagated nearly parallel to the notch-axis, got arrested and a crack ensued from the shear band tip. They attributed the difference in their and Kalthoff's experimental results to different value of material parameters. We note that Kalthoff listed only the Rockwell hardness number for the steel tested and did not provide stress-strain curves. Mason et al. (1994a) have given the shear stress vs. the logarithmic shear strain curve for the C-300 maraging steel, and Zhou et al. (1996b) have evaluated the material parameters by curve fitting.

Needleman and Tvergaard (1995), Zhout at al. (1996b) and Batra and Nechitailo (1997) have used the finite element method to simulate Kalthoff's experiment and employed different constitutive relations to model the thermoviscoplastic response of the material. Each of these investigations assumed that a plane strain state of deformation prevails in the plate. Batra and Nechitailo (1997) also modeled the deformations of the projectile. Needleman and Tvergaard (1995) enforced essential boundary conditions at the impacted face with the maximum value of prescribed velocity equal to one-half of the initial velocity of the projectile. However, Zhou et al. (1996b) presumed that the maximum value of the prescribed velocity equals the initial velocity of the striker. Needleman and Tvergaard (1995) accounted for the softening of the material due to the evolution of the porosity and also due to the temperature rise but the other investigations considered thermal softening only. These works did not study the effect of different material parameters on the deformations of the plate material adjacent to the notch-tip. Here we model the thermoviscoplastic response of the material by the Johnson-Cook (1983) relation and analyze the effect of the change in the value of each material parameter on the deformations of the plate material close to the notch-tip. In each case, the deformations of the projectile are also considered and both the plate and the striker are taken to be made of the same material. The effect of the impact speed, notch-tip radius, and the length of the projectile on the deformations of the plate are also investigated. By assuming that the brittle failure ensues when the maximum tensile principal stress at a point equals twice the yield stress of the material in a quasistatic simple tension or compression test and a shear band initiates when the effective plastic strain at a point

equals 0.5, we also delineate the effect of material and other parameters on the initiation of a failure mode.

2 Formulation of the Problem

A schematic sketch of the problem studied is given in Fig. 1. In the referential description equations governing the thermomechanical deformations of the projectile and the prenotched plate are

$$\rho J = \rho_O \text{ , J= det F,} \qquad (1)$$

$$\rho_O \dot{V} = \text{Div T,} \qquad (2)$$

$$\text{T } F^T = \text{F } T^T \qquad (3)$$

$$\rho_O \dot{e} = \text{-Div Q + tr}(T \dot{F^T}). \qquad (4)$$

Here ρ is the present mass density of the material particle whose mass density in the reference configuration is ρ_O, F the deformation gradient, V the velocity of a material particle, a superimposed dot indicates material time derivative, T the first Piola-Kirchhoff stress tensor, e the specific internal energy, Q the heat fulx measured per unit reference area, and Div the divergence operator with respect to coordinates in the reference configuration. Here we assume the deformations to be locally adiabatic, thus Q = 0. All of the plastic working is converted into heating even though Farren and Taylor (1925) and Sulijoadikusumo and Dillon (1979) proposed that only 90 to 95% of plastic working is converted into heating. Mason et al. (1994b) have shown that the fraction of plastic working converted into heating depends upon the strain, strain-rate and the material of the body.

Both the projectile and the plate are assumed to be made of the same homogeneous and isotropic thermoviscoplastic material which is modeled by the following constitutive relations.

$$\sigma = \text{-p1 + s, p = K}(\rho/\rho_o - 1), \sigma = J^{-1}\, \text{T}\, F^T, \tag{5}$$

$$\overset{\nabla}{\sigma} = \dot{\sigma} + \text{W}\sigma - \sigma\,\text{W, 2W} - \text{grad v} - (grad\ v)^T, \tag{6}$$

$$\overset{\nabla}{s} = 2\mu \overline{D}^e,\ trD^p = 0,\ \overline{D} = \text{D} - \frac{1}{3}\text{tr(D)1}, \tag{7}$$

$$\dot{e} = c\dot{T} + tr(\sigma D^e),\ \text{2D} = \text{grad v} + (grad\ v)^T,\ D^e = \text{D} - D^p - \alpha \dot{T}1, \tag{8}$$

$$D^p = \Lambda s, \sigma_{eff} = (\frac{3}{2} tr(ss^T))^{1/2}, \tag{9}$$

$$\sigma_m = (\text{A} + \text{B}(\varepsilon_p)^n)(1 + \text{Cln}(\dot{\varepsilon}_p / \dot{\varepsilon}_o^p)\left(1 - \left(\frac{T - T_O}{T_m - T_o}\right)^m\right), \tag{10}$$

$$\dot{\varepsilon}_p = \left(\frac{2}{3} tr(\overline{D}^p \overline{D}^p)\right)^{1/2},\ \varepsilon_p = \int \dot{\varepsilon}_p dt, \tag{11}$$

$$\Lambda = 0 \text{ if either } \sigma_{eff} < \sigma_m \text{ or } \sigma_{eff} = \sigma_m \text{ and } tr(\overset{\nabla}{s}\, s) \le 0, \text{ and} \tag{12}$$

$$\Lambda > 0 \text{ if either } \sigma_{eff} > \sigma_m \text{ or } \sigma_{eff} = \sigma_m \text{ and } tr(\overset{\nabla}{s}\, s) > 0. \tag{13}$$

whenever (13) holds Λ is a solution of the nonlinear equation

$$\sigma_{eff} = \sigma_m. \tag{14}$$

Here σ is the Cauchy stress tensor, σ_{eff} the equivalent or effective stress, s the deviatoric Cauchy stress tensor, p the pressure, K the bulk modulus, α the coefficient of

thermal expansion, $\overset{\nabla}{\sigma}$ the Jaumann derivative of σ, W the spin tensor, μ the shear modulus, D the strain-rate tensor, $\overline{D}$ the deviatoric strain-rate tensor, T the present temperature of a material particle, and grad the gradient operator with respect to coordinates in the present configuration. The strain-rate tensor is assumed to have an additive decomposition into an elastic part, D^e, and a plastic part, D^p, and the strain-rate $\alpha \dot{T} 1$ due to thermal expansion. Equation $(9)_1$ states that D^p is parallel to s, and eqn. (14) is the von-Mises yield criterion with the present value of the yield stress depending on the effective plastic strain, ε_p, the effective plastic strain-rate, $\dot{\varepsilon}_p$, and the non-dimensional temperature, $(T - T_O)/(T_m - T_O)$, where T_O is the reference temperature and T_m is related to the melting temperature of the material. Equation (10) is the Johnson-Cook relation expressing the effective stress σ_m in terms of $\varepsilon_p, \dot{\varepsilon}_p$ and T. In eqn. (10) A is the yield stress of the material in a quasistatic simple tension or compression test, parameters B and n characterize the strain-hardening of the material, and T_m and m the thermal softening of the material.

Initially the prenotched plate is at rest, stress free and at a uniform temperature T_O. The projectile is stress free, at a uniform temperature T_O, is moving with a uniform velocity V_O parallel to the axis of the notch, and at time t = 0 impacts the plate at normal incidence.

All bounding surfaces of the projectile and the prenotched plate are thermally insulated, and all of these except for the impacted faces are traction free. At the contact surface

$[V.n] = 0,\ [n.\sigma n] = 0,\ f_t = -(n.\sigma n)(\mu_S + (\mu_k - \mu_S)e^{-\beta v_{rel}})t,$ (15)

$t = v_{rel}/|v_{rel}|,$

Where [f] denotes the jump in the values of f on the two sides of the contact surface, n is a unit outward normal to the surface, f_t is the tangential traction acting along the unit tangent vector t, and v_{rel} equals the relative velocity of sliding between the two contacting surfaces. μ_S and μ_k are the static and the kinetic coefficients of friction, respectively, and β describes the dependence of the frictional force upon the relative speed of sliding. Values of μ_S, μ_k and β depend upon the roughness of the contacting surfaces.

In order to determine whether a brittle or a ductile fracture initiates first, the brittle failure is assumed to occur at a point when the maximum tensile principal stress there equals twice the quasistatic yield stress of the material in a simple tension or compression test. The criterion for the initiation of a shear band is described in Section 3. However, no such failure or fracture criterion has been implemented in the code; thus a material point can undergo unlimited plastic deformations. Even though the projectile is assumed to be deformable, details of its deformations are not described in order to stay focussed on the deformations of the plate material near the notch-tip.

3 Computation and Discussion of Results

We employ the large scale explicit finite element code DYNA2D developed by Whirley at al. (1992) to analyze the aforestated problem. It uses four noded quadrilateral elements with one-point integration rule, the conditionally stable central-difference method for time integration, and an hour-glass control algorithm to suppress the spurious modes. The finite element mesh shown in Fig. 2 has sixty elements around the notch-tip, and the element size gradually increases with distance from the notch-tip. For one set of material parameters results were also computed with 30 and 48 elements around the notch-tip; otherwise the mesh design was similar to that shown in Fig. 2. The three meshes gave essentially identical results. Results presented herein are obtained with the mesh depicted in Fig. 2 with $7.85\,\mu$m x $23.6\,\mu$m elements abutting the notch-tip. The hour-glass viscosity coefficient was set to 0,4 to suppress spurious modes. Results for one case were also computed with the hour-glass viscosity equal to 0.1 and were found to be virtually indistinguishable from those for hour-glass viscosity equal to 0.4. Because of the assumption of locally adiabatic deformations, the energy equation is trivially integrated, and the size of the time step is governed by the mechanical problem. The time step size equals 0.6 times the time taken by the dilatational wave to travel the shortest dimension of any element in the mesh. The time step size is greatly reduced as the elements get distorted during the deformation process.

In DYNA2D the effects of thermal expansion are neglected. This has no effect on the computed plastic strains since the plastic strain-rate is proportional to the deviatoric Cauchy stress tensor. Material points where the maximum tensile principal stress occurs

are not heated because of the small plastic strains induced there. Thus the computed values of the maximum tensile principal stress should be reasonable.

We analyze the effect on the deformations near the notch-tip of each material parameter in the Johnson-Cook relation, the notch-tip radius, impact speed and the length of the projectile which controls the duration of the loading pulse. When conducting the parametric studies, only one variable is changed at a time. Base values of the material (for a typical steel) and geometric parameters used to compute numerical results are listed below.

A=791.2MPa, B=509.51MPa, C=0.014, n=0.26,

ε_O^p =1/s, m=1.03, K=157GPa, μ=76GPa, T_m = 1033K, c=452 J/(kg K), ρ_O= 7850 kg/m^3, r_O = 0.15mm, V_O = 50m/s, μ_S = 0.18, μ_k = 0.05 and β = 0.0055.

The values of the material parameters in the Johnson-Cook relation are taken from Rajendran's report (1992). For large variations in temperature, as are likely to occur near the notch-tip, nearly all of these material parameters depend upon the temperature, e.g. see Klepaczo et al. (1987). However, this temperature dependence has not been considered here mainly because of the lack of such data.

By assuming that the plate material is linear elastic, a plane strain state of deformation prevails, velocity is instantaneously applied normal to the impact face, and Poisson's ratio for the material of the plate equals 0.25. Lee and Freund (1990) found that the near-filed mode-mixity parameter equals –0.25 over the time interval of interest, i.e., before waves reflected from the far end have arrived at the notch tip. Thus both mode-I and mode-II deformations occur near the notch-tip but the latter are predominant. In an

attempt to delineate which parameters might strongly influence deformations near the notch-tip of a thermoviscoplastic plate, we have used DYNA2D to numerically simulate simple shearing deformations of a homogeneous block of the material at an average strain-rate of 5 x 10^4 /s. It is close to the maximum value of the effective plastic strain-rate computed in the simulations of the Kalthoff experiment. Figures 3a through 3g depict the effective stress vs. the effective plastic strain curves for different values of material parameters A, B, C, n, m, T_m and the nominal shear strain-rate $\dot{\varepsilon}_o$. It is clear that lower value of T_m and higher values of A increase the magnitude of the initial negative slope of the effective stress vs. the effective plastic strain curves. For a simple shearing problem, Wright and Walter (1987) pointed out that the initial negative slope of the effective stress vs. the effective plastic strain curve strongly influences the initiation of a shear band. Stevens and Batra (1998) studied the Taylor impact test for a tungsten heavy alloy (WHA) rod, and assumes that the rod was either made of pure tungsten (W), or a homogeneous iron-nickel tungsten (Fe-Ni-W) alloy, or Fe-Ni-W particles randomly interspread among W particles. They found that a shear band formed at the point on the rod's mantle where the mushroomed region transitioned into the straight rod, only in the rod with the largest value of the initial negative slope of the effective stress vs. effective strain curve.

As was noted by Batra and Nechitailo (1997) the computed value of the maximum velocity imparted to the plate particles on the impact face was found to be one-half of the initial velocity of the projectile.

We now discuss results for the prenotched plate with values of variables listed in (16) except for m, which is set equal to 0.6. This material exhibits enhanced thermal softening and a shear band should initiate when the effective plastic strain slightly exceeds the value at which the effective stress peaks. The impact of the plate by the rod causes a compressive wave to travel into the plate towards the notch-tip. As soon as a wave arrives at the notch-tip, the material there is significantly deformed. The velocity field in the region surrounding the notch-tip, plotted in Fig. 4 for two different values of the time reckoned from the instant of impact, shows that initially the material above the upper flat surface of the notch moves rather slowly and that below the lower surface of the notch moves rapidly in the direction of V_o. Material particles near the traction free lower surface of the notch also move upward due to the Poisson effect. This upward movement of particles essentially subsides once the material near the notch-tip has been severely deformed and is no longer circular. The lower surface of the notch close to the notch-tip is displaced upwards by about 0.05 mm while the upper surface has barely moved. The displacement in the direction of V_o of particles on the lower surface of the notch stretches material lines on the upper curved surface of the notch and induces there a tensile hoop stress. The maximum tensile principal stress occurs at a point, usually a little away from the notch surface, that in the reference configuration makes an angle of approximately 70^o with the notch-axis; the time history of the maximum tensile principal stress, $\sigma^t_{\max}$, at a point in this region is depicted in Fig. 5. Note that $\sigma^t_{\max}$ need not always occur at the same material point. However, the maximum effective plastic strain occurs at a point on the notch surface that in the undeformed configuration

makes an angle of nearly -45^{o} with the notch-axis. The principal stress with the greatest magnitude in the region surrounding this point is compressive. The time histories of the effective plastic strain, the effective stress, the effective plastic strain-rate and the temperature at this material point are exhibited in Figs. 6a and 6b. It is clear that the effective plastic strain-rate, the effective plastic strain and the nondimensional temperature grow rapidly. However the effective stress first increases extremely fast, and then gradually decreases. The rate of change of these quantities strongly depends upon the notch-tip radius and the thermal softening characteristics of the plate. The effective stress peaks at a rather small value of the effective plastic strain. For a simple shearing problem, Wright and Walter (1987) computed a catastrophic drop in the shear stress within a shear band which was subsequently confirmed by torsional experiments on thin-walled HY-100 steel tubes of Marchand and Duffy (1988). For a simple shearing problem, Batra and Kim (1990) found that the sudden drop in the shear stress caused an elastic unloading wave to emanate out of the shear banded region. However, in plane strain and axisymmetric problems, the rate of drop of the effective stress is generally much less than that in a simple shearing problem because in the former class of problems, the material surrounding the shear banded material constrains the latter from severely deforming; e.g. see Batra and Ko (1993). Figure 7 exhibits the deformed shape of the material adjacent to the notch-tip at times t = 20 and 24 μs . It is evident that the material abutting the bottom surface of the notch-tip is intensely deformed. An opening in the shape of a leaflet develops there which subsequently closes at the notch surface thereby forming an elliptical open area. In order to ensure that this phenomenon is not mesh-dependent, the problem was reanalyzed with the finite element mesh shown in Fig. 8. The

aspect ratio of the elements around the notch-tip for this mesh is close to one. Results obtained with meshes of Figs. 2 and 8 were virtually the same.

Time histories, plotted in Fig. 6, of different variables at a material point do not clearly indicate when, if at all, a shear band initiates at this material point. Mason et al. (1994) estimated shear strains of 100% within a 200-300 μm wide shear band formed in a prenotched plate of C-300 maraging steel. Marchand and Duffy (1988) conducted torsional tests on thin-walled tubes made of a HY-100 steel and measured shear strains of upto 20 within a band. They postulated that a shear band initiates when the torque required to deform the tube suddenly drops. Zhou at al. (1998) assumed a relationship between effective plastic strain and the effective plastic strain-rate at the tip of a shear band. For a C-300 maraging steel, their relation (5) with values listed in their Table 2 gives the effective plastic strain at the shear band tip to be 0.17 and 0.0636 for effective plastic strain-rates of 4 x 10^4/s and 4 x 10^5/s respectively. Batra and Kim (1992) numerically studied the initiation and development of shear bands in simple shearing deformations of twelve materials and concluded that a shear band initiates when the shear stress has dropped to 90% of its peak value. However, Deltort (1994) hypothesized that a shear band initiates when the shear stress has dropped to 80% of its maximum value. Batra and Rattazzi (1997) studied the initiation and propagation of a shear band in a thick walled steel tube and investigated the effect of the following four criteria for the initiation of a shear band: (I) the effective plastic strain equals 0.5, (ii) the effective plastic strain equals 1.0, (iii) the effective stress has dropped to 90% of its peak value, and (iv) the effective stress has dropped to 80% of its maximum value. As was also found by Batra

and Rattazzi (1997) these four definitions of the initiation of a shear band give quite different results for the present problem. We note that Tresca (1878) observed shear bands during the hot forging of a platinum bar and conjectured that the tangential velocity is discontinuous across a shear band. Batra and Ko's (1993) computations showed that this indeed was the case. This criterion for the development of a shear band could not be adopted for the present problem mainly because the band did not propagate far enough from the notch-tip for most cases studied.

We now delineate the effect of different parameters on the time of initiation , t_{is}, of a shear band according to criterion (I). Figures 9a and 9b depict the dependence of t_{is} on different material and geometric parameters, and the impact speed. A four-fold increase in the value of C increases t_{is} ny only about 6%. Values of m, T_m, B, A, V_o and r_o strongly influence when a shear band initiates. t_{is} decreases with an increase in V_o and a decrease in r_o, B, m and T_m. For the three values 0.13, 0.25 and 0.52 of the strain hardening exponent n, the shear band initiates essentially at the same time. Also the length of the projectile had no effect on t_{is}. t_{is} increases when A is changed in either direction from the base value. Results could not be satisfactorily computed for A=0.39GPA because the plate material near the bottom of the projectile/plate impact surface got severely deformed. Even though the data points in Fig. 9 have been joined by straight lines, there is no implication that such is indeed the case. The intent is to identify parameters which play a prominent role.

According to criteria (I)-(iv) the time of initiation of a shear band equals 17, 24, 14.5 and 20 μs respectively. As noted earlier, the value of t_{is} depends upon the criterion used.

The speed of propagation of a shear band also depends upon the criterion used to define the shear band tip, and was found to be 50m/s for most of the cases studied here. Henceforth we use criterion (I) to define a shear band.

Assuming that brittle fracture initiates when the maximum tensile principal stress equals twice the yield stress of the material in a quasistatic simple tension or compression test, we have plotted in Figs. 9c and 9d the dependence of the time of initiation of the brittle fracture upon different material and geometric parameters. A comparison of these results with those plotted in Figs. 9a and 9b reveals which failure mode will initiate first. It is clear that a material with smaller value of n will first experience brittle failure and a shear band will first initiate in the material with a higher value of n. As expected, a shear band will first initiate in a material exhibiting increased thermal softening due to lower value of m. The value of T_m does not noticeably change the time of initiation of the brittle fracture but significantly affects the time of initiation of a shear band. The value of the quasistatic yield stress, A, or the strength of the material has a predominant effect on the failure mode. An increase in the value of A considerably delays the initiation of a shear band but lowers the time of initiation of the brittle failure. However, higher values of B delay the initiation both the shear band and the brittle failure. An increase in the value of n has a little effect on the time of initiation of a shear band but noticeably delays the onset of brittle failure. Similarly, an increase in the value of C has a very small effect on the time of initiation of the shear band but considerably decreases the time of initiation of the brittle failure.

Whereas the length of the projectile has virtually no effect on the time of initiation of a shear band, it strongly influences the time of initiation of the brittle failure. For longer

projectiles, the brittle failure will first ensue at a point near the upper surface of the notch. The time of initiation of a shear band significantly decreases with an increase in the impact speed. For a projectile speed of 25 m/s, brittle failure will occur first but for projectile speeds, V_o, greater than or equal to 50 m/s, a shear band will initiate first at a point near the notch tip. For V_o = 50m/s, a decrease in the notch tip radius decreases the time of initiation of a shear band and the brittle failure. For r_o = 0.05 and 0.1mm, a shear band will initiate sooner than the brittle failure.

The foregoing observations on the failure mode depend upon the criteria used to define a shear band and the onset of brittle failure.

We now delineate the effect of different parameters on the deformations of the material adjacent to the notch-tip.

3.1 Effect of Thermal Softening

Two material parameters, m and T_m, influence the thermal softening of the material.

3.1.1 Effect of the value of the thermal softening exponent, m.

The effect of decreasing the value of m is to enhance the thermal softening of the material; cf. Fig. 3b. Figure 10 depicts the contours of the effective plastic strain for m=0.6, 0.7, 0.8, 0.9 and 1.03 when the maximum effective plastic strain at any point near the notch tip equals 1.0; the corresponding times are 24.25, 27, 31, 33 and 35 μs respectively. These plots reveal that two shear bands originate from the bottom surface of the deformed notch-tip; one band propagates at about -10^o to the notch ligament and the other at -128^o. As the value of m is increased or the thermal softening is decreased, the band propagating at -128^o to the notch-axis subsides and only one band

propagates at nearly -10^O to the notch-axis. Recall that Kalthoff measured the angle between the shear band and the notch-axis to be between -10^O and -15^O. As expected, the time measured from the instant of impact, when the the maximum effective plastic strain equals 1.0 increases with an increase in the value of m. The time histories of the effective plastic strain and the effective stress for element E, shown in Fig. 7a, are similar to each other for all values of m considered (e.g. see Fig. 6) except that for m=0.6, the effective plastic strain suddenly increased from 1.4 at t = 27.3 μs to 2.7 at 27.4 μs. This is due to the severe deformations of the element E. For a fixed value of time t, the radial distance through which a shear band defined by any of the four aforestated criteria had propagated decreases with an increase in the value of m.

3.1.2 Effect of the value of T_m

As should be clear from the effective stress vs. the effective plastic strain curves of Fig. 3b, a decrease in the value of T_m enhances the thermal softening effect**.** Thus the effects of decreasing T_m should be similar. Figure 11 depicts contours of the effective plastic strain when the maximum effective plastic strain at any point on the near the notch-tip equals 1.0; the values of the time when this occurs are 24, 28, 35 μs for T_m = 653, 780 and 1033K respectively. A comparison of these plots with those given in Fig. 10 reveals that indeed the results are qualitatively similar and shear bands initiate sooner with a decrease in T_m or m. For T_m = 653K the effective plastic strain exceeds 0.5 in the 0.17-mm thick region abutting the notch-surface and extending in the reference configuration from $\theta = 25^O$ to $\theta = -90^O$ where positive θ is the angle measured counterclockswise from the notch-axis. The thickness or the angular width of this region decreases as one moves

away from the notch surface. The speed of the band, defines as a contour of effective plastic strain of 0.5, first increases from about 10 m/s at the instant of initiation to approximately 50 m/s when it has propagated radially through 0.3 mm and then decreases. The width of the band and the radial distance through which it propagates decreases with an increase in the value of T_m. For T_m = 1413K, the maximum effective plastic strain never reaches 1.0 in any element near the notch-tip, and for T_m = 1033K the width of the shear banded region(i.e. where the effective plastic strain equals atleast 0.5) adjacent to the notch-tip equals 0.14 mm and it extends from $\theta = -27^o$ to $\theta = -80^o$ in the circumferential direction and 0.1mm in the radial direction.

3.2 **Effect of Quasistatic Yield Stress, A**

The values of the quasistatic yield stress, A, strongly influence the deformations of the material near the notch-tip. Recall that the projectile and the plate are made of the same material. For five different values of A, Fig. 12 exhibits contours of effective plastic strain when the effective plastic strain at any point near the notch-tip equals 1.0; this happens at t = 30.75, 31, 32 and 36 μs for A= 2.376, 1.584, 1.18 and 0.63GPa respectively. Whereas for lower values of A, there are two intensely deformed regions originating from the the point on the bottom surface of the deformed notch-tip, there is only one such region for the highest value 2.376Gpa of A. Note that the value of A determines the strength of a steel. For very high strength steels, only one shear band propagating essentially parallel to the axis of the notch forms. Also, deformations of the material adjacent to the notch-tip are similar to that shown in Fig. 7 for low values of A but no leaflet like opening develops for A=2.376GPa even though the maximum effective plastic strain there exceeds 1.0. Figure 13 depicts at t =24 μs the deformed mesh near the

notch surface for A= 2.376GPa and also the velocity field. Whereas for lower values of A, the material particles adjacent to the traction free lower surface of the notch move essentially horizontally at t = 24 μs , for the higher value of A, their velocity has a small downward component. For A= 2.376GPa the shear band defined as the region in which the effective plastic strain exceeds 0.5 was 71 μm wide near the notch-tip and extended 0.48 mm in the radial direction. The band width near the notch-tip decreased from 150 μm for A= 0.63GPa to 71 μm for A=2.376GPa.

For A = 0.39Gpa, the notch closed near the impacted end at t = 19 μs . In order to circumvent this, the notch width near the impacted end was increased to 0.5mm by keeping the lower traction free surface of the notch horizontal and making the upper one inclined to obtain a notch opening of 0.3 mm at a distance of 20 mm from the impacted end. In this case the mesh near the bottom of the target/projectile interface was severely distorted.

3.3 Effect of Strain-Hardening

Two material parameters, B and n, influence the strain hardening of the material; smaller values of n for ε_p < 1 and higher values of B enhance the strain hardening effect of the material. For ε_p > 1, a material with higher value of n will exhibit more strain hardening effect. As pointed out earlier, higher values of B result in larger values of the time, t_{iS} , of the initiation of a shear band. Also, only one shear band originates at the notch-tip and propagates nearly horizontally, i.e., parallel to the axis of the notch. Figure 14 depicts contours of the effective plastic strain and the deformed shape of the notch-tip at t = 38 μs for a material with B=1.108Gpa. The maximum effective plastic strain at the notch-tip

equals 0.76. It is evident that the surface of the notch-tip is not as severely distorted as for lower values of B, and only a few elements in the region where the deformed notch-tip meets the lower surface of the notch exhibit intense plastic deformations. Similar deformation patterns were observed for a material with n = 0.13. We should add that for B=0.203Gpa, a lealfet like opening akin to that exhibited in Fig 7b formed. Figure 15 evinces, for four values of B and two values of n, the time history of the temperature in an element abutting the notch surface and situated in the reference configuration on a line that makes an angle of 45^o clockwise with the notch-axis. Lower values of B and n result in higher final temperatures at this element. These values of temperatures compare favorably with those experimentally measured by Zhou et al. (1996a).

3.4 Effect of Strain-Rate Hardening

As should be obvious from the plot in Fig. 16 of the time history of the evolution of the effective plastic strain at element E for C = 0.004, 0.007 and 0.028, values of C within the range studied influence a little the initiation of a shear band. Other results such as the deformed surfaces of the notch-tip, the shear band speed, and the velocity field in the deforming region were also essentially unaffected by the value of C.

3.5 Effect of Notch-tip Radius, r_o

The maximum tensile principal stress induced at any point near the surface of the notch-tip and normalized by the quasistatic yield stress of the material equals 2.02 for r_o = 0.05mm, and 2.27 for r_o = 0.1, 0.15 and 0.2mm. Thus the maximum principal tensile stress is essentially independent of the notch-tip radius; Batra and Nechitailo's (1997) results for larger values of r_o gave a similar trend. At t = 18 μs the deformed surface of

the notch-tip for r_o = 0.05 mm looks similar to that shown in Fig. 7b in the sense that a leaflet like opening develops in the region where the deformed notch surface meets the bottom traction-free surface of the notch. Both the upper and lower traction free surfaces of the notch move upwards, the lower one moves up by 0.043 mm and the upper one by 0.013 mm; thus the gap between these surfaces decreases from 0.1 mm at t = 0 to 0.068 mm at t = 18 μs. Recall that for r_o = 0.15 mm, the upper traction free surface of the notch scarcely moved. As shown in Fig. 9b the time of initiation of the shear band, i.e., the time when the maximum effective plastic strain at a point on the notch surface equals 0.5, decreases sharply with a decrease in the notch-tip radius.

For different values of r_o, we have plotted in Figs. 17a and 17b the time-history of the effective plastic strain and the effective stress for element E. For r_o = 0.05 mm, the effective stress drops catastrophically and the effective plastic strain increases immensely at t $\cong$ 18 μs. The drop of the effective stress to zero indicates that the temperature of the material point E has reached the presumed melting temperature of 1033K. At t = 18 μs, a leaflet like opening somewhat similar to that shown in Fig. 7b developed.

Figure 17c depicts the plot of $\ln \dot{\varepsilon}_p$ vs. $\ln r_o$ at t = 8.1, 9 and 9.5 μs, $\dot{\varepsilon}_p$ and r_o have been normalized by 1/s and 1 mm respectively. Here $\dot{\varepsilon}_p$ equals the effective plastic strain-rate in the element abutting the notch-tip. Assuming that $\dot{\varepsilon}_p \ \alpha \ r_o^{\alpha}$, we conclude from the slopes of the best fit straight lines to the computed values that α = 0, -0.1 and –0.4 at t = 8.1, 9 and 9.5 μs respectively. At t = 8.1 μs the material near the notch-tip just starts

deforming plastically. Thus the order of the singularity at the notch-tip changes with an increase in the plastic deformation there.

We note that for r_O = 0.05mm the notch opening near the impacted surface of the plate was increased by keeping the lower notch surface horizontal and making the upper one inclined for about 20 mm. For t < 18 μs the notch surfaces stayed apart but they contacted at t $\cong$ 18 μs at the point where the upper inclined notch-surface met the lower horizontal notch-surface. It seems that forces at the contact surface had little influence on the deformations near the notch-tip since the material there had already been intensely deformed.

3.6 Effect of Projectile Length

The duration of the loading pulse at the projectile/target interface is directly proportional to the length of the projectile. Whereas for a 75 mm long projectile the maximum effective plastic strain at any point near the notch-tip reached 1.0 at t = 35 μs , it equalled 1.7 at t = 40 μs for 112.5 mm and 150 mm long projectiles. For a 150 mm long projectile, contours of effective plastic strain and the deformed mesh near the notch tip at t = 40 μs are exhibited in Fig. 18. Only one shear band emanates from the point where the deformed notch-tip meets the bottom nearly horizontal surface of the notch and propagates, in the direction of the impact velocity, at an angle of -10^O to the horizontal axis. There is no leaflet like open region developed near the bottom of the deformed notch-tip which look similar to the deformed notch-tip for A = 2.376Gpa.

3.7 Effect of Impact Speed, V_O

Figures 19 a and 19b exhibit for element E marked in Fig. 7b the time histories of the effective plastic strain and the effective stress for different values of the impact speed

V_o. For V_o = 25 m/s the maximum effective plastic strain induced at any point near the notch-tip is less than 0.3. The value of the maximum effective plastic strain increases with an increase in the impact speed. For $V_o \leq 25$ m/s there is no shear band formed according to any one of the four aforestated criteria. However, for V_o = 25 m/s, the maximum tensile principal stress equals 2.14 times the quasistatic yield stress, A, of the material. Thus if the brittle failure of the material occurs when the maximum principal tensile stress equals 2A, then the brittle failure will occur at low impact speeds. At high impact speeds, the maximum effective plastic strain reached the critical value of 0.5 before the maximum tensile principal stress becomes 2A, thus a shear band initiates first. Once a material point fails, new surfaces are created and the boundary conditions change; this has not been pursued here. In order to satisfactorily compute results for V_o = 75 m/s, the upper surface of the notch near the impacted end was made inclined as described before.

For low impact speeds, the notch-tip is not intensely deformed and the computed surface of the notch-tip is smooth. For V_o = 75 m/s, a leaflet like opening develops as shown in Fig. 7c and two shear bands, one at -10^o and the other at -128^o emanate from the area containing the leaflet.

We have plotted in Fig. 19c $\ln \dot{\varepsilon}_p$ vs $\ln V_o$ for three different values of time; $\dot{\varepsilon}_p$ and V_o have been normalized by 1/s and 1 m/s respectively. Here $\dot{\varepsilon}_p$ equals the effective plastic strain-rate in the element abutting the notch-tip. By fitting straight lines by the least squares method we find that $\dot{\varepsilon}_p \ \alpha \ V_o^{\beta}$ with β = 0, 1.25 and 1.92 for t = 8.1, 9 and 9.5

μs respectively. Thus strain-rate induced at the notch-tip soon after the arrival of a loading wave is independent of the speed of the projectile. However, subsequent values of $\dot{\varepsilon}_p$ increase sharply with an increase in V_O.

3.8 Plate made of a C-300 steel

Mason et al. (1994) and Zhou et al. (1996a) tested prenotched plates made of a C-300 steel. Zhou et al. (1996) have given the time histories of the temperature at material points approximately 3 mm and 6 mm from the notch-tip, band speed and the length of a shear band. They modeled the strain and strain-rate hardening of the material by power law type relations and the thermal softening by an exponentially decaying function. Since strain-rate hardening plays a less noticeable role and the strain-hardening in the Johnson-Cook model is analogous to a power law type function, we changed the thermal softening function in eqn. (10) to the one used by Zhou et al. and arrived at

$$\sigma_m = \max[(A + B(\varepsilon_p)^n)(1 + C\ln(\dot{\varepsilon}_p / \dot{\varepsilon}_O^p))(1 - \delta(\exp((T - T_O)/\kappa) - 1)), 0], \qquad (17)$$

where T_O equals the room temperature. Values of material parameters A, B, n, C, $\dot{\varepsilon}_O$, and κ are obtained by fitting curves to their data and used to compute results discussed herein are listed below.

A = 2GPa, B = 94.5MPa, n = 0.2, C= 0.0165, T_O = 293K,

$\dot{\varepsilon}_O^p$ = 1.3 x 10^{-13}/s, κ = 500K.

Values of geometric parameters and other material parameters are the same as those listed in (16).

For values of material parameters given in (18), $\sigma_m = 0$ when T=698 K. Generally $\sigma_m = 0$ for a perfect fluid. Thus the material point defined by (17) and (18) will behave like a perfect fluid for T $\geq$ 698K. Zhou et al. (1996b, 1998) assumed that it behaves like a viscous fluid when $\varepsilon_p \geq 0.17$ and 0.0636 for $\dot{\varepsilon}_p = 4 \times 10^4$/s and 4×10^5/s respectively. We have also computed results with $\kappa = 800$K which implies that the material point turns into a perfect fluid at T = 941K; the latent heat required to melt a solid particle has been neglected.

Figure 20 depicts the effective stress vs. the effective plastic strain curves for the C-300 steel with $\kappa = 500$ K and 800 K obtained by analyzing with DYNA2D a simple shearing problem at a nominal strain-rate of 5×10^4/s. The thermal softening exhibited by the material defined by (17) and (18) is significantly more than that in the C-300 steel for which the experimental effective stress vs. the effective strain curve is given in Fig. 9 of Zhou et al. (1998); it seems like that they ignored the effect of thermal softening when fitting a curve to the test values. Here, an initial boundary-value problem corresponding to a simple shearing of a block has been analyzed. For each value of κ, the maximum tensile principal stress induced at any point equalled 1.9 times the quasistatic yield stress of the material in simple tension or compression. For $\kappa = 500$ K and 800 K a shear band according to criterion (I) defined above initiated at t $\cong$ 20.5 and 23 μs respectively and propagated into the plate at an average speed of 350 m/s. For the two values of κ, we have plotted in Fig. 21, the time histories of the effective plastic strain, the effective stress, the effective plastic strain-rate and the normalized temperature for the element E depicted in Fig. 7c. For $\kappa = 500$ K a shear band initiates in element E at t $\cong$ 20.5 μs and

the temperature there equals 603 K; the material point melts at t $\cong$ 22 μs. The effective plastic strain-rate, $\dot{\varepsilon}_p$, at the instant of the initiation of the shear band at point E equals 8 x 10^7 /s. Note that $\dot{\varepsilon}_p = 10^7$ /s when the effective stress at E has the peak value. For $\dot{\varepsilon}_p = 8 \times 10^7$ /s, Zhou et al.'s (1998) eqn. (5) implies that the effective plastic strain at the tip of the shear band is 0.04 which is very small. Since the contour of effective plastic strain of 0.04 travels much faster than that of 0.5 (e.g. see Needleman (1989), Zhu and Batra (1991)) the computed band speed will far exceed 350 m/s found here for the contour of $\varepsilon_p = 0.5$. Figure 22 shows for $\kappa = 500$ K the deformed mesh and contours of the effective plastic strain at t = 22.2 μs. Only a small amount of material near the bottom of the notch-tip is intensely deformed and the contour of the effective plastic strain of 0.17 has propagated to a point 0.5 mm from the notch-tip. Results for $\kappa = 800$ K are similar to those for $\kappa = 500$ K except that the initiation of the shear band in delayed a little.

The computed value of the temperature in element E is comparable to that measured by Zhou et al. (1998). However our computations could not be carried further in time because of the excessive distortions of elements surrounding the element E. Zhou et al. (1998, 1996b) have not elaborated upon the technique, if any, employed to overcome the severe distortion of elements containing the failed material.

Mason et al. (1994) have estimated the shear band speed and the time of initiation, t_{is}, to be 320 m/s and 26 μs respectively. Zhou et al. (1996a) measured the maximum shear band speed to be 2000 m/s in the same C-300 steel. For $\kappa = 500$ k and 800 k, our

computed values are t_{is} = 20.5 and 23 μs respectively, and the average shear band speed for each value of κ equals 350 m/s.

4. Conclusions

We have analyzed finite plane strain transient deformations in a prenotched plate impacted on the side by a projectile moving parallel to the axis of the notch. The projectile and the plate are made of the same material which exhibits strain hardening, strain-rate hardening and thermal softening. The thermoviscoplastic response of the material is modeled by the Johnson-Cook relation. The deformations of the plate are assumed to be locally adiabatic and no failure criterion is included. The problem is analyzed for several values of the material and geometric parameters by using the large scale explicit finite element code DYNA2D. For one set of material and geometric parameters, results computed with four different reasonably fine finite element meshes were found to be virtually identical to each other. Results presented in this Thesis and the conclusions drawn are based on the finest finite element mesh used that had 60 elements around the notch-tip. For a notch-tip radius of 0.15 mm, the size of the elements abutting the notch-tip equalled 7.85 μm x 23.6 85 μm .

For all of the cases analyzed, the bottom surface of the notch moves upwards and the upper surface essentially stays stationary except when the notch-tip radius equals 0.05mm. For the latter case both surfaces move upwards, however the lower one moves by a larger amount than the upper one with the result that the notch opening is decreased as also happens for other problems studied. The lower notch surface is also displaced in the direction of the velocity of the projectile, the notch tip is deformed and line elements near the upper part of the notch surface are stretched. The maximum principal stress is

tensile near this part of the notch-tip and compressive near the bottom of the deformed notch-tip.

It is found that for strongly strain-hardening or high-strength (very high values of the yield stress in a quasistatic simple tension or compression test) steels, a shear band initiates from the bottom of the deformed notch-tip and propagates in the direction of the impact velocity at an angle of about -10^{o} with the axis of the notch. The maximum computed shear band speed equals approximately 100 m/s. However, for moderate strength steels, a leaflet like opening develops near the bottom of the deformed surface of the notch-tip, and two shear bands – one at -10^{o} and the other at -128^{o} to the notch-axis propagate into the plate material.

For all values of the material and geometric parameters considered with the Johnson-Cook model the maximum tensile principal stress equals about 2.2 times the yield stress of the material in a quasistatic simple tension or compression test. For impact speeds below approximately 30 m/s, the maximum effective plastic strain induced is less than 0.4. With the assumptions that a shear band initiates when the effective plastic strain equals at least 0.5 and the brittle failure occurs when the maximum tensile principal stress equals twice the quasistatic yield stress of the material, a brittle failure will occur at low values of the impact speed and a ductile failure at high impact speeds in conformity with the observations of Kalthoff. We note that in problems where the computed effective plastic strain exceeded 0.5, it occurred before the maximum tensile principal stress attained its critical value implying thereby that a shear band initiated first.

The initial plastic strain-rate at the notch-tip at t = 8.1 μs when a loading wave arrives there is independent of V_o and r_o, that at t = 9 μs is proportional to $V_o^{1.25}/r_o^{0.3}$ and

$V_o^{1.92}/r_o^{0.4}$. The exponents of V_o and r_o will very likely depend upon the constitutive relation employed to model the thermoviscoplastic response of the material.

We have also investigated the dynamic deformations of a prenotched plate made of a C-300 steel modeled by the modified Johnson-Cook relation with the thermal softening function replaced by an exponential one proposed by Zhou et al. (1996b). For the material parameters obtained by fitting curves to Zhou et al.'s data, the average shear band speed was found to be 350 m/s and the temperature rise at the initiation of a shear band to be 350^o C. The maximum tensile principal stress equalled 1.9 times the yield stress of the material in a quasistatic simple tension or compression test.

5. References

Batra, R.C. and Kim, C.H. (1992). Analysis of shear bands in twelve materials. Int. J. Plasticity. 8, 425-452.

Batra, R.C. and Kim, C.H. (1990). Adiabatic shear banding in elasto-viscoplastic nonpolar and dipolar materials. Int. J. Plasticity. 6, 127-141.

Batra, R.C. and Ko, K.I. (1993). Analysis of shear bands in dynamic axisymetric compression of a thermoviscoplastic cylinder. Int. J. Engng. Sci. 31, 529-547.

Batra, R.C. and Nechitailo, N.V. (1997). Analysis of failure modes in dynamically loaded pre-notched steel plates. Int. J. Plasticity. 13, 291-308.

Batra, R.C and Rattazzi, D. (1997). Adiabatic shear banding in a thick-walled steel tube. Comp. Mechs. 20, 412-426.

Deltort, B. (1994). Experimental and numerical aspects of adiabatic shear in a 4340 steel. J. Physique Colloque C8. 4, 447-452.

Farren, W.S. and Taylor, G.I. (1925). The heat developed during plastic extrusion of a metal. Proc. Roy. Soc. A207, 422-426.

Johnson, G.R. and Cook, W.H. (1983). A constitutive model and data for metals subjected to large strains, high strain rates and high temperatures. Proc. 7th Int. Symp. Ballistics, The Hague, The Netherlands, 541-548.

Kalthoff, J.F. (1987) Shadow optical analysis of dynamic shear fracture, SPIE, Vol. 1814, Photomechanics and speckle Meteorology, 531-538.

Kalthoff, J.F. and Winkler, S. (1987). Failure mode transition at high rates of shear loading. In Impact Loading and Dynamic Behavior of Materials, eds. C.Y. Chiem et al., 185-195, Informationsgesellaschaft Verlag Bremen.

Klepaczko, J.R., Lipinski, P. and Molinari, A. (1987). An analysis of the thermoplastic catastrophic shear in some metals. Proc. Int. Conf on Impact loading and Dynamic Behavior of Materials, eds. C.Y. Chiem et al., 685-794, Informationsgesellaschaft Verlag Bremen.

Lee, Y.J. and Freund, L.B. (1990). Fracture initiation due to asymmetric impact loading of an edge cracked plate. J. Appl. Mech. 57, 104-111.

Marchand, A. and Duffy, J. (1988). An experimental study of the formation process of adiabatic shear bands in a structural steel. J. Mechs. Phys. Solids. 36, 251-283.

Mason, J.J., Rosakis, A.J. and Ravichandran, G. (1994a). Full field measurements of the dynamic deformation field around a growing adiabatic shear band tip of a dynamically loaded crack or notch. J. Mech. Phys. Solids. 42, 1679-1697.

Mason, J.J, Rosakis, A.J. and Ravichandran, G. (1994b). On the strain and strain-rate dependence of the fraction of plastic work converted to heat: an experimental study using high speed infrared detectors and Kolsky bar. Mechs. Materials. 17, 135-150.

Needleman, A. (1989). Dynamic shear band in plane strain. J. Appl. Mech. 56, 1-8.

Needleman, A. and Tvergaard, V. (1995). Analysis of brittle-ductile transition under dynamic shear loading. Int. J. Solids Structures. 44, 2571-2590.

Rajendran, A.M. (1992). High strain-rate behavior of metals, ceramics and concrete. Report No. WL-TR-92-4006. Wright-Patterson Air Force Base.

Stevens, J.B. and Batra, R.C. (1998). Adiabatic shear bands in the Taylor impact test for a WHA rod. Int. J. Plasticity. 14 (to appear).

Sulijoadikusumo, A.V. and Dillon, O.W., Jr. (1979). Temperature distribution for steady axisymmetric extrusion with an application to Ti-6Al-4V, Part I. J. Thermal Stresses. 2, 97.

Tresca, H. (1878). On further application of the flow of solids. Proc. Inst. Mech. Eng. 30, 301-345.

Whirley, R.G., Englemann, B.E. and Hallquist, J.O. (1992). DYNA2D, A nonlinear, explicit, two-dimensional finite element code for solid mechanics, user manual. Lawrence Livermore National Laboratory Report, UCRL-MA-110630.

Wright, T.W. and Walter, J.W. (1987). On stress collapse in adiabatic shear bands. J. Mech. Phys. Solids. 35, 701-720.

Zhou, M., Rosakis, A.J. and Ravichandran, G. (1996a). Dynamically shear bands in prenotched plates: I-Experimental investigations of temperature signatures and propagating speed. J. Mech. Phys. Solids. 44, 981-1006.

Zhou, M., Rosakis, A.J. and Ravichandran, G. (1996b). Dynamically propagating shear bands in prenotched plate: II-Finite element simulations. J. Mech. Phys. Solids. 44, 1007-1032.

Zhou, M., Rosakis, A.J. and Ravichandran, G. (1998). On the growth of shear bands and failure mode transition in prenotched plates: a comparison of singly and doubly notched specimens. Int. J. Plasticity. 14, 435-451.

Zhu, Z.G. and Batra, R.C. (1991). Shear band development in a thermally softening viscoplastic body. Computers & Structures. 39, 459-472.

6. Appendix

The following is a sample input file.

```
         MELT.TEMP=1033                                                  92
    24506144427    0    0    0    0    0    0    0    0
    1    0    0      12.0      25.0    1    1    1
    0    0    2    4    1       1.0       .18   .60E-01   .55E-02
       38.       0.0    0       0.6      0.01      00.0      00.0
0.0
      33.0       1.0    0    0    0    0    0    0      0.00
    1    0    0    0    0    0    0
    1       0.4    1       1.5      0.06    0
    1   12      7.85    1    1      0.40    1       1.5      0.06    0
  JOHNSON-COOK MODEL. (material 1 defined for the target)
     76.0079.219E-02509.51E-03       .26     0.014      1.03     1033.
298.
1.0000E-06   452E-06
       5.5       0.0       0.0       0.0       0.0


   EQUATION OF STATE (volumetric behavior):  This is linear polynomial
  0.0      157.       0.0       0.0       0.0       0.0       0.0
  1.0
    2   12      7.85    1    1      0.40    1       1.5      0.06    0
   JOHNSON-COOK MODEL.(material 2 defined for the projectile)
     76.0079.219E-02509.51E-03       .26     0.014      1.03     1033.
298.
1.0000E-06   452E-06
       5.5       0.0       0.0       0.0       0.0


  EQUATION OF STATE (volumetric behavior):  This is linear polynomial
  0.0      157.       0.0       0.0       0.0       0.0       0.0
  1.0
    1   .0       50.756069183349609         .106066912412643
    .
    .
    .
45061   .0      -76.199996948242188      -50.799999237060547
    1    1    2   33   32    1
    .
    .
    .
4442745060450614499544994    2
    1  0.00E+00  0.00E+00    0
42025  0.00E+00  0.00E+00    0
42026  5.00E-02  0.00E+00    0
45061  5.00E-02  0.00E+00    0
```

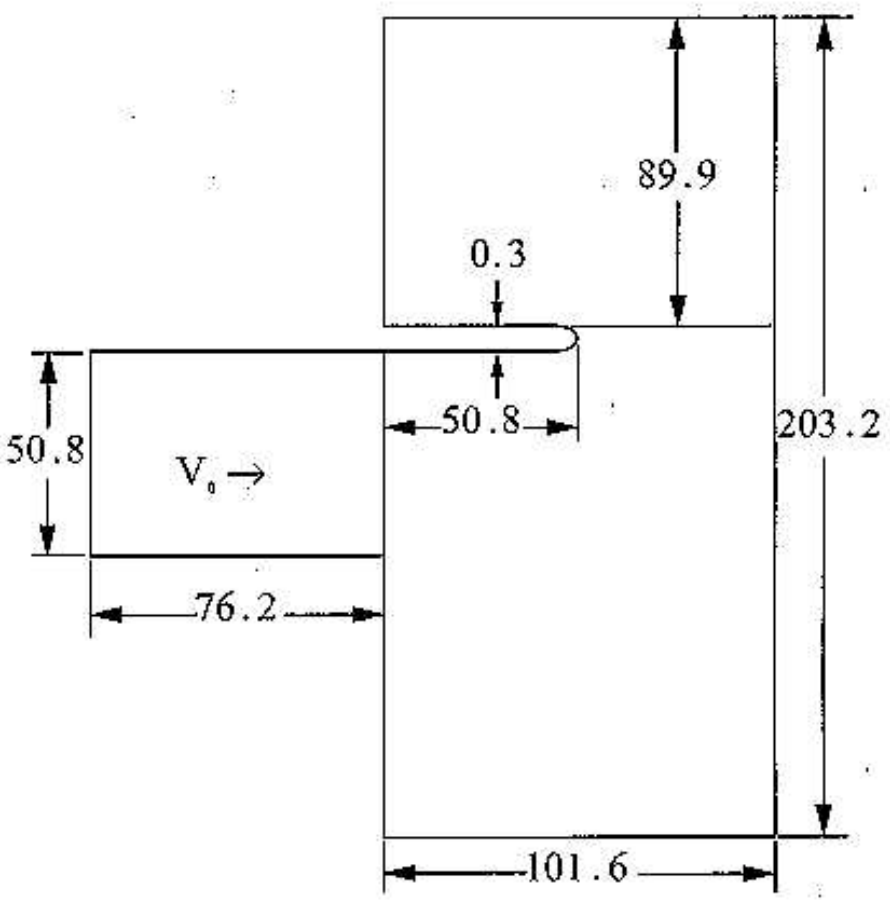

All dimensions are in mm (Sketch not to scale)

Figure 1. A schematic sketch of the problem studied.

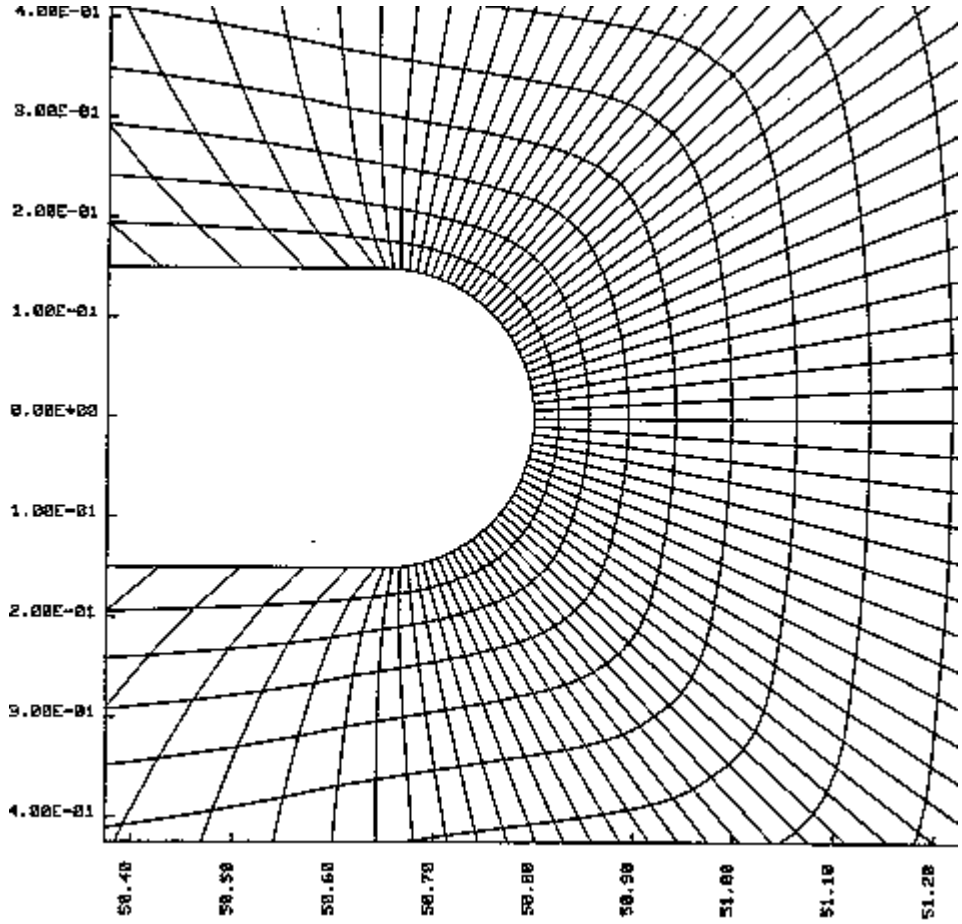

Figure 2. Details of the finite element mesh near the notch tip.

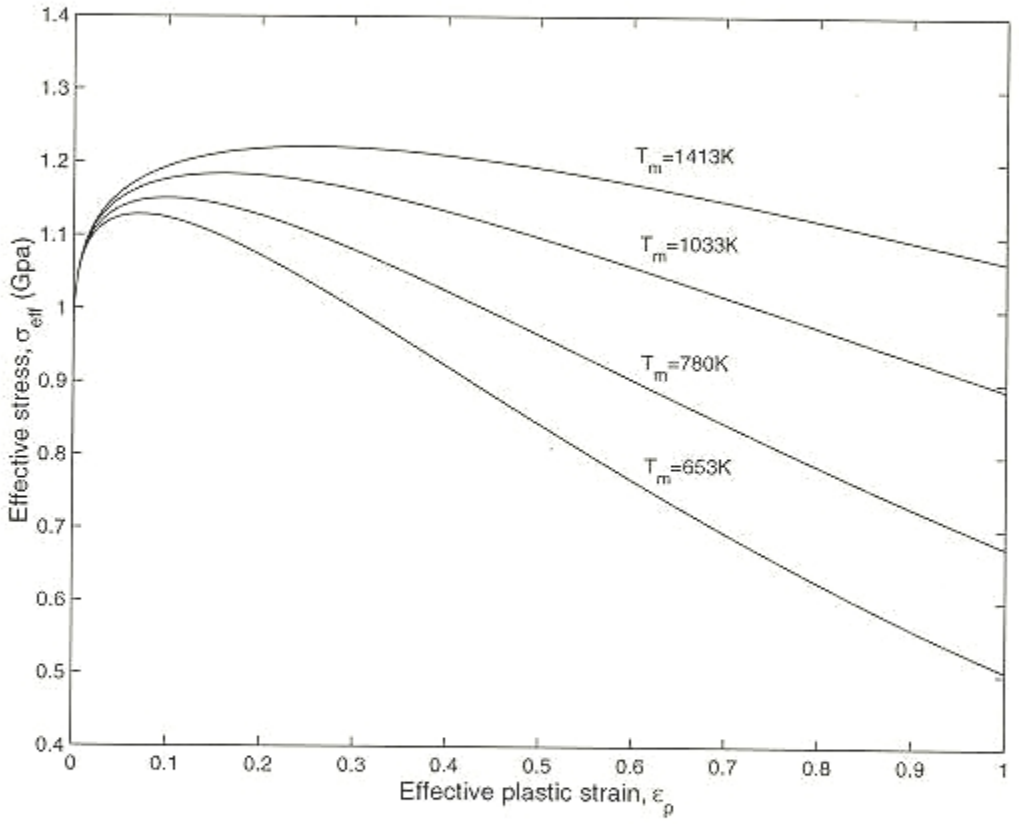

Figure 3a. Effective stress vs. effective plastic strain during simple shearing deformation of a typical steel at nominal strain-rate of 50,000/s for different values of material parameters.

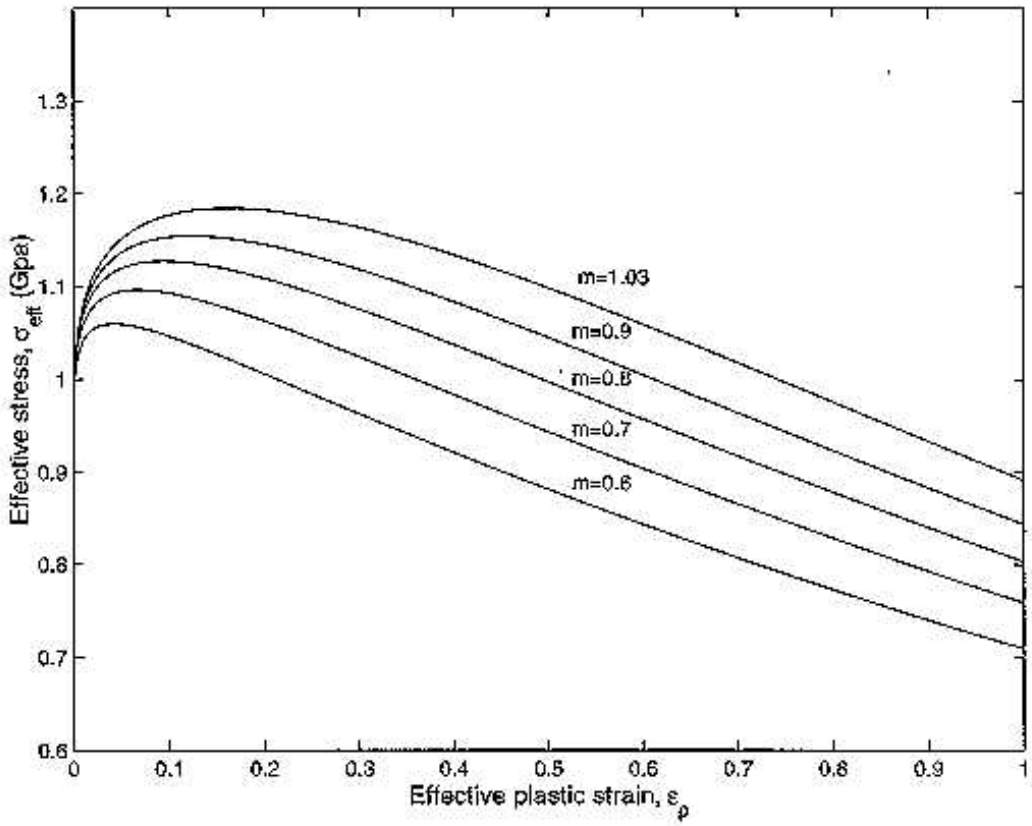

Figure 3b. Effective stress vs. effective plastic strain during simple shearing deformation of a typical steel at nominal strain-rate of 50,000/s for different values of material parameters.

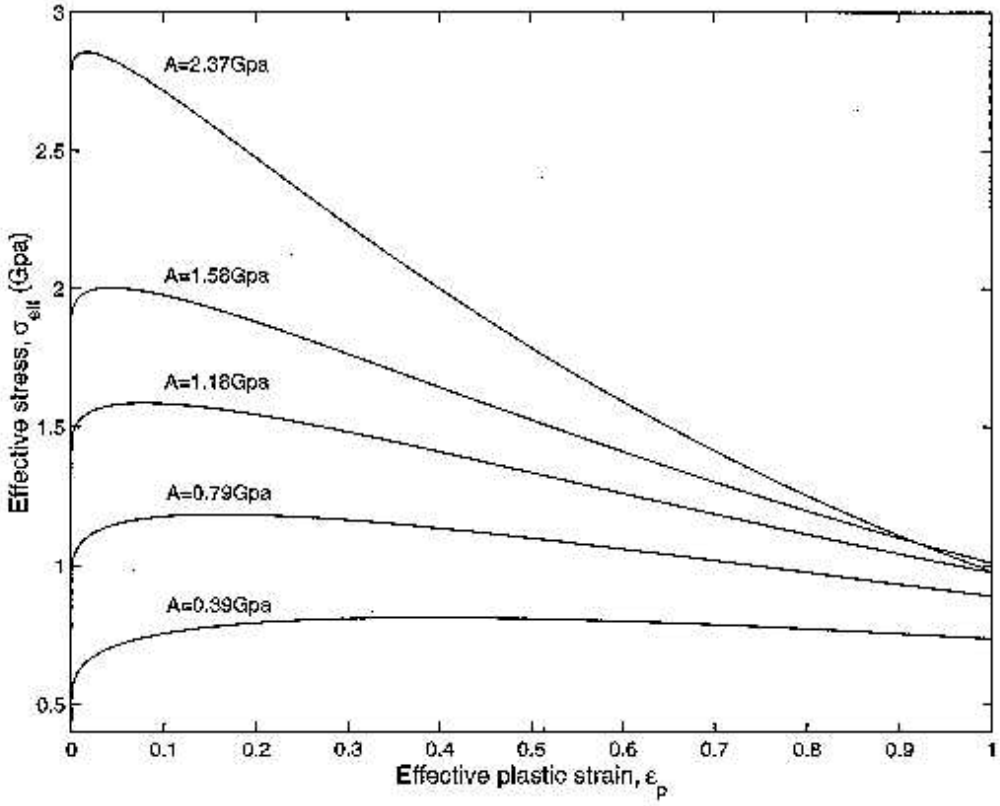

Figure 3c. Effective stress vs. effective plastic strain during simple shearing deformation of a typical steel at nominal strain-rate of 50,000/s for different values of material parameters.

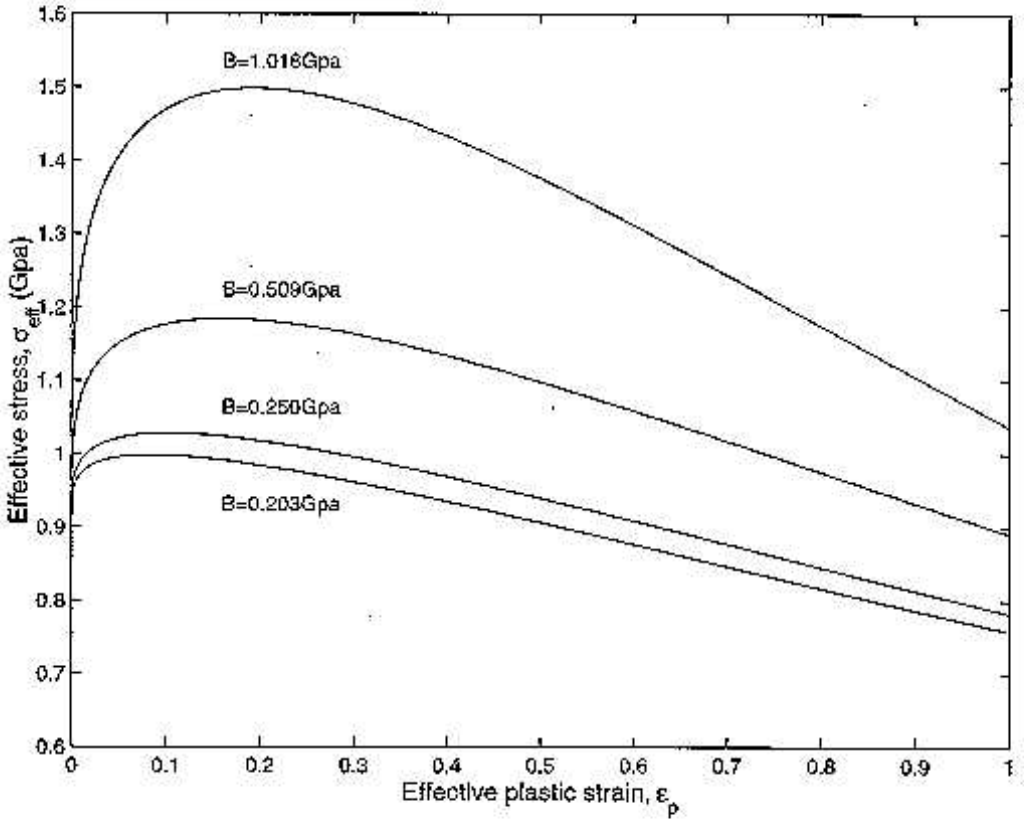

Figure 3d. Effective stress vs. effective plastic strain during simple shearing deformation of a typical steel at nominal strain-rate of 50,000/s for different values of material parameters.

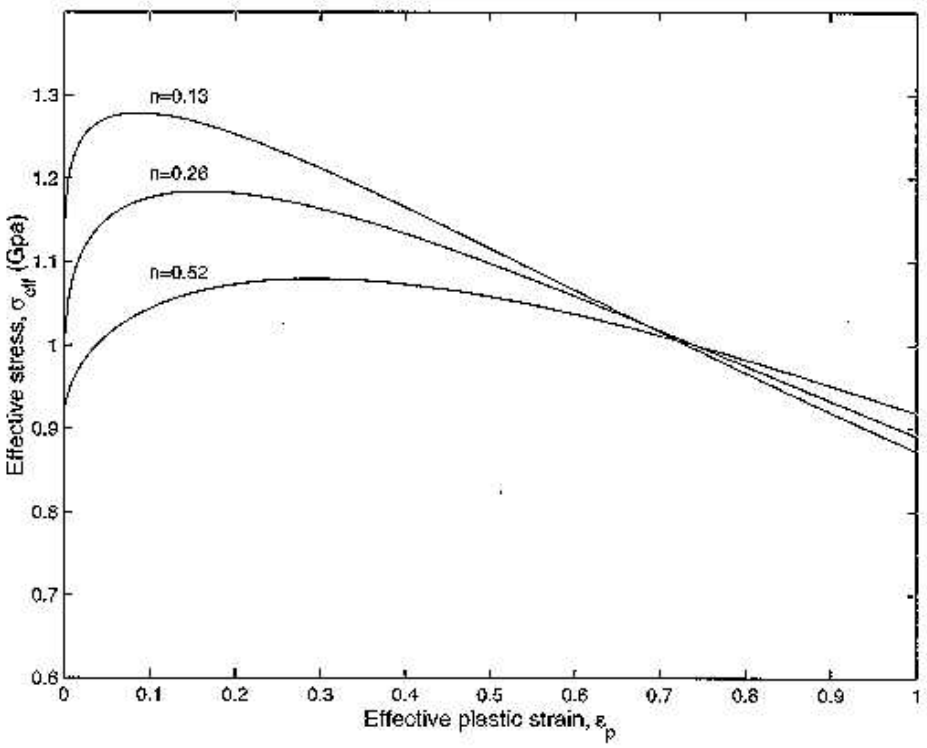

Figure 3e. Effective stress vs. effective plastic strain during simple shearing deformation of a typical steel at nominal strain-rate of 50,000/s for different values of material parameters.

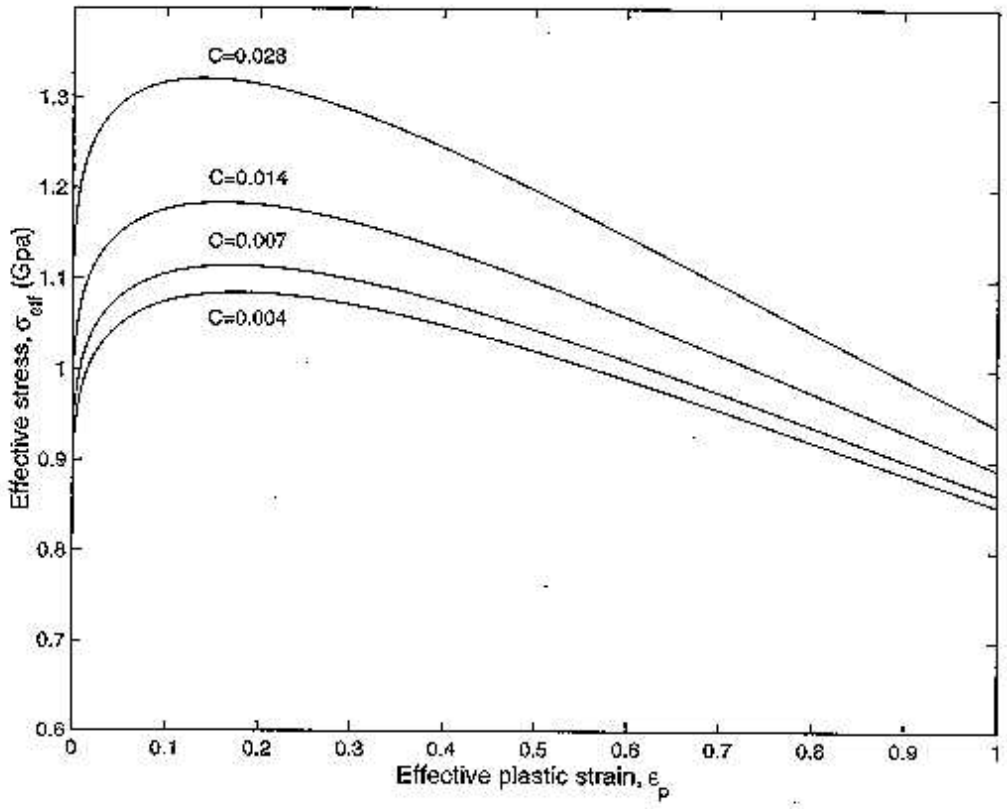

Figure 3f. Effective stress vs. effective plastic strain during simple shearing deformation of a typical steel at nominal strain-rate of 50,000/s for different values of material parameters.

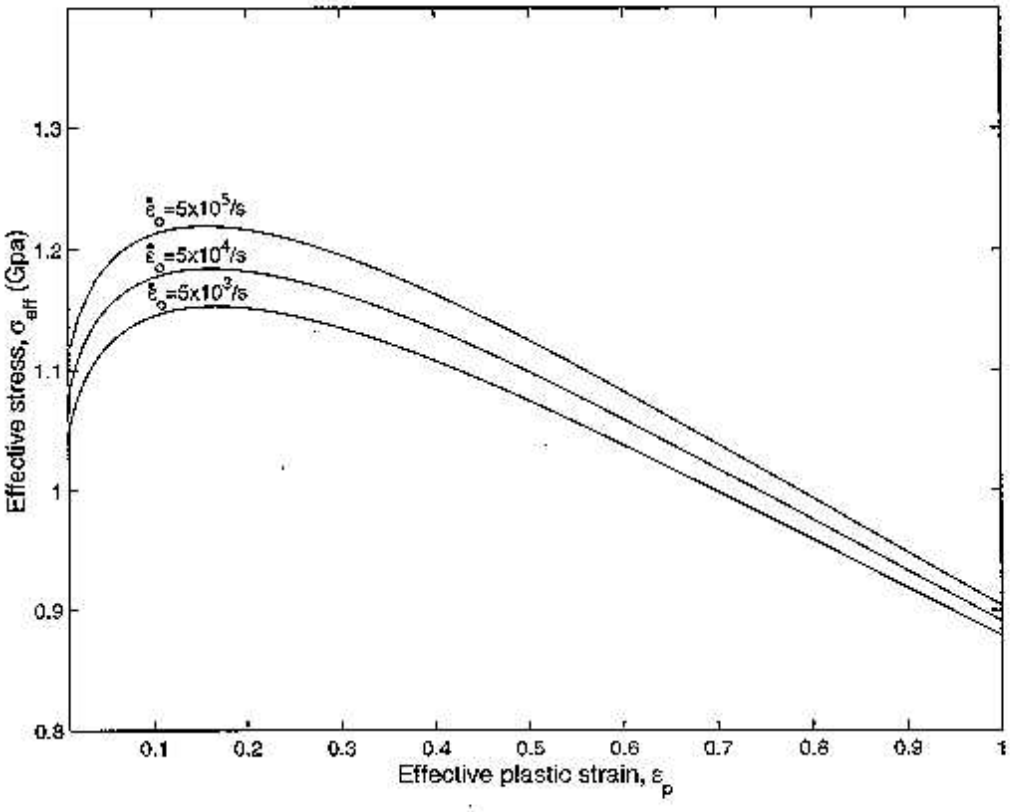

Figure 3g. Effective stress vs. effective plastic strain during simple shearing deformation of a typical steel at nominal strain-rate of 50,000/s for different values of material parameters.

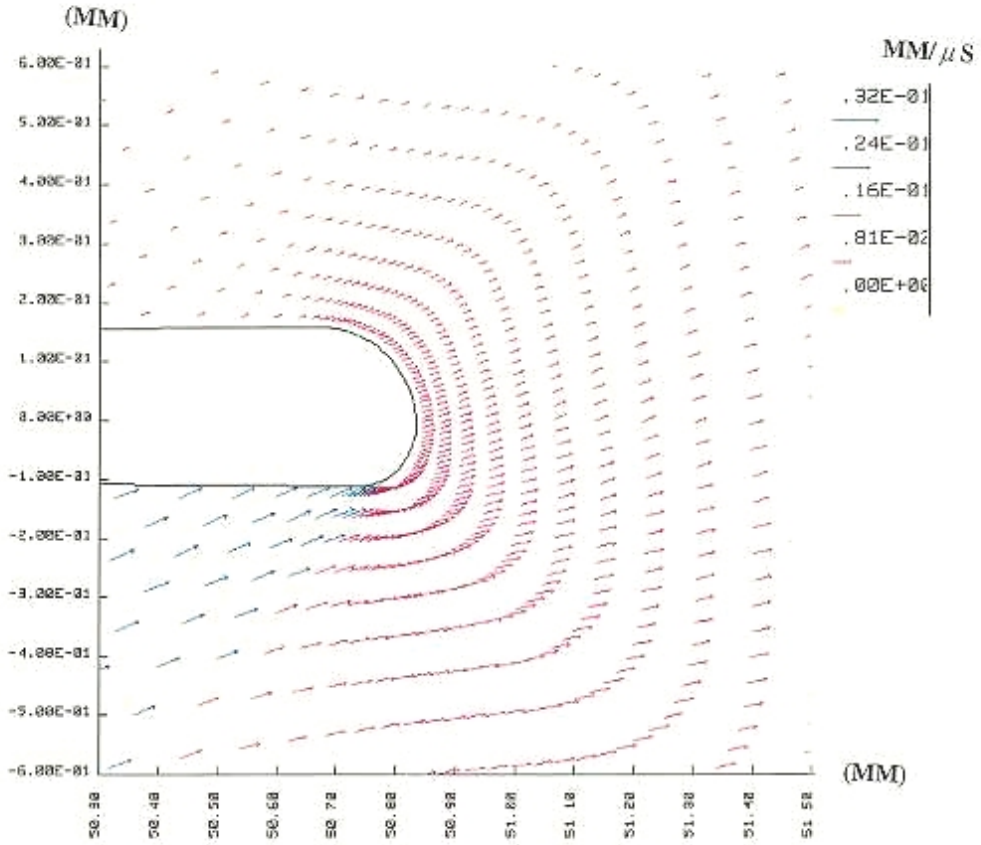

Figure 4a. Velocity Field at t=13 microseconds in the region surrounding the notch-tip. (m=0.6)

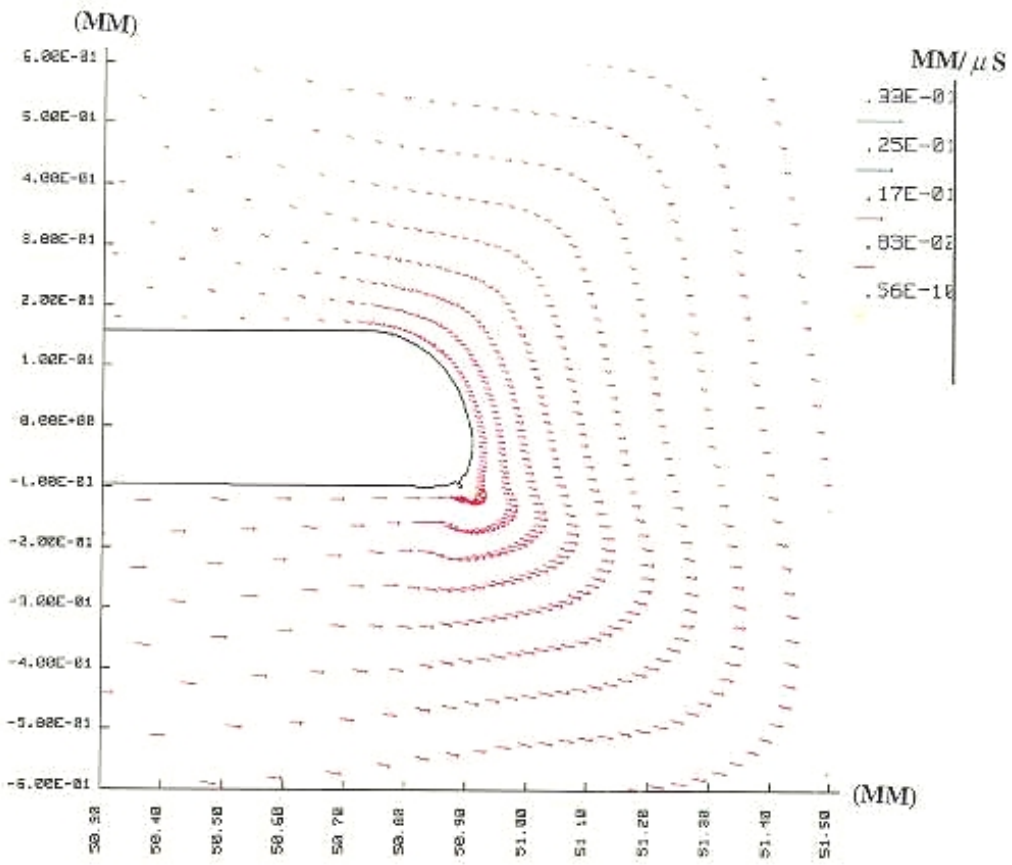

Figure 4b. Velocity Field at t=13 microseconds in the region surrounding the notch-tip. (m=0.6)

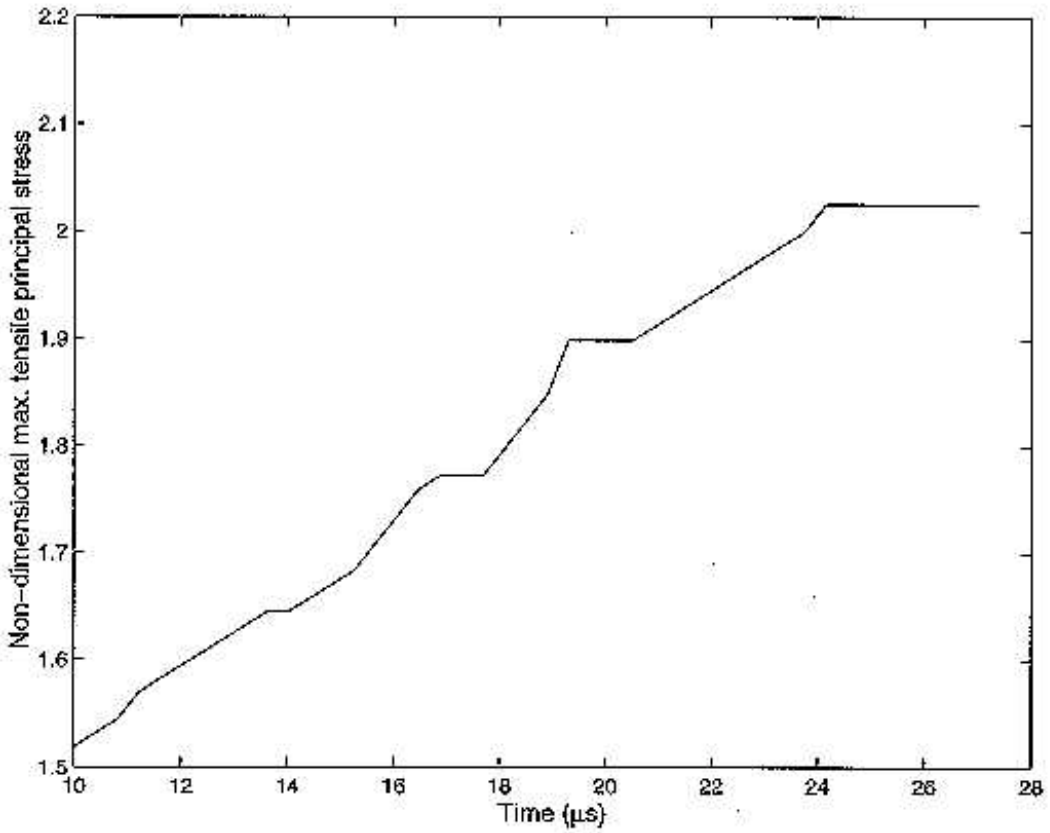

Figure 5. Time-history of the maximum tensile principal stress in the vicinity of the point on the notch surface that makes, in the reference configuration, an angle of 70^0 with the notch-axis (m=0.6)

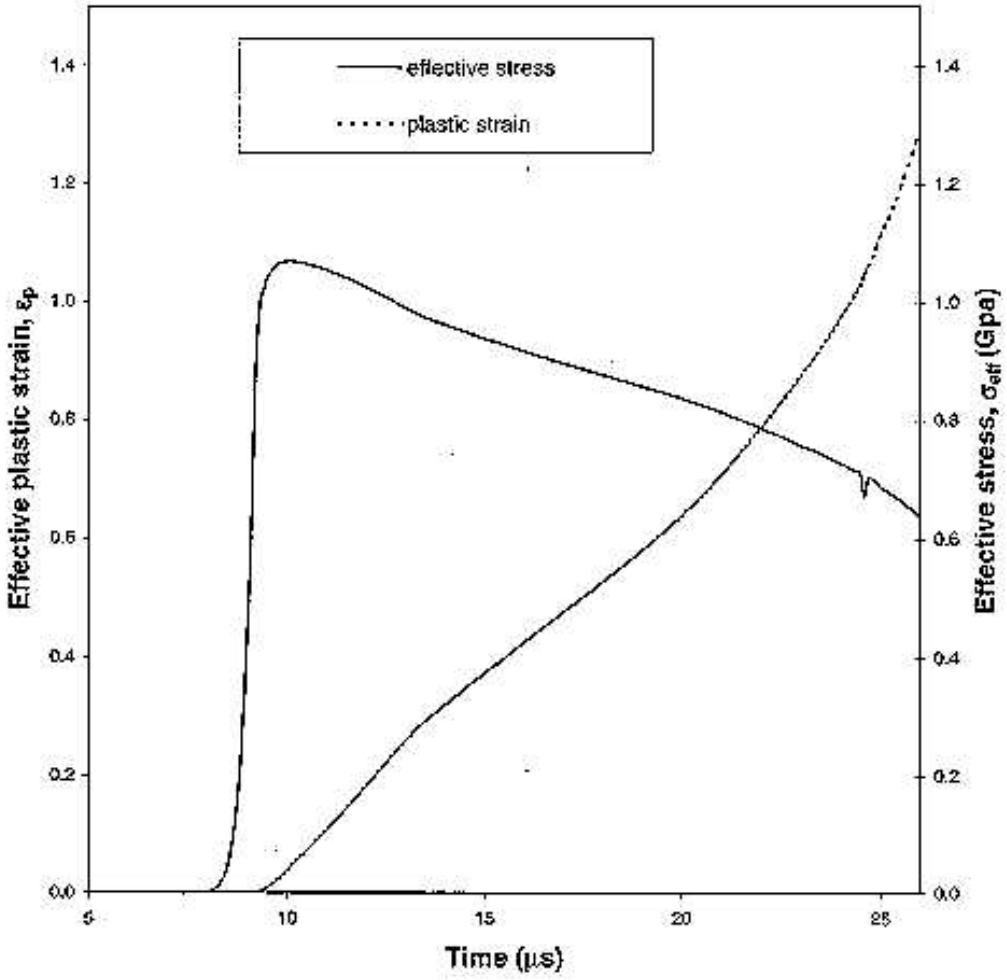

Figure 6a. Time history of the effective plastic strain and the effective stress at a point on the notch surface that makes an angle of $-\ 45^0$ with the notch-axis in the reference configuration.

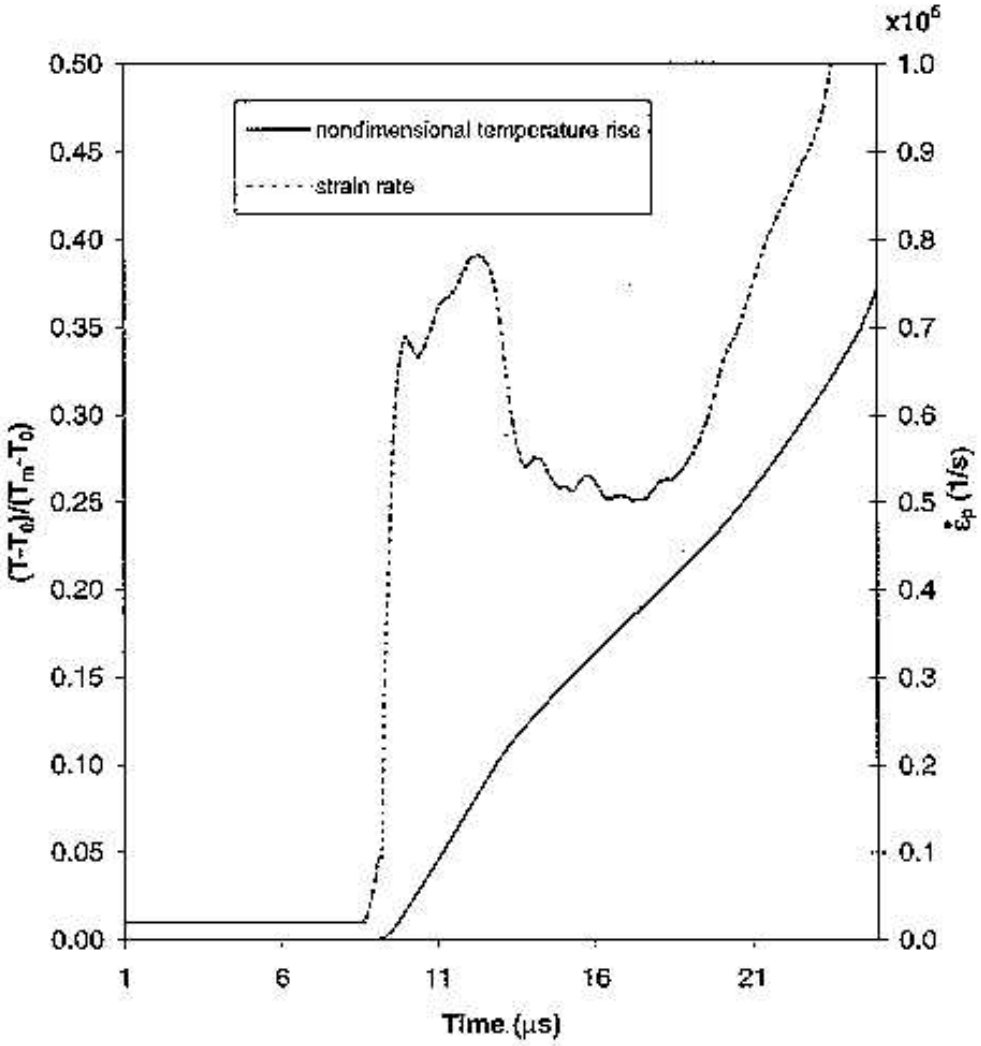

Figure 6b. Time history of the effective plastic strain and the effective stress at a point on the notch surface that makes an angle of $-\ 45^0$ with the notch-axis in the reference configuration.

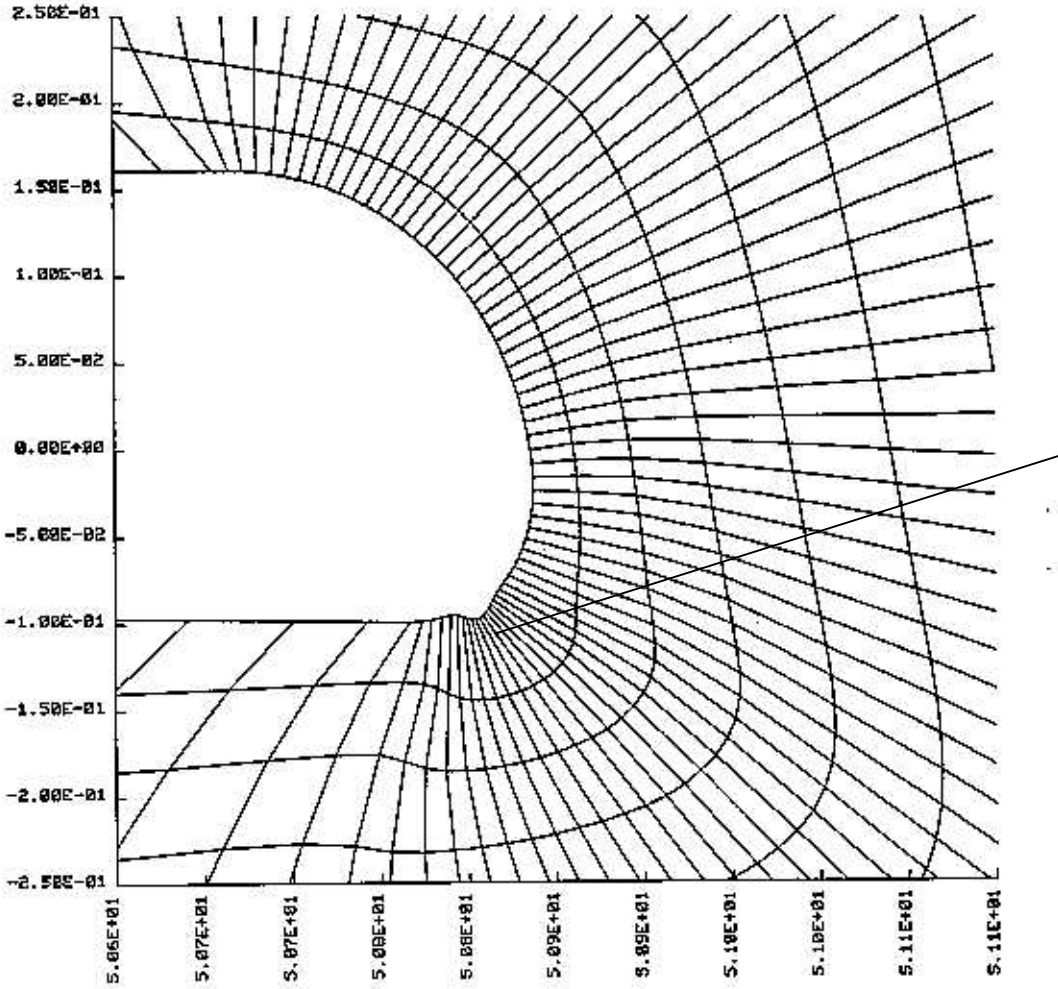

Figure 7a. Deformed shape of the material with m=0.6 near the notch-tip at t=20 μs .

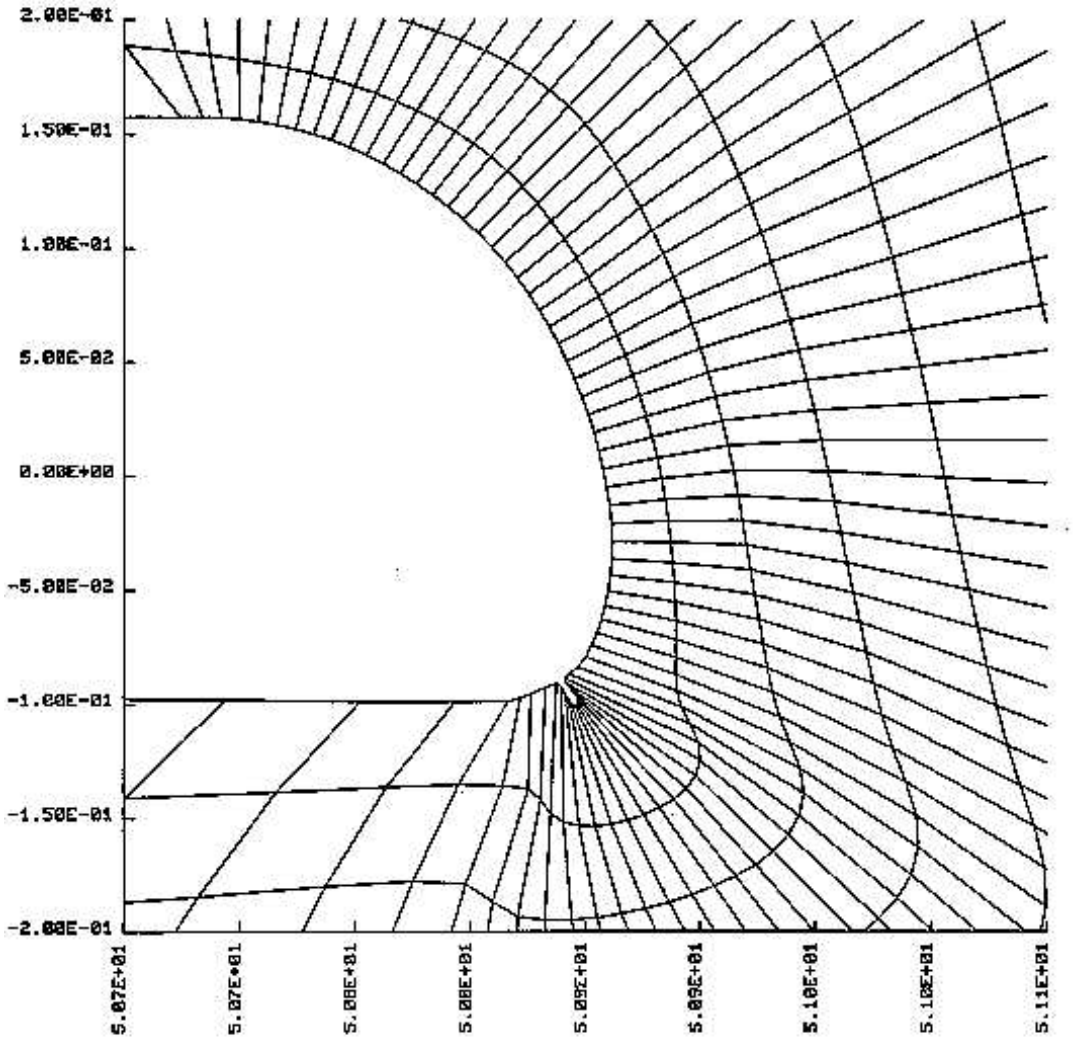

Figure 7b. Deformed shape of the material with m=0.6 near the notch-tip at t=24 μs .

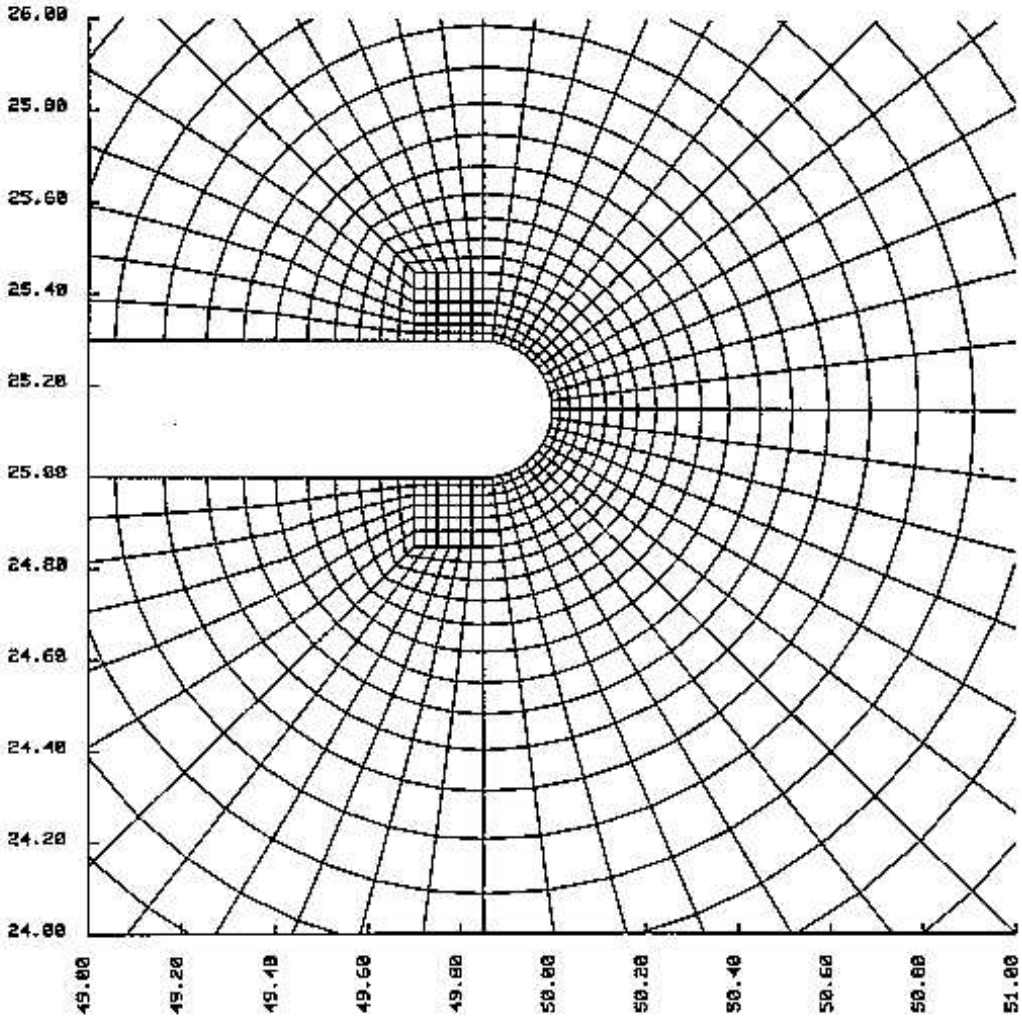

Figure 8. Details of an alternate finite element mesh near the notch-tip.

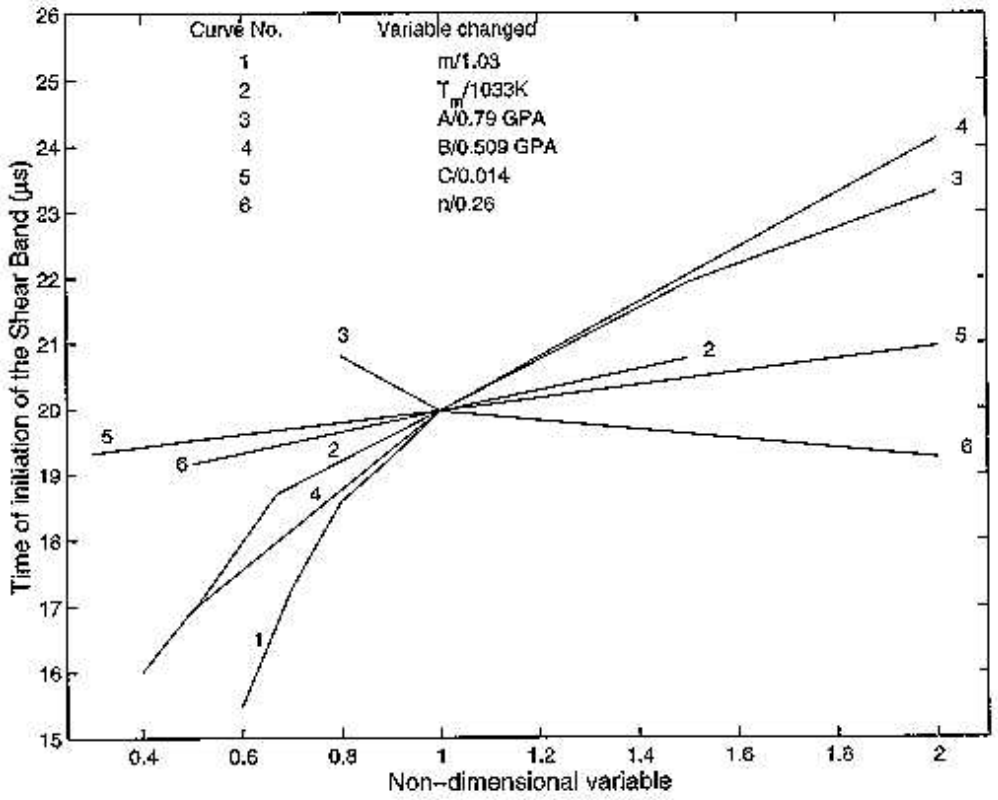

Figure 9a. Effect of different material variables on the time of initiation of a shear band. A shear band is assumed to initiate when the maximum effective plastic strain at any point equals 0.5.

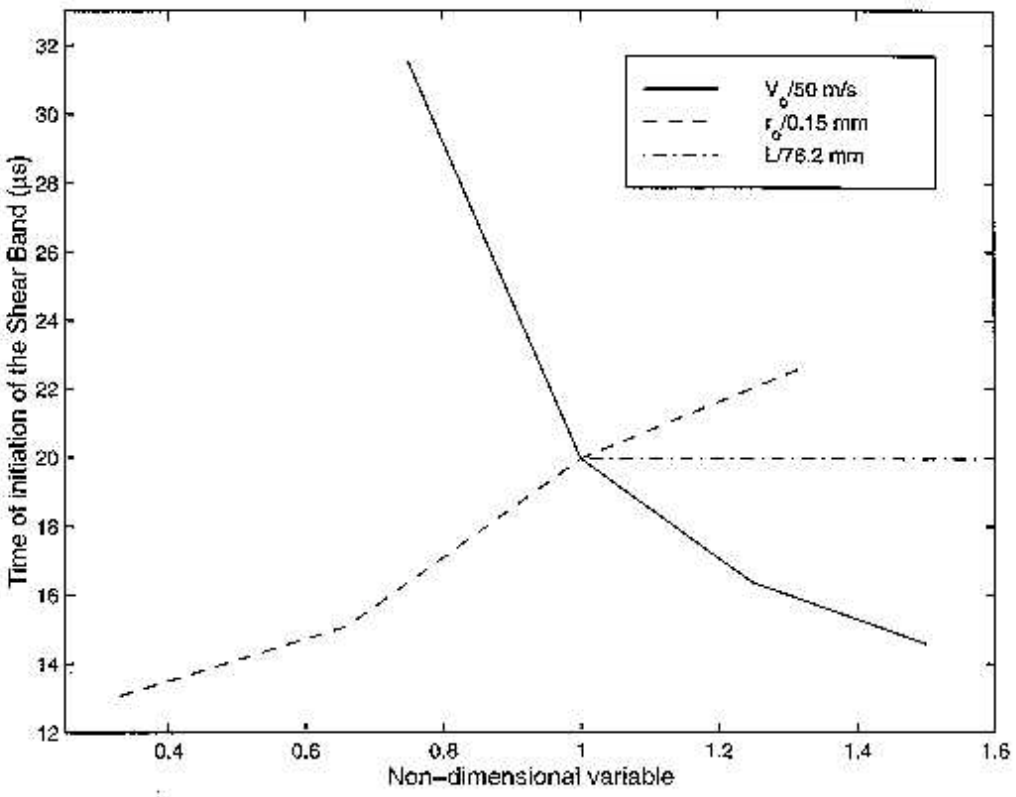

Figure 9b. Effect of impact speed, notch-tip radius and the length of the projectile on the time of initiation of a shear band.

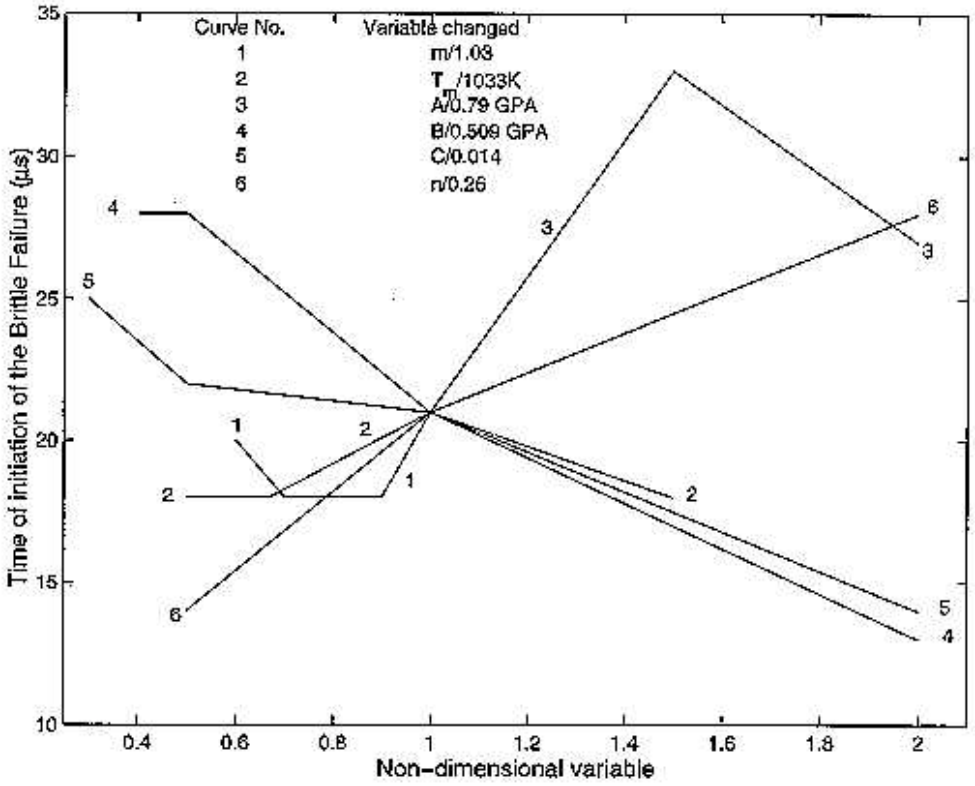

Figure 9c. Effect of material parameters on the time of initiation of brittle fracture. The brittle fracture is assumed to occur when the maximum tensile principal stress at a point equals twice the yield stress of the material in a quasistatic simple tension/compression test.

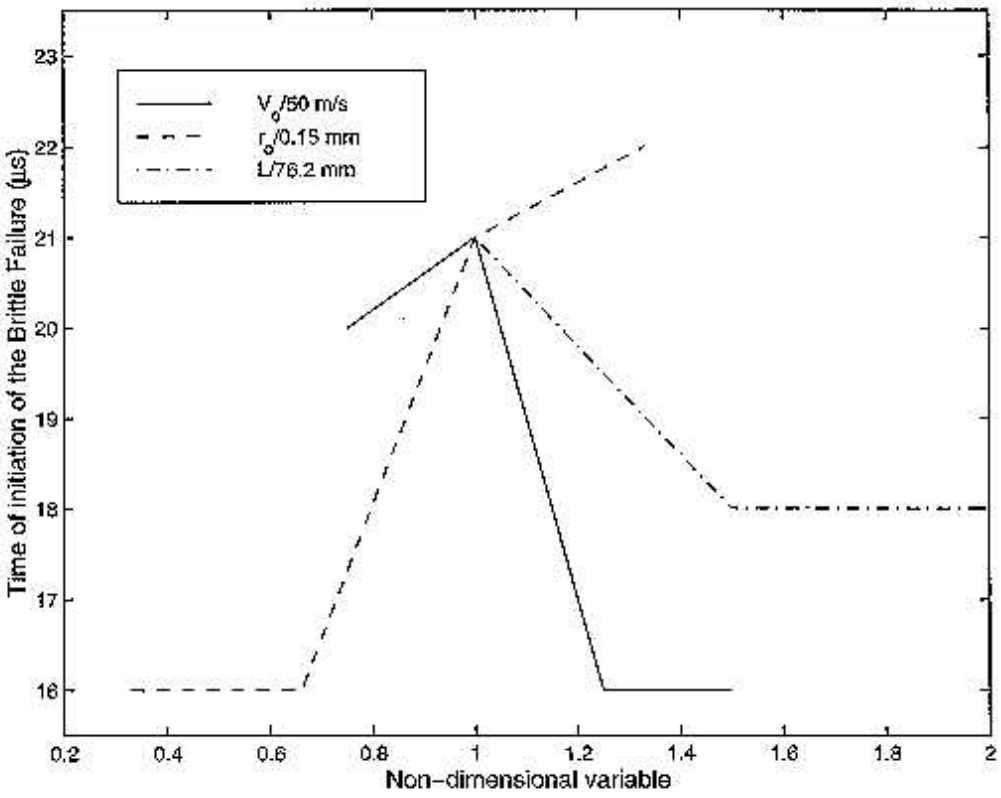

Figure 9d. Effect of impact speed, notch-tip radius and the length of the projectile on the time of initiation of brittle failure.

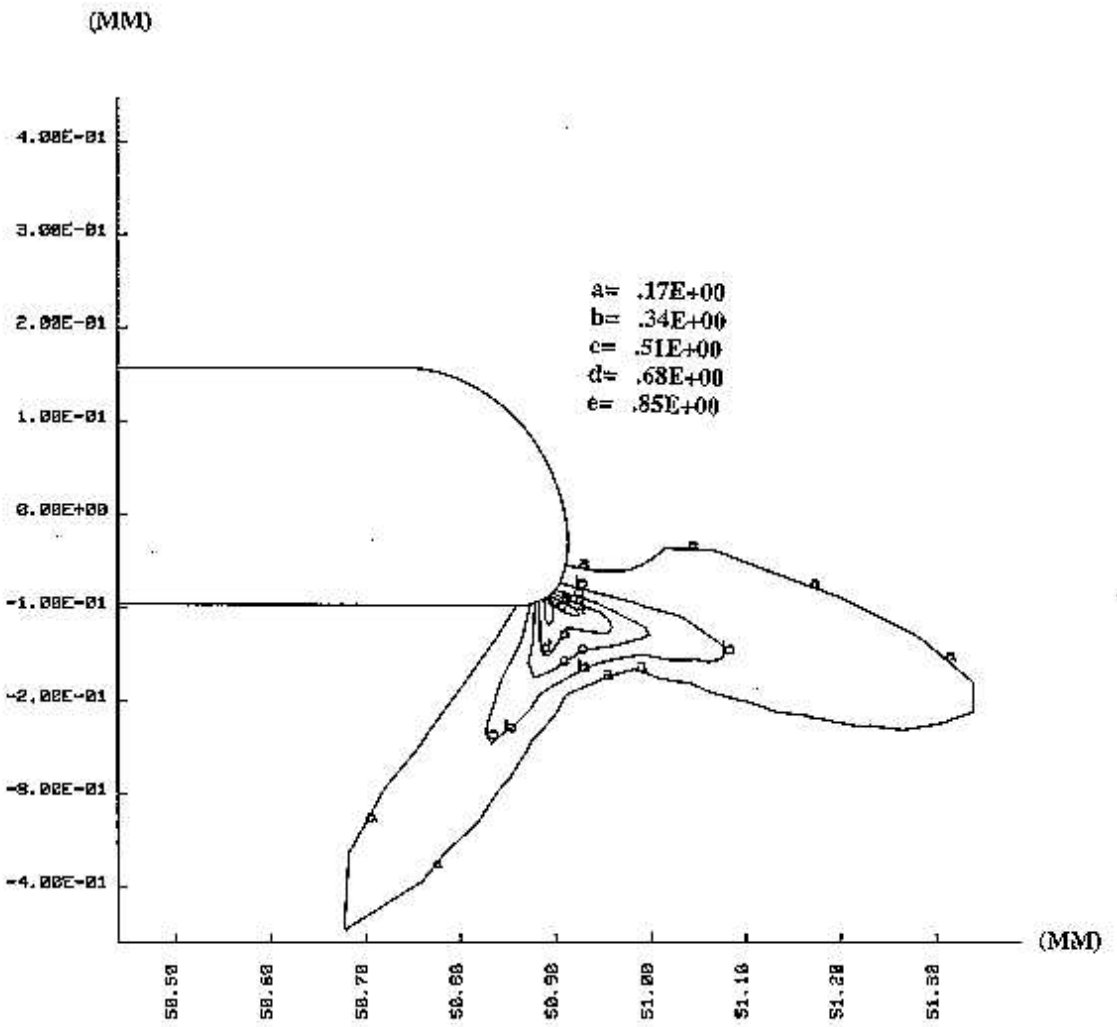

Figure 10a. Contour of the effective plastic strain for m=0.6 when the maximum effective plastic strain at any point near the notch-tip equals 1.0 for at t = $24.25\mu s$.

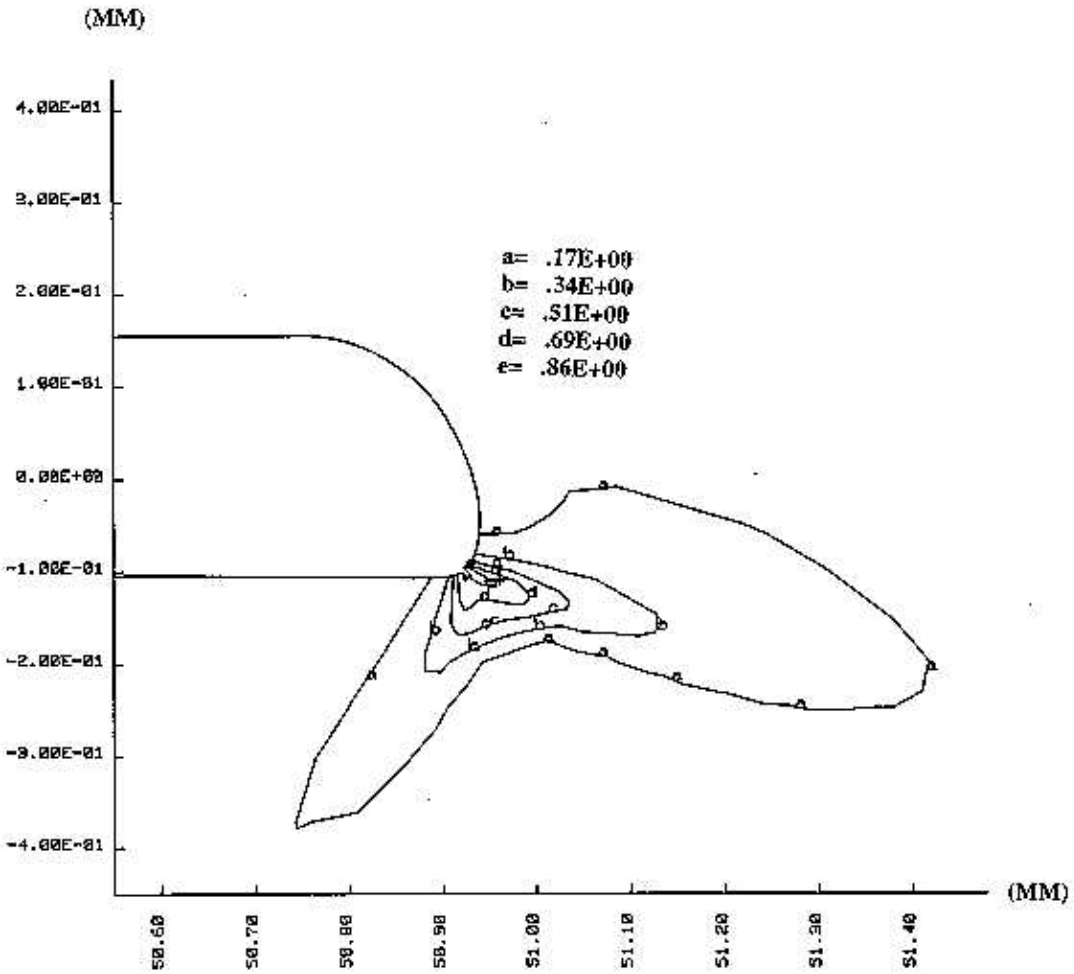

Figure 10b. Contour of the effective plastic strain for m=0.7 when the maximum effective plastic strain at any point near the notch-tip equals 1.0 at t = 27 μs .

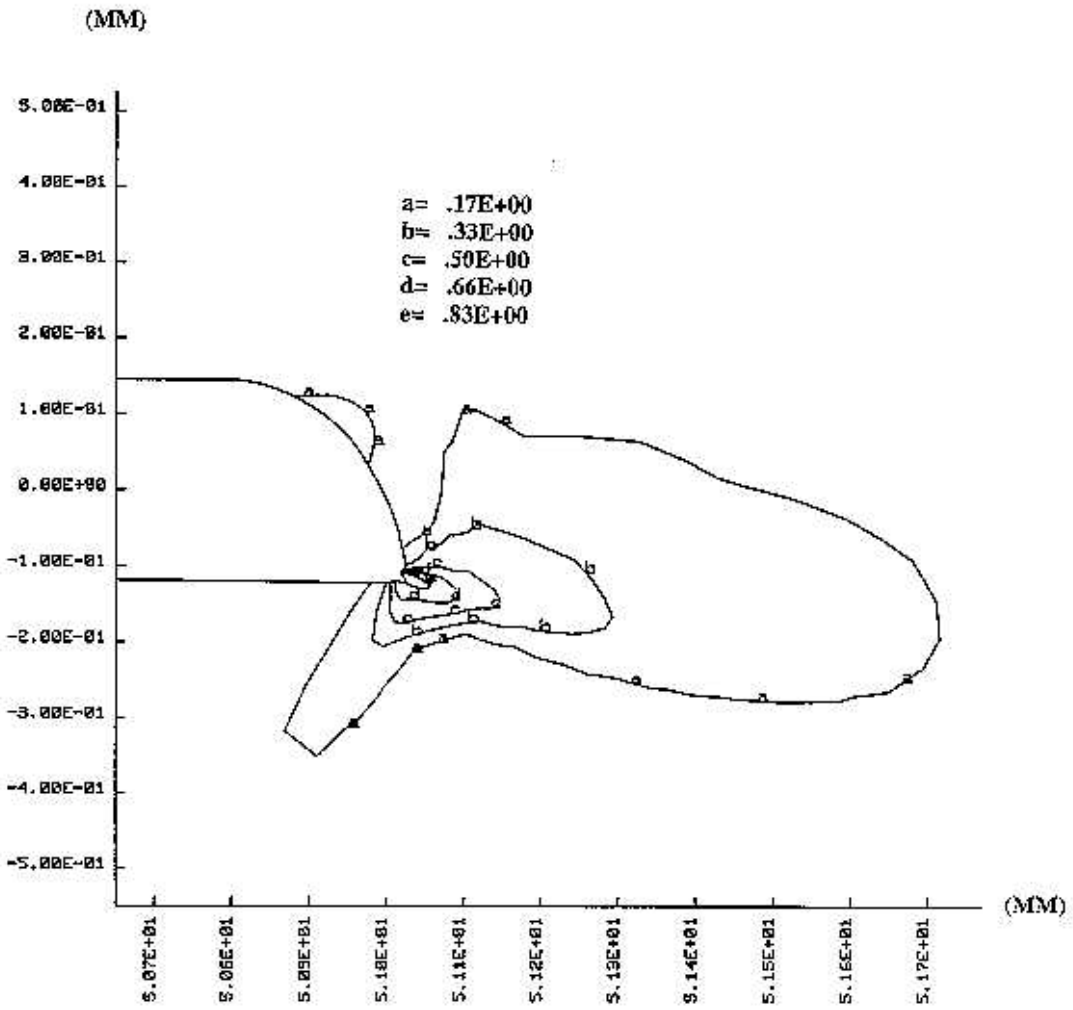

Figure 10c. Contour of the effective plastic strain for m=0.8 when the maximum effective plastic strain at any point near the notch-tip equals 1.0 at t = 31 μs .

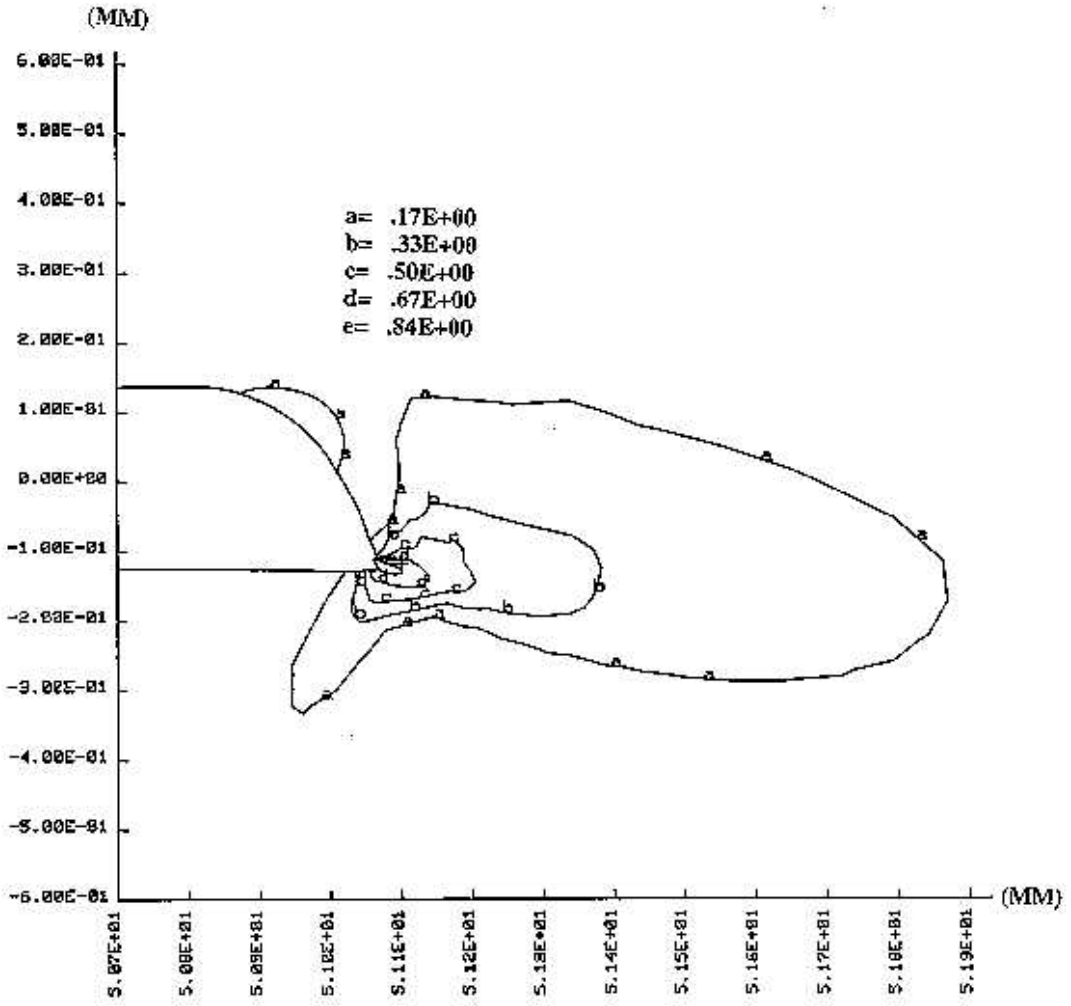

Figure 10d. Contour of the effective plastic strain for m=0.9 when the maximum effective plastic strain at any point near the notch-tip equals 1.0 at t = 33 μs .

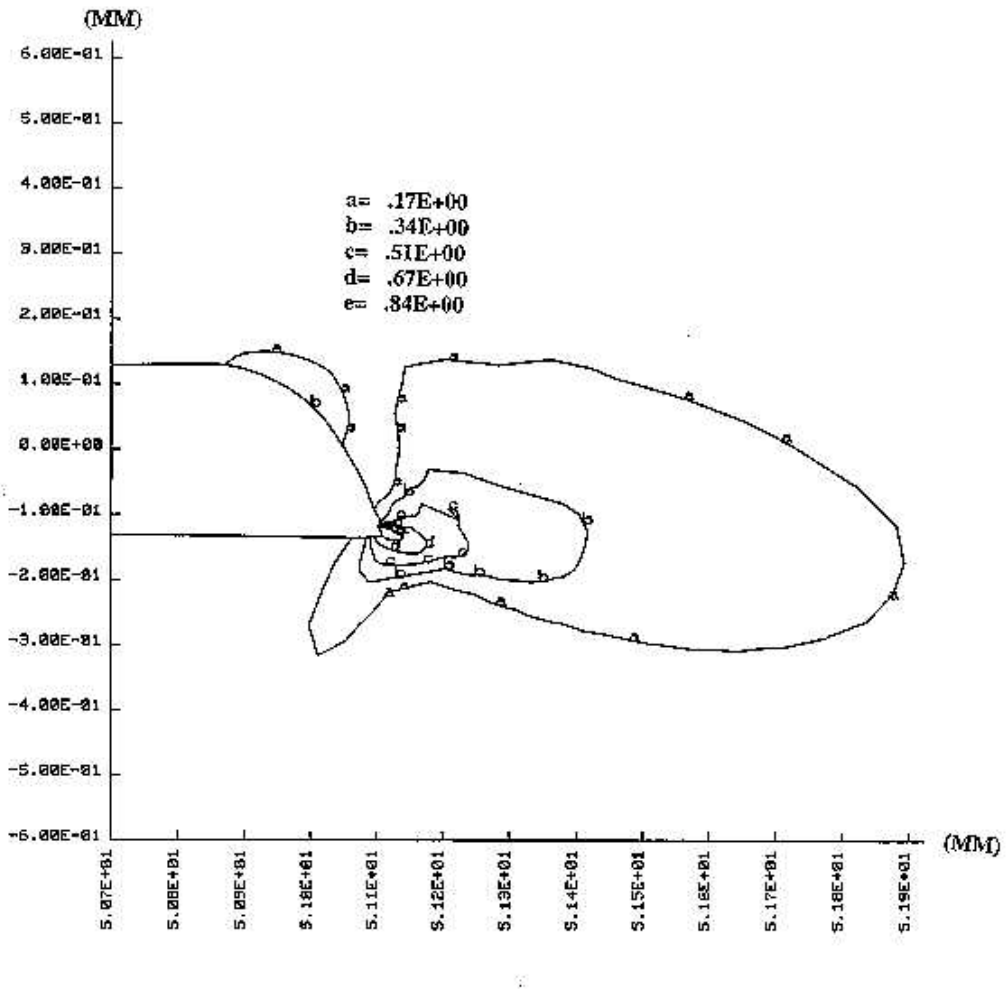

Figure 10e. Contour of the effective plastic strain for m=1.03 when the maximum effective plastic strain at any point near the notch-tip equals 1.0 at t = 35 μs .

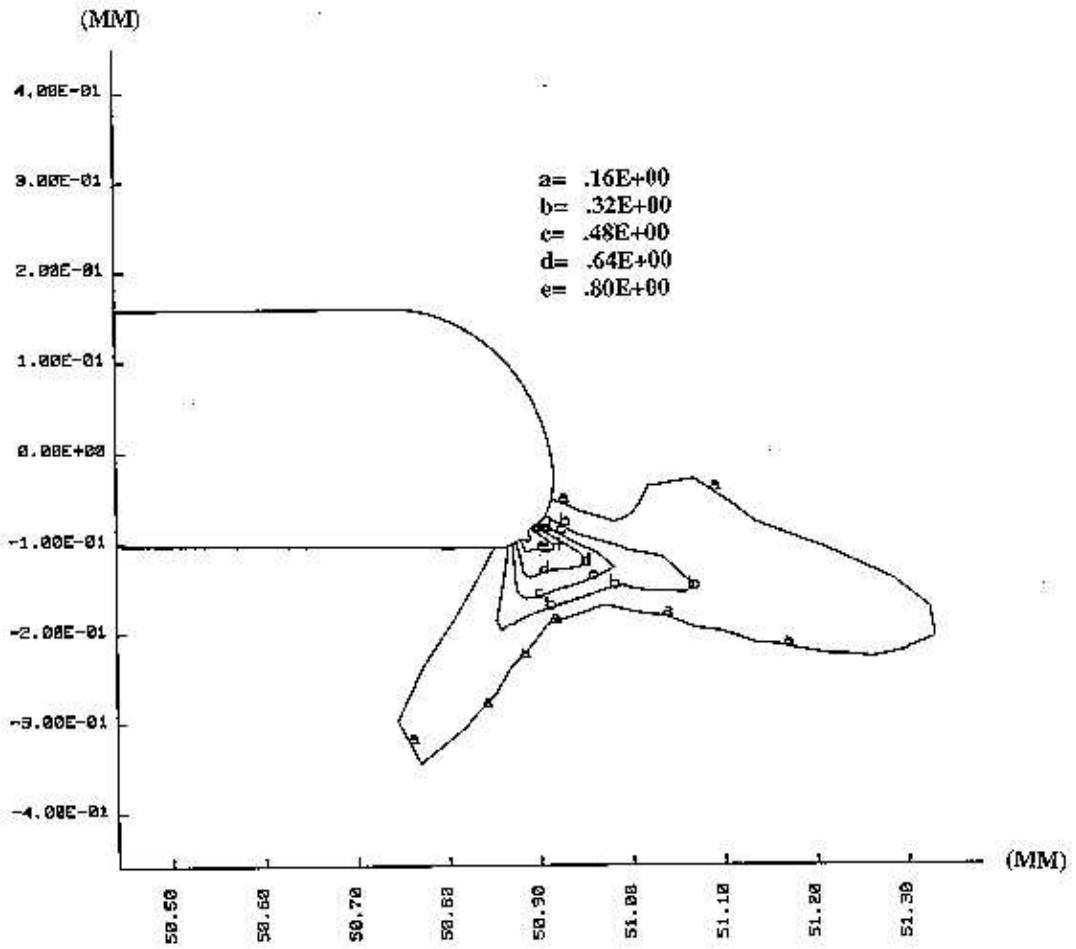

Figure 11a. Contours of the effective plastic strain for different values of T_m when the maximum effective plastic strain at any point near the notch-tip equals 1.0 for T_m =653K at t =24 μs

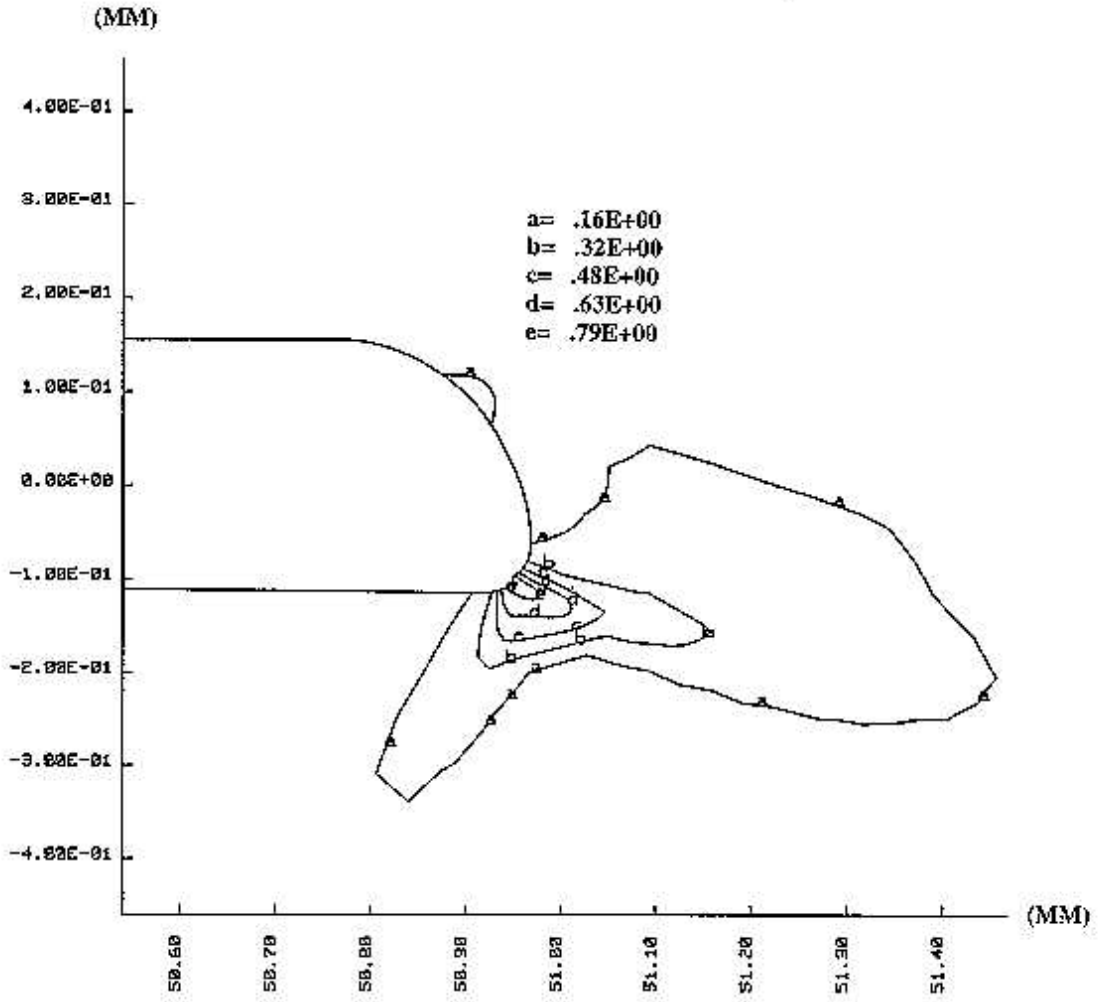

Figure 11b. Contours of the effective plastic strain for different values of T_m when the maximum effective plastic strain at any point near the notch-tip equals 1.0 for T_m =780K at t =28 μs

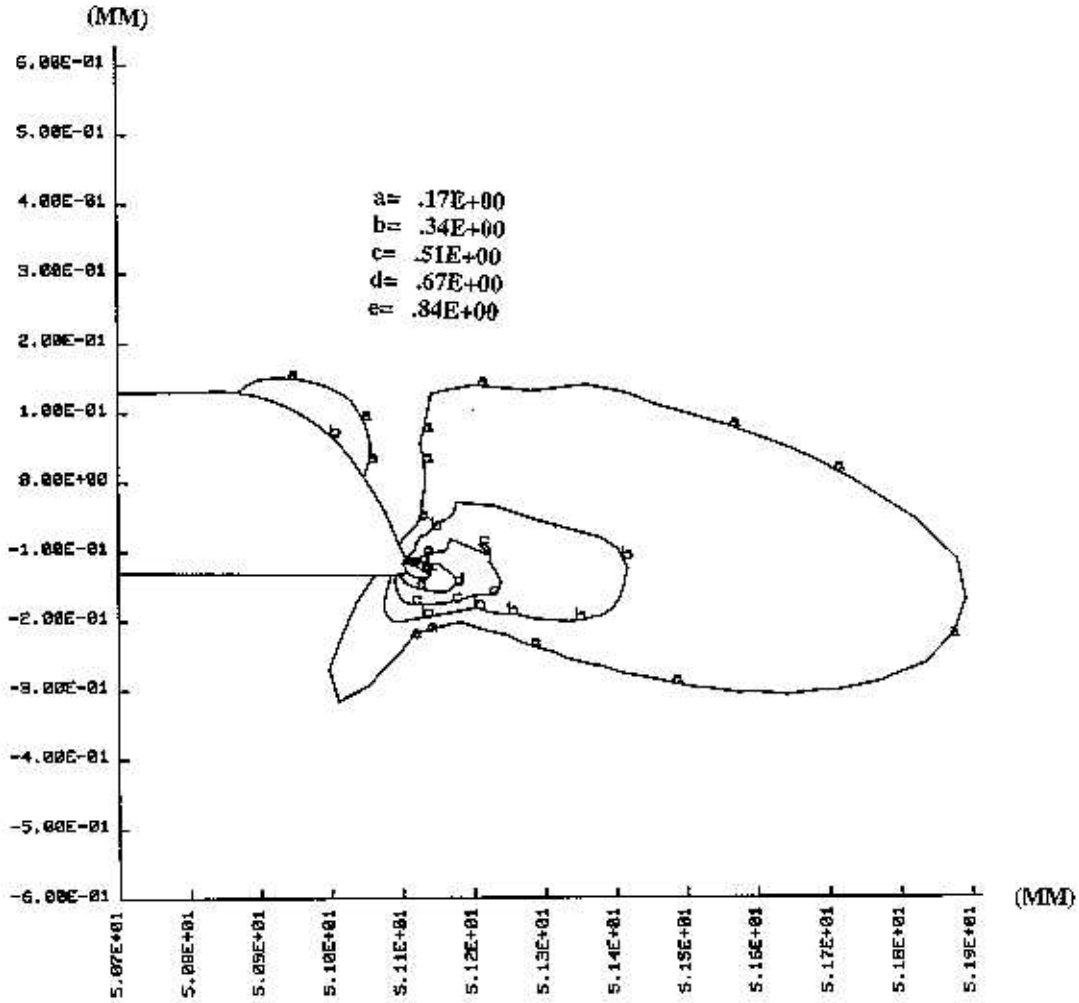

Figure 11c. Contours of the effective plastic strain for different values of T_m when the maximum effective plastic strain at any point near the notch-tip equals 1.0 for T_m =1033K at t =35 μs

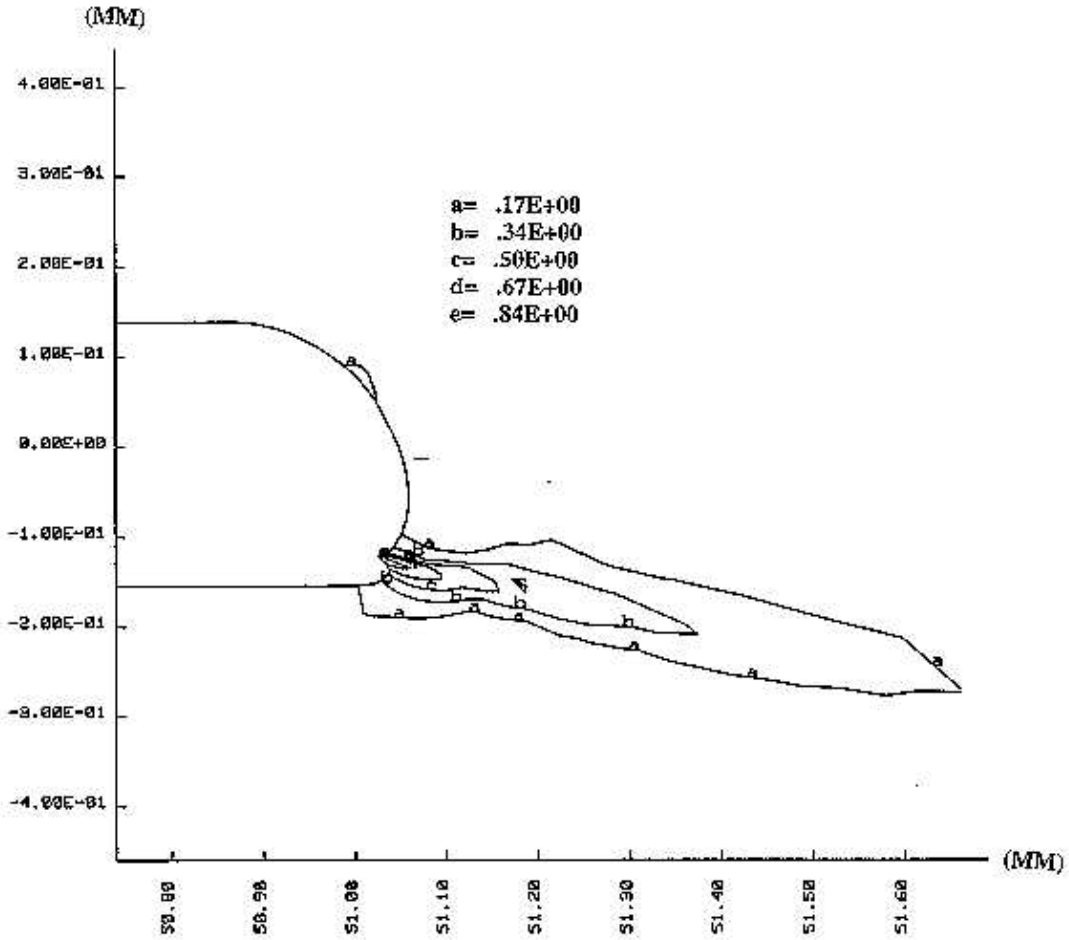

Figure 12a. Contours of the effective plastic strain for A=2.376GPA when the maximum effective plastic strain at any point near the notch -tip equals 1.0 at t = 30.75 μs

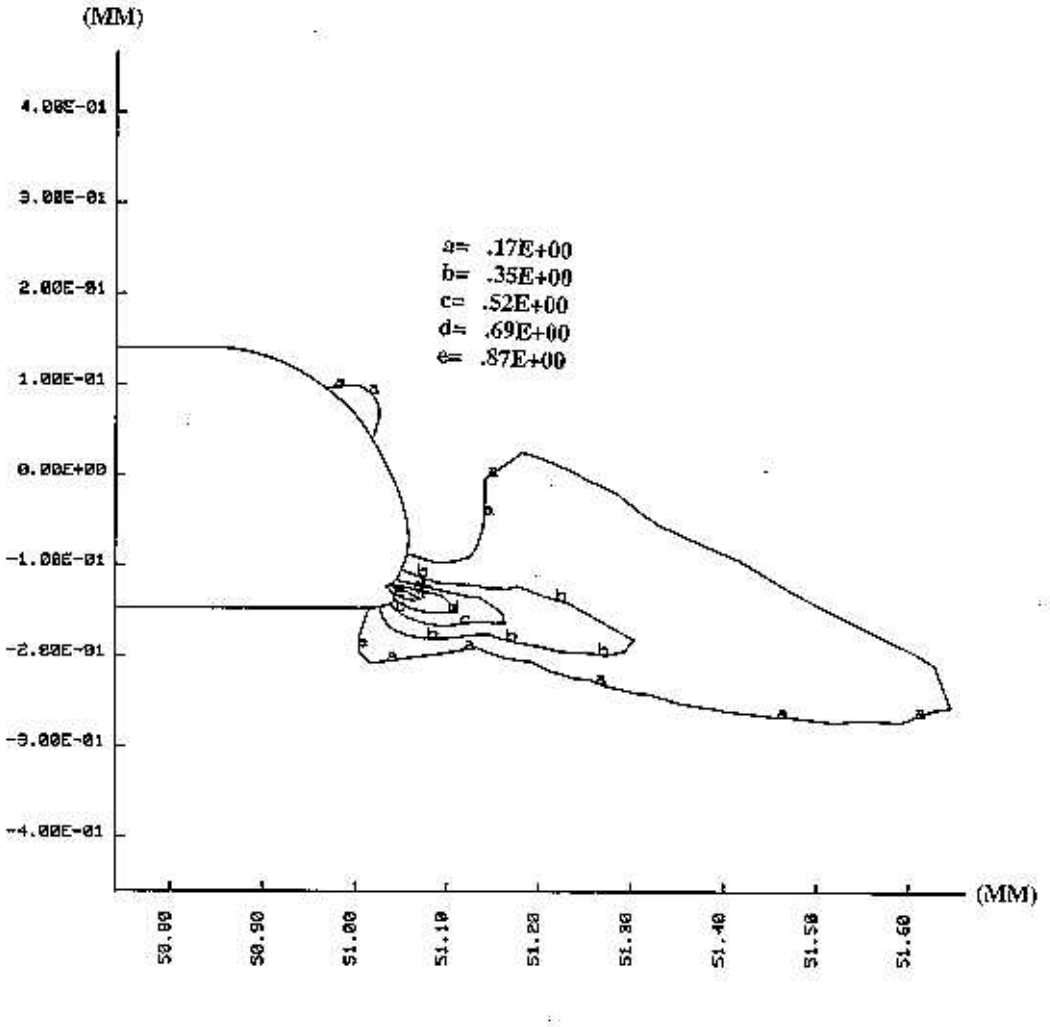

Figure 12b. Contours of the effective plastic strain for A=1.584GPA when the maximum effective plastic strain at any point near the notch -tip equals 1.0 at t = 31 μs

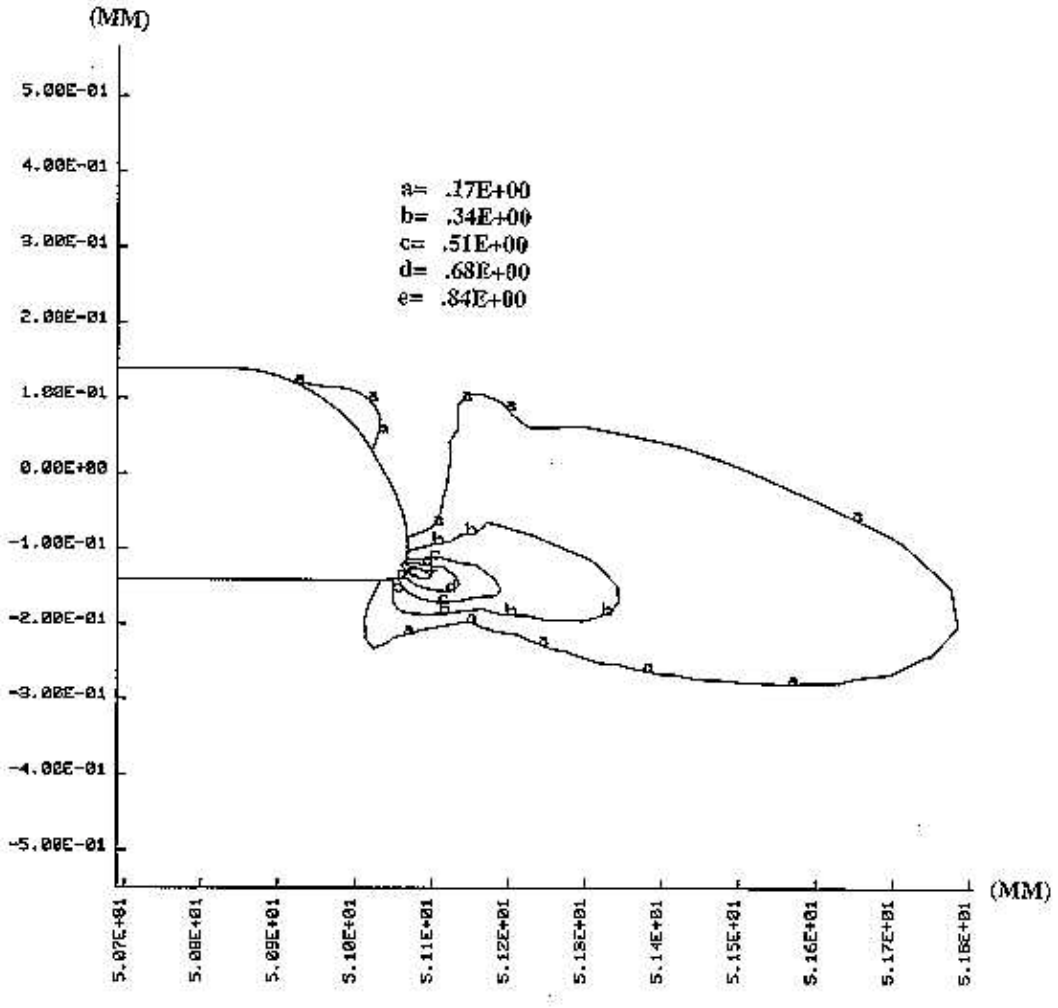

Figure 12c. Contours of the effective plastic strain for A=1.18GPA when the maximum effective plastic strain at any point near the notch -tip equals 1.0 at t = 32 μs

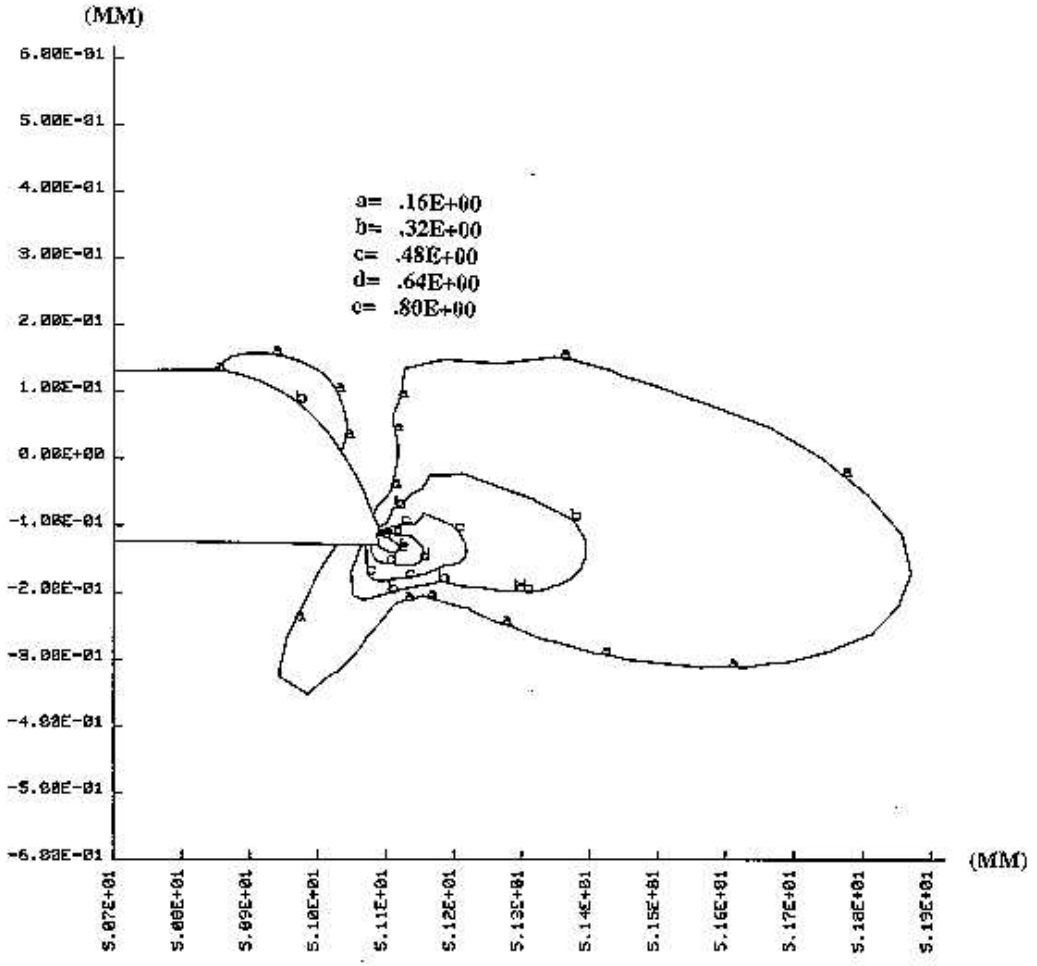

Figure 12d. Contours of the effective plastic strain for A=0.63GPA when the maximum effective plastic strain at any point near the notch -tip equals 1.0 at t = 36 μs

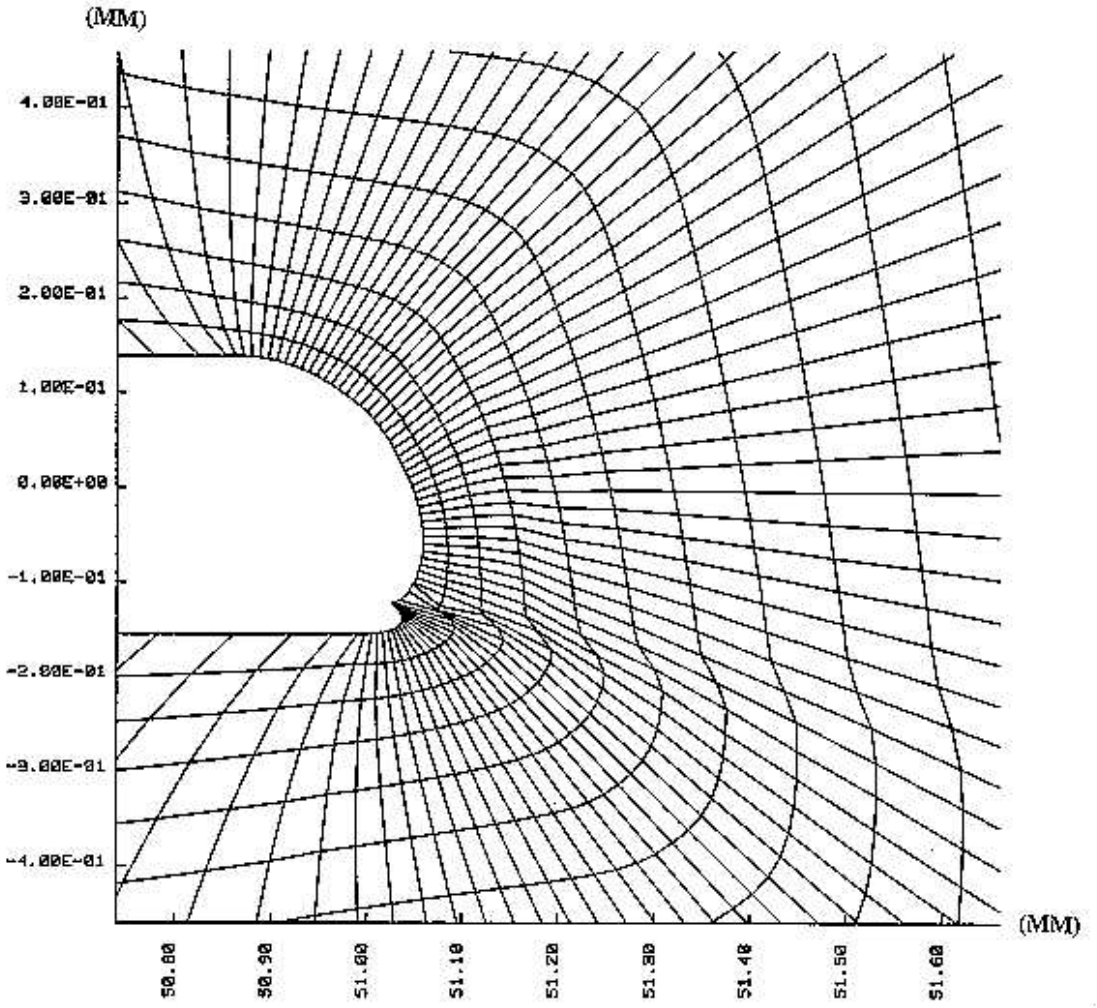

Figure 13a. The deformed mesh near the notch surface for A=2.376GPA at t = 30.75 μs .

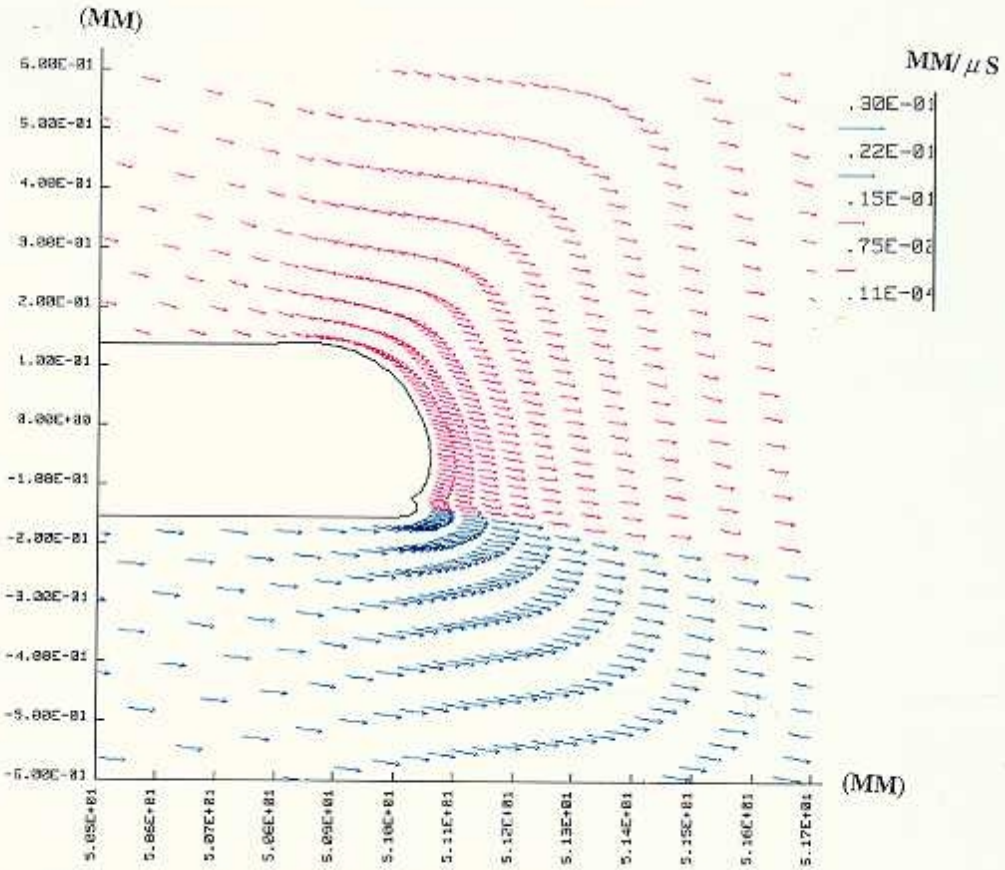

Figure 13b. Velocity field near the notch surface for A=2.376GPA at t = 30.75 μs .

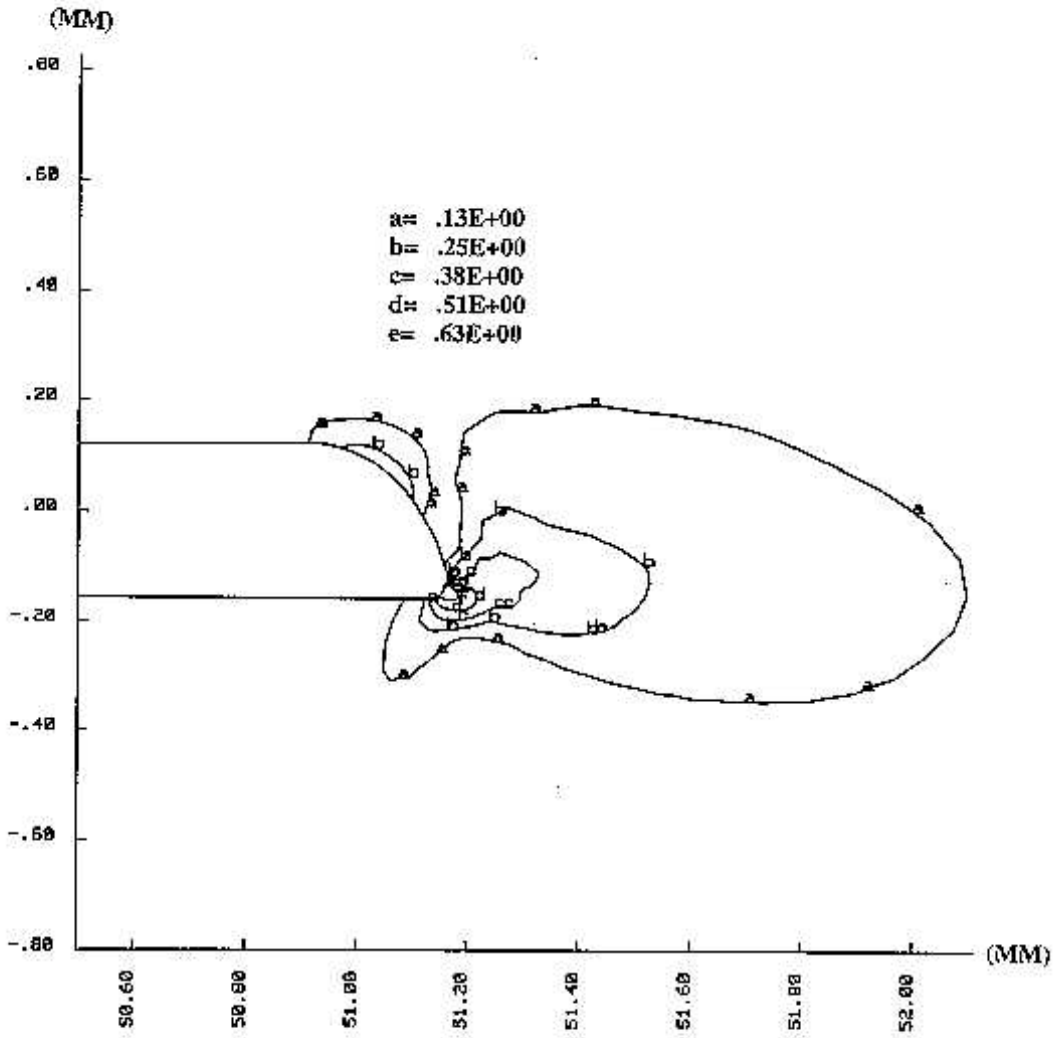

Figure 14a. Contours of the effective plastic strain at t=38 μs for material with B = 1.018GPA.

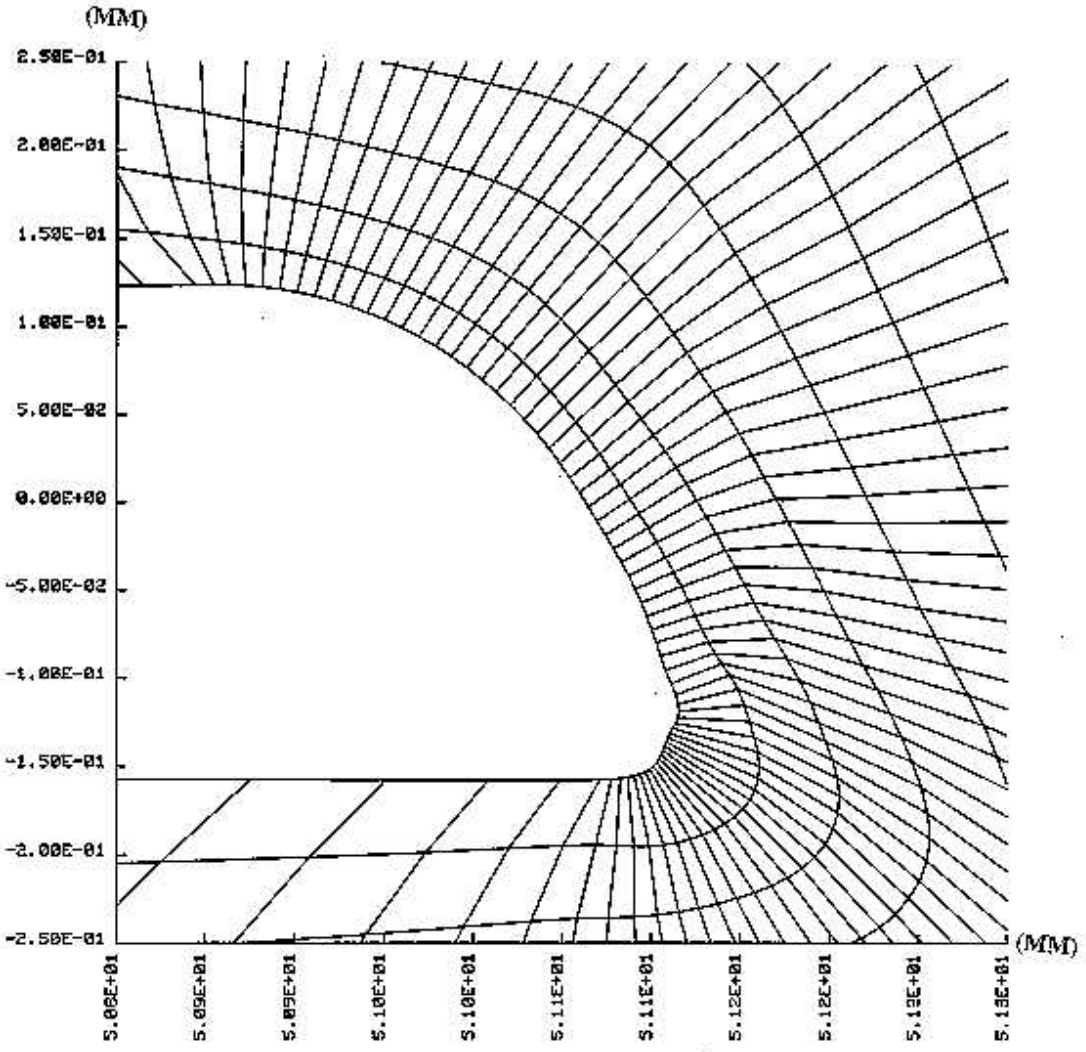

Figure 14b. Deformed notch-tip at t=38 μs for a material with B = 1.018GPA.

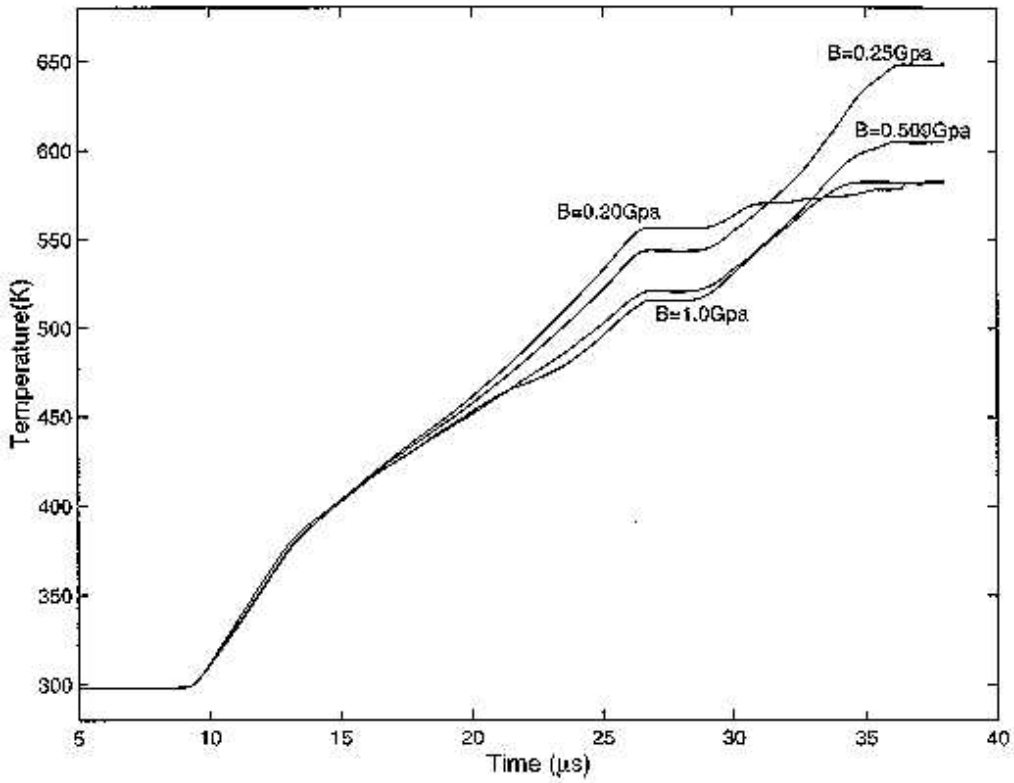

Figure 15a. Time history of the temperature in element E (see Fig. 7b for its location) for four values of B.

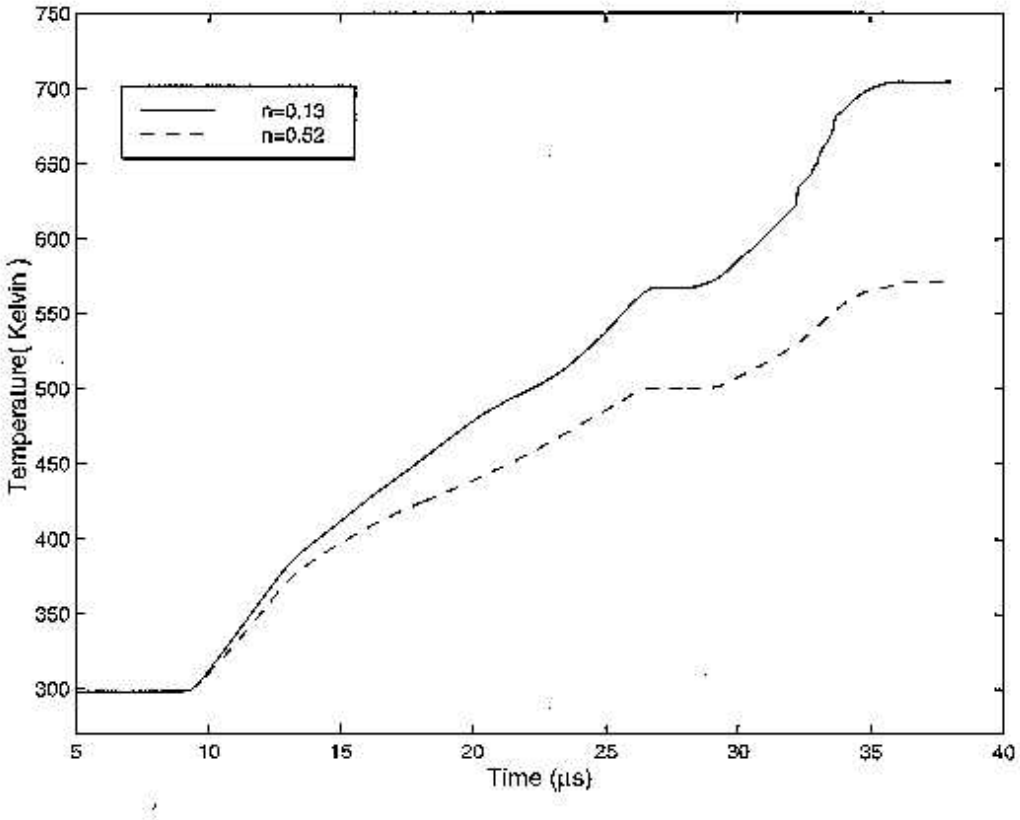

Figure 15b. Time history of the temperature in element E (see Fig. 7b for its location) for two values of n.

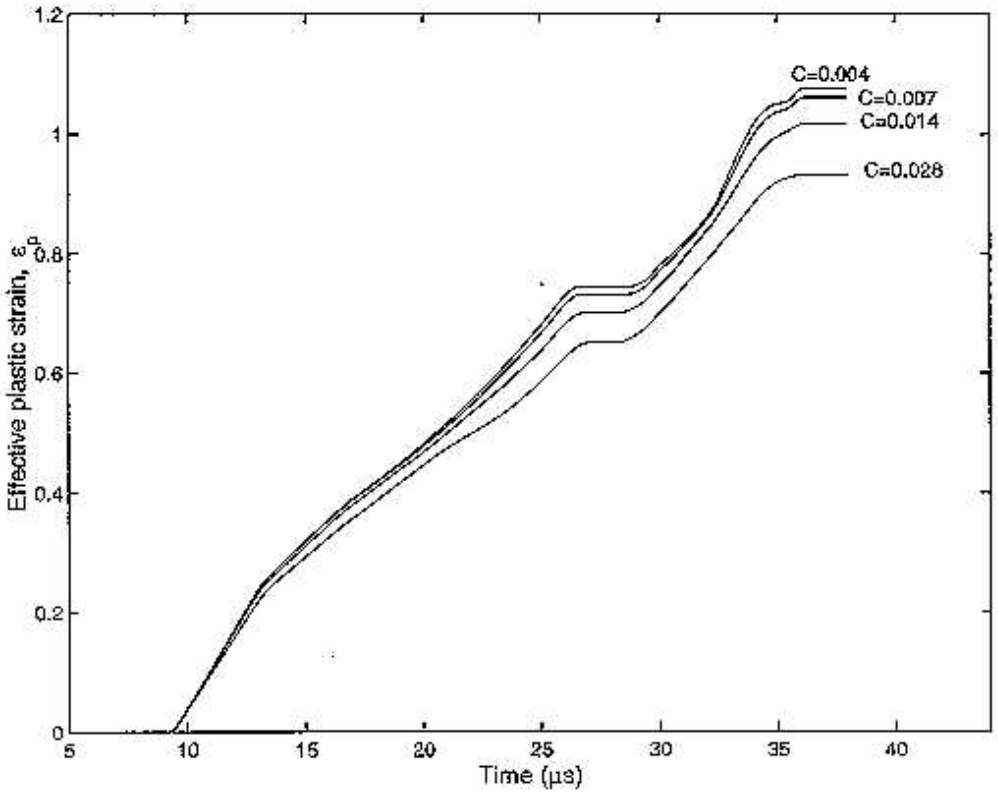

Figure 16. Time history of the evolution of the effective plastic strain in element E (see Fig. 7b for its location) for C = 0.004, 0.007, 0.014 and 0.028.

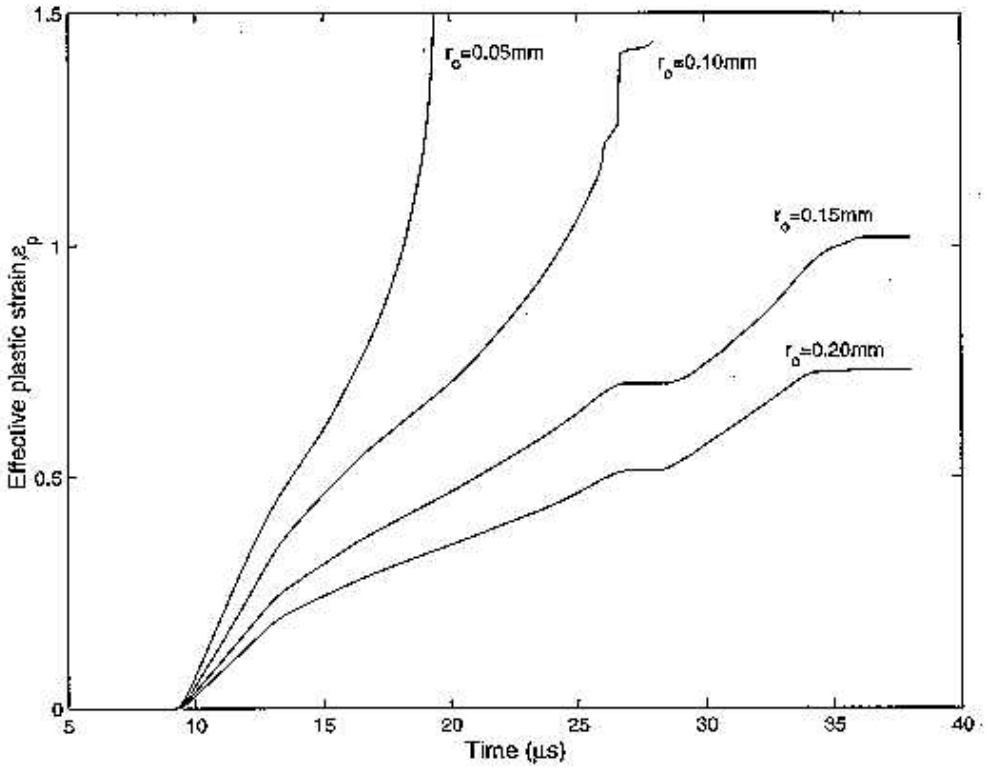

Figure 17a. Time history of the effective plastic strain for element E (see Fig. 7b for its location) for different values of the notch-tip radius, r_0.

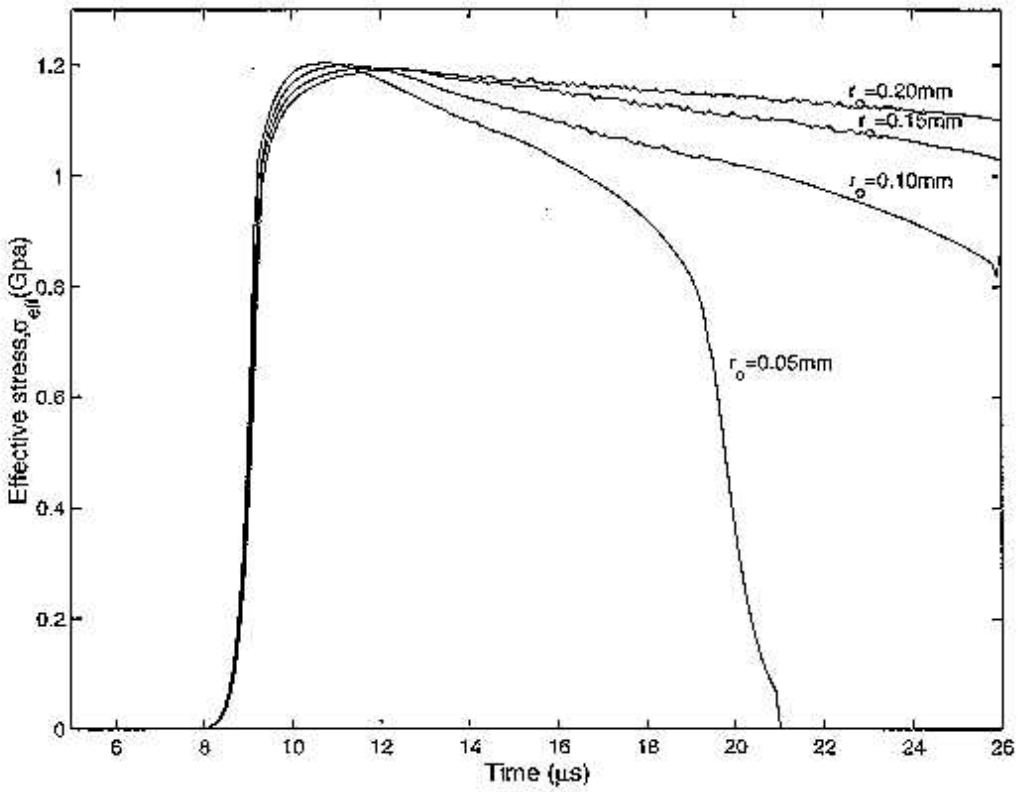

Figure 17b. Time history of the effective stress for element E (see Fig. 7b for its location) for different values of the notch-tip radius, r_0.

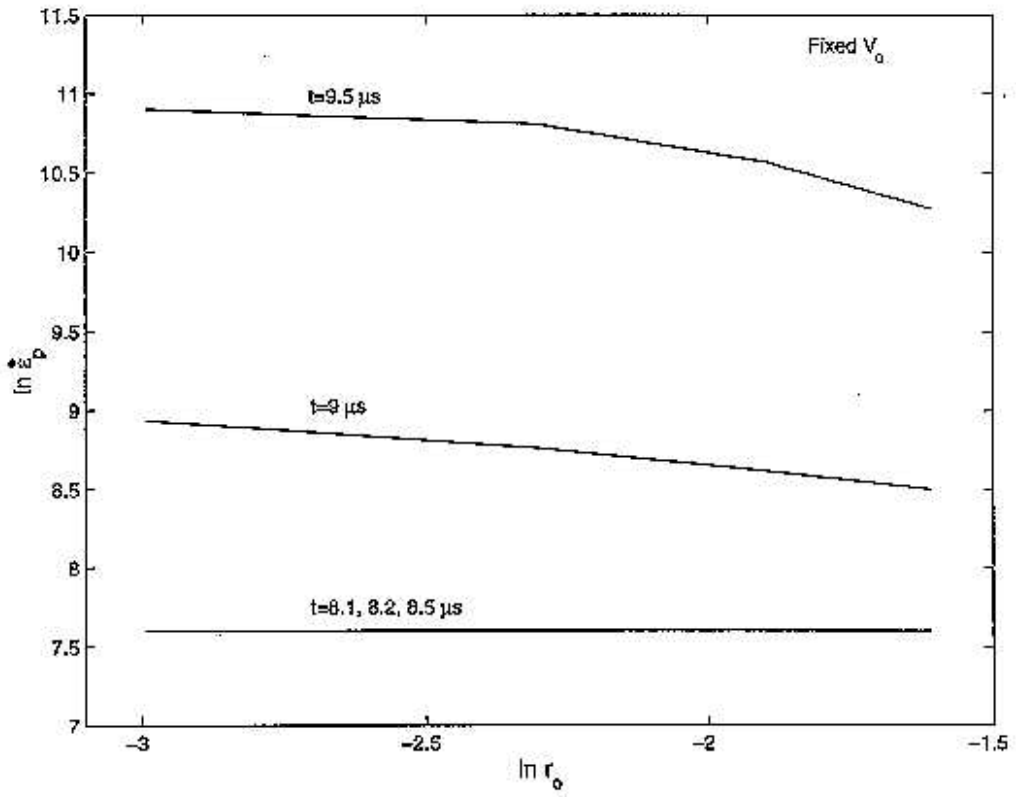

Figure 17c. Variation of ln $\dot{\varepsilon}_p$ with ln r_0 at t=8.1, 9 and 9.5 μs .

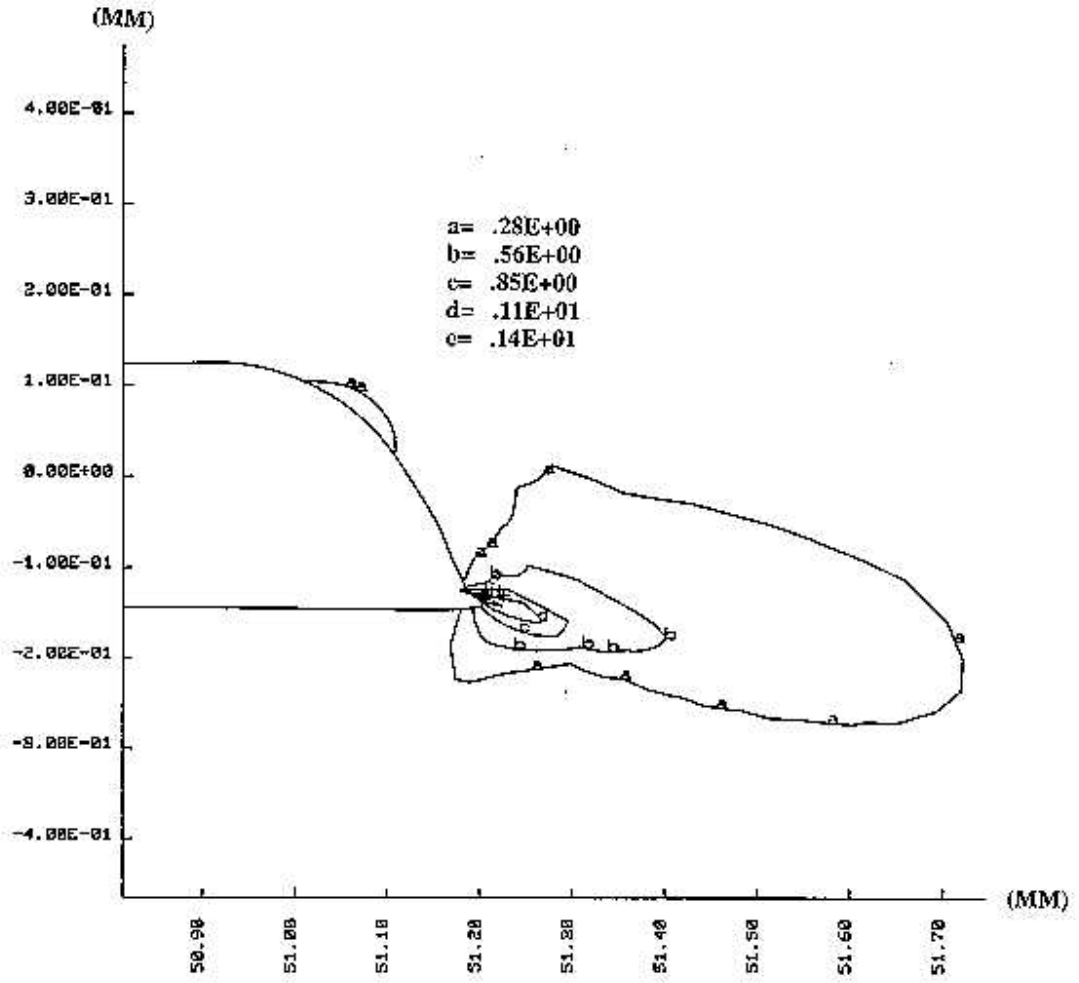

Figure 18a. Contours of the effective plastic strain at t = 40 μs for the 100m long projectile.

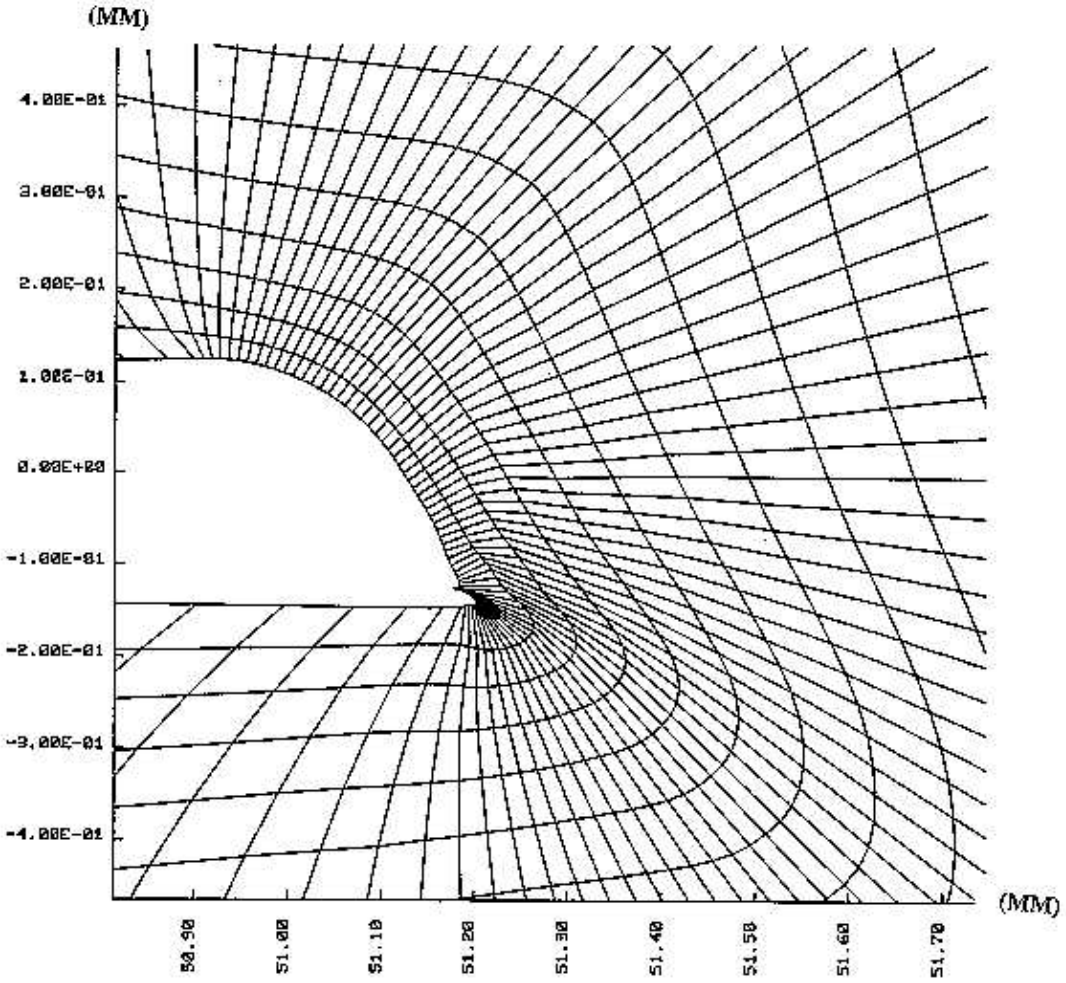

Figure 18b. Deformed mesh near the notch surface of at t = 40 μs for the 100mm long projectile.

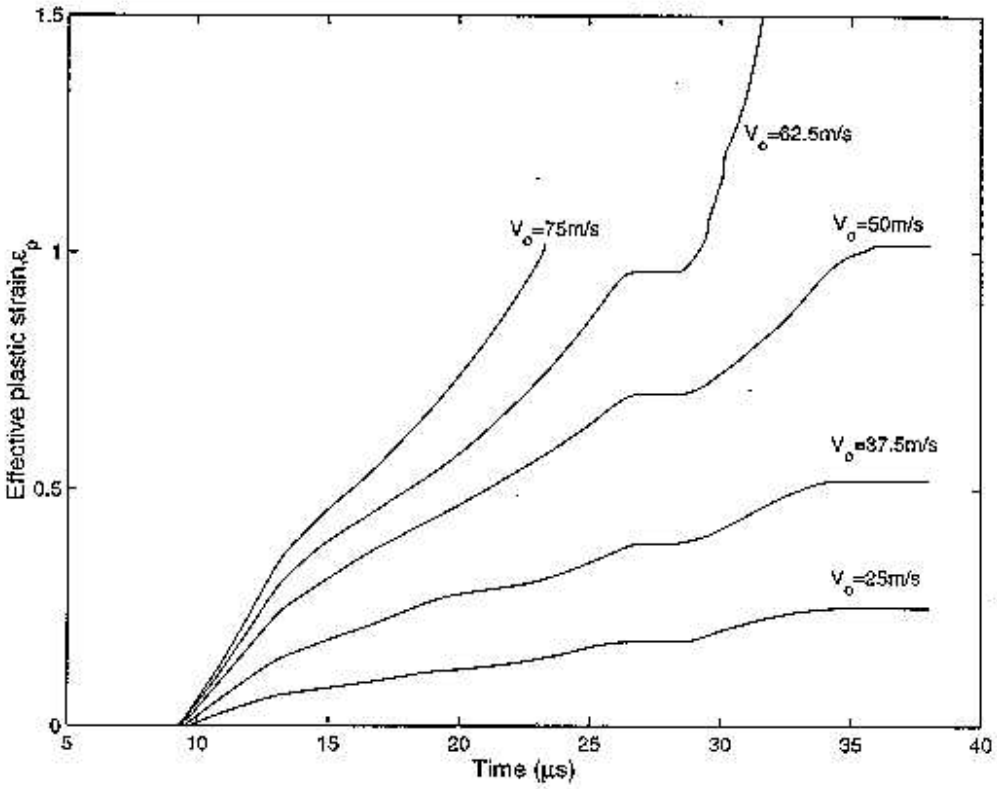

Figure 19a. Time history of the effective plastic strain for different values of the impact velocity, V_0

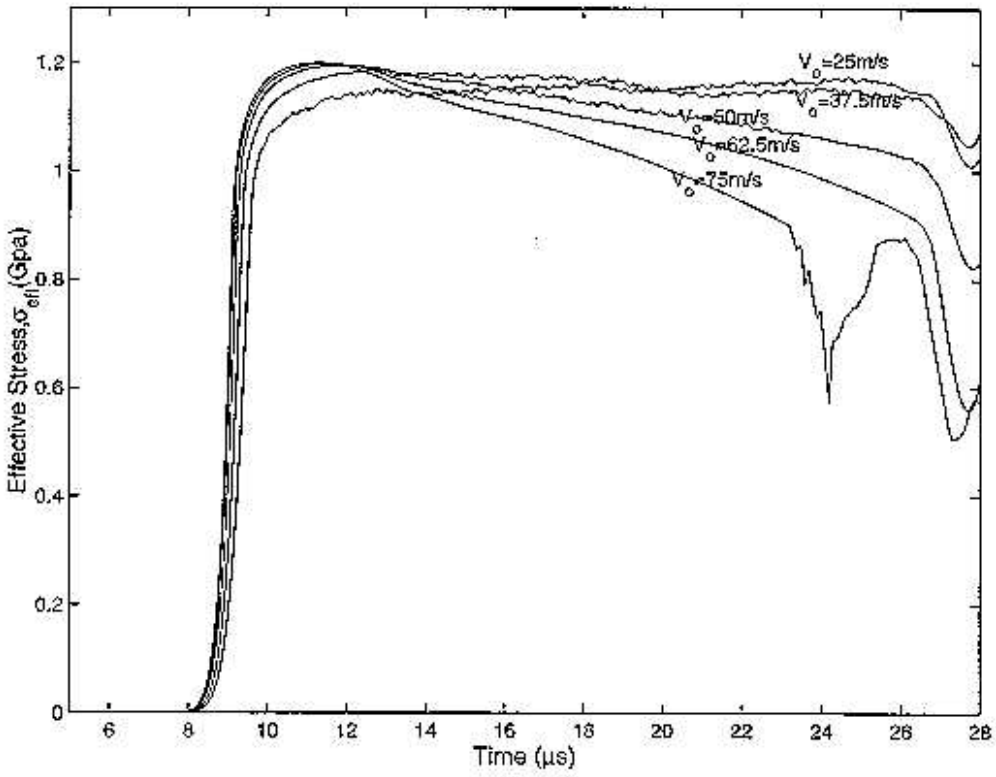

Figure 19b. Time history of the effective stress for different values of the impact velocity, V_0

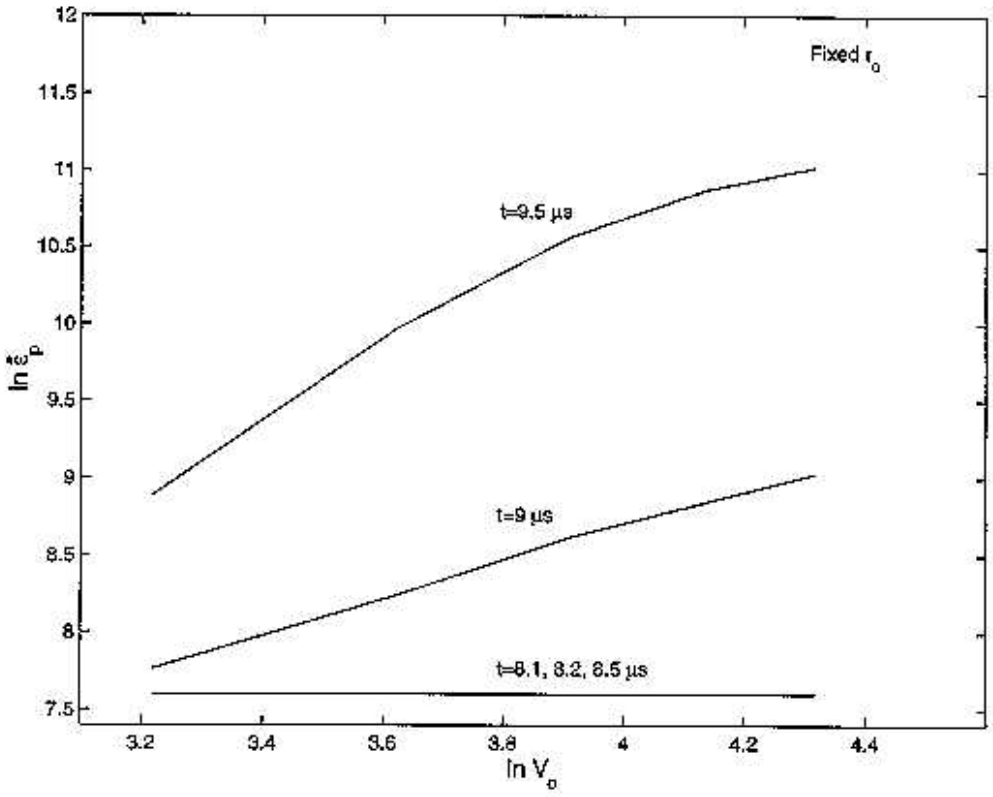

Figure 19c. Variation of $\ln \dot{\varepsilon}_p$ with $\ln V_0$ at t=8.1, 9 and 9.5 μs .

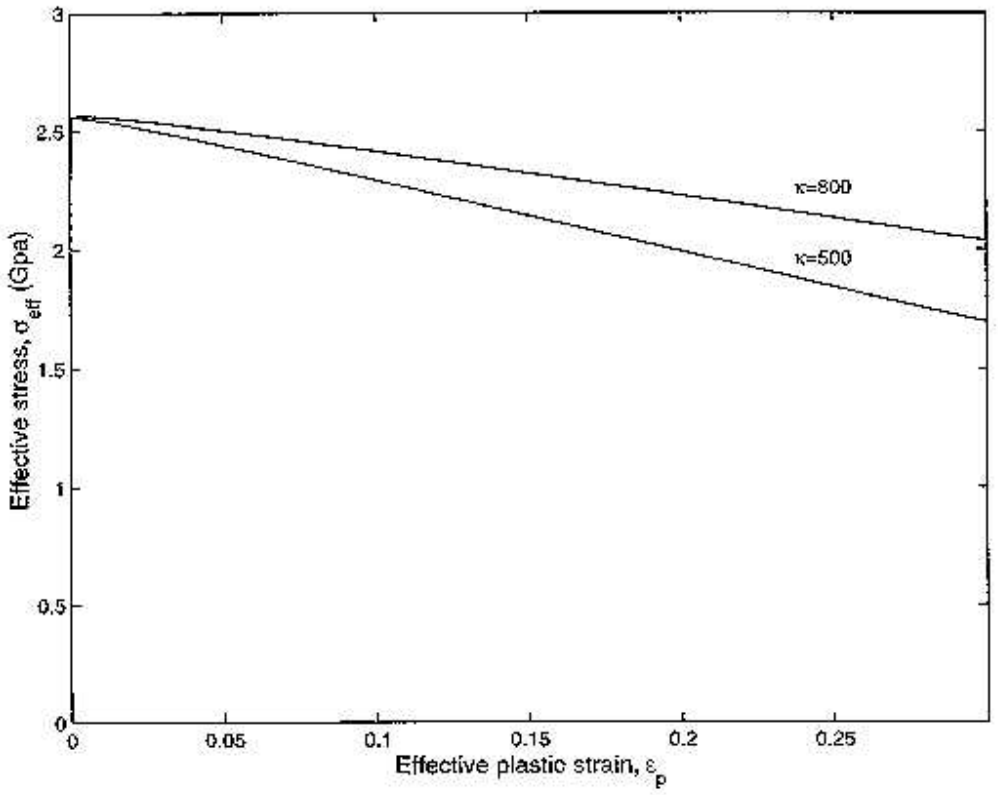

Figure 20a. Effective stress vs. effective plastic strain for simple shearing deformations of a C-300 steel at a strain -rate of $5x\,10^4$ /s.

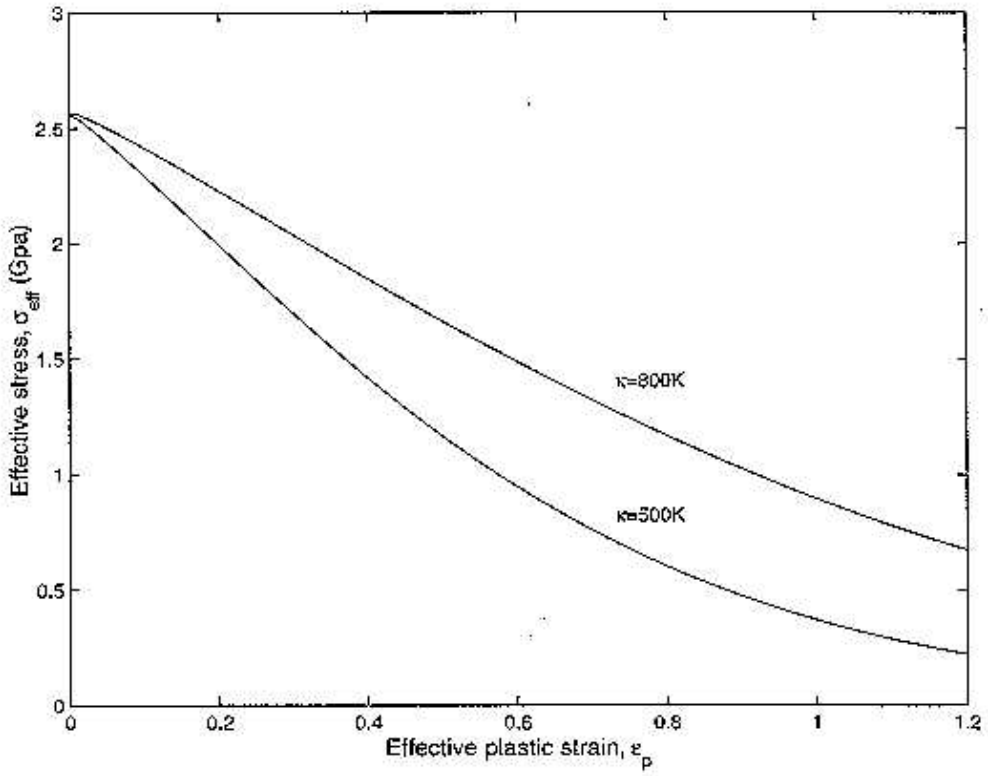

Figure 20b. Effective stress vs. effective plastic strain for simple shearing deformations of a C-300 Steel being deformed at a strain rate of 50,000/s.

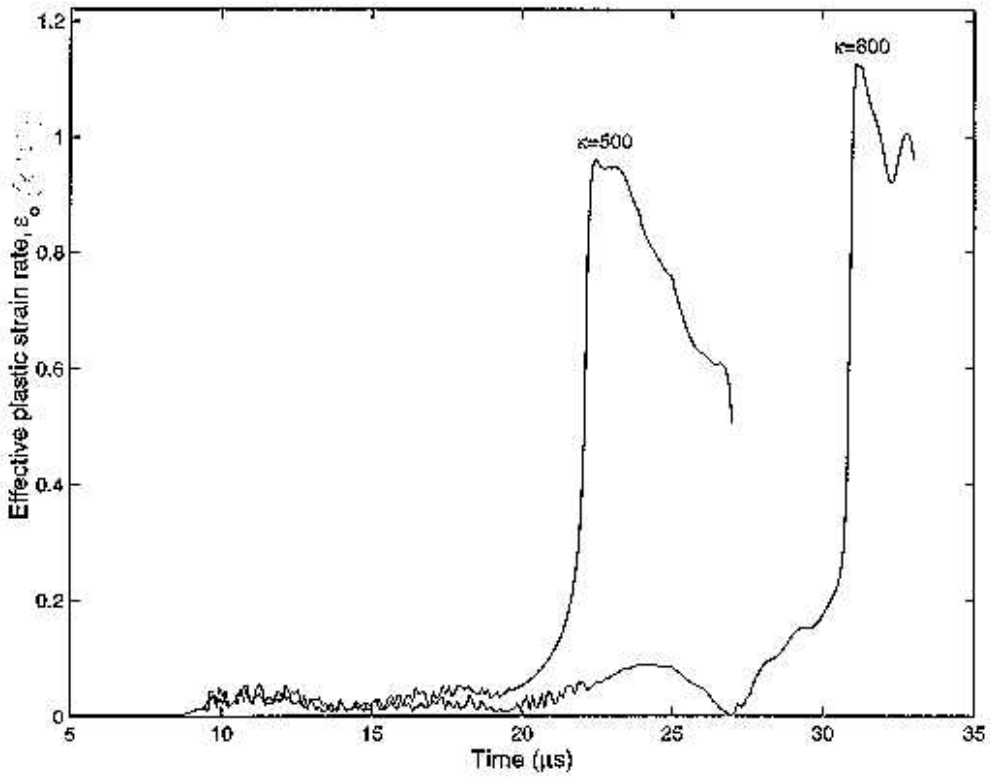

Figure 20c. Time history of the effective plastic strain-rate for simple shearing deformations of a C-300 steel at a strain -rate of 5×10^4 /s.

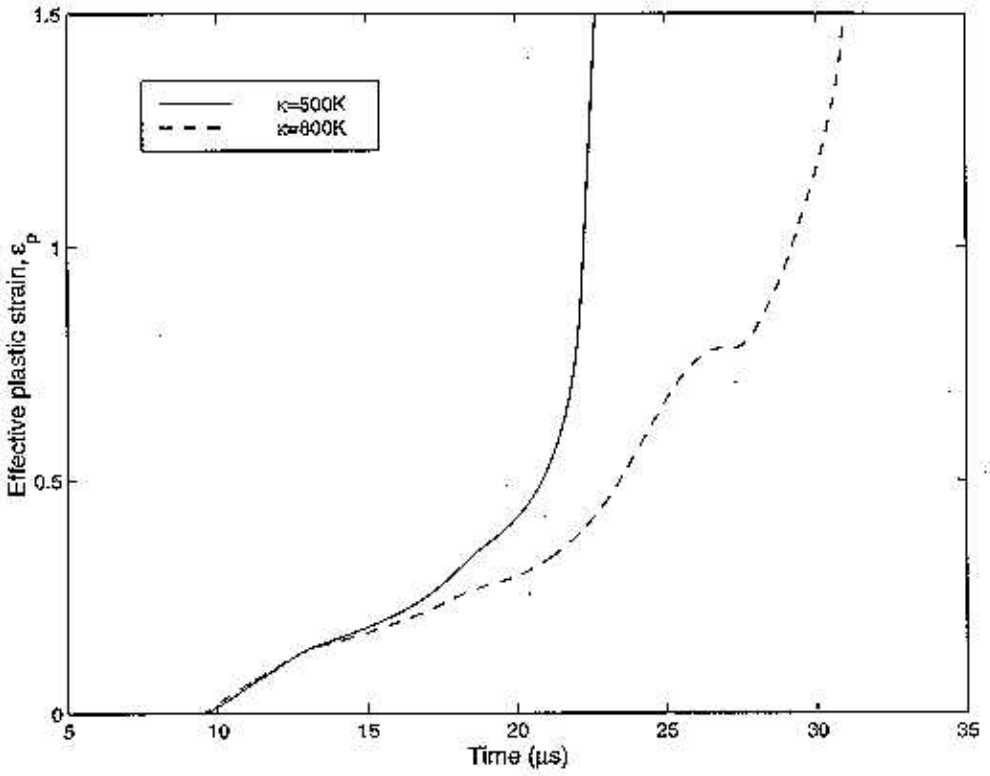

Figure 21a. Time history of the effective plastic strain for element E (see Fig. 7b for its location).

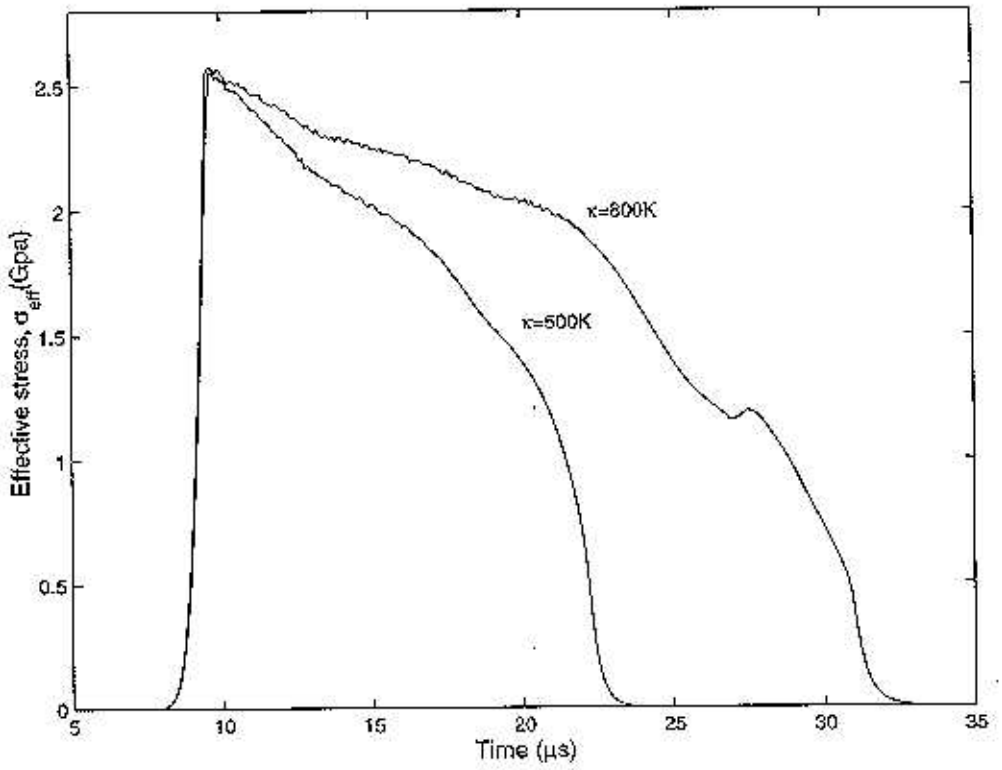

Figure 21b. Time history of the effective stress for element E (see Fig. 7b for its location).

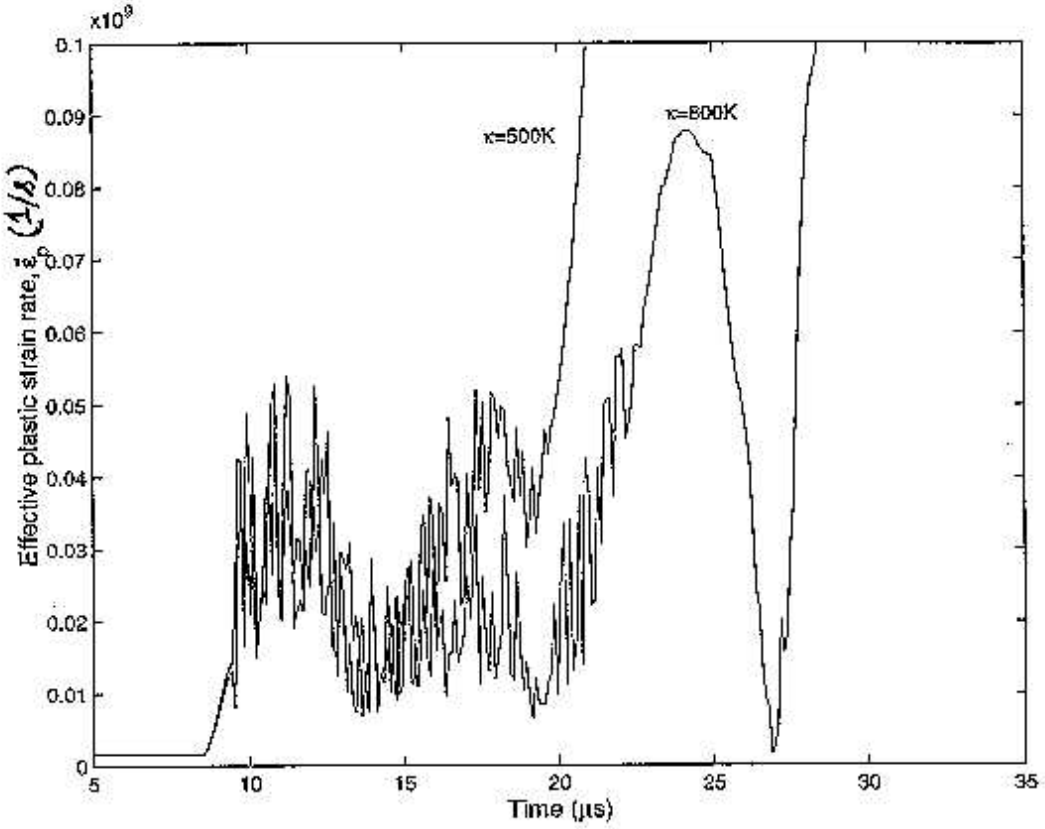

Figure 21c. Time history of the effective plastic strain-rate for element E (see Fig. 7b for its location).

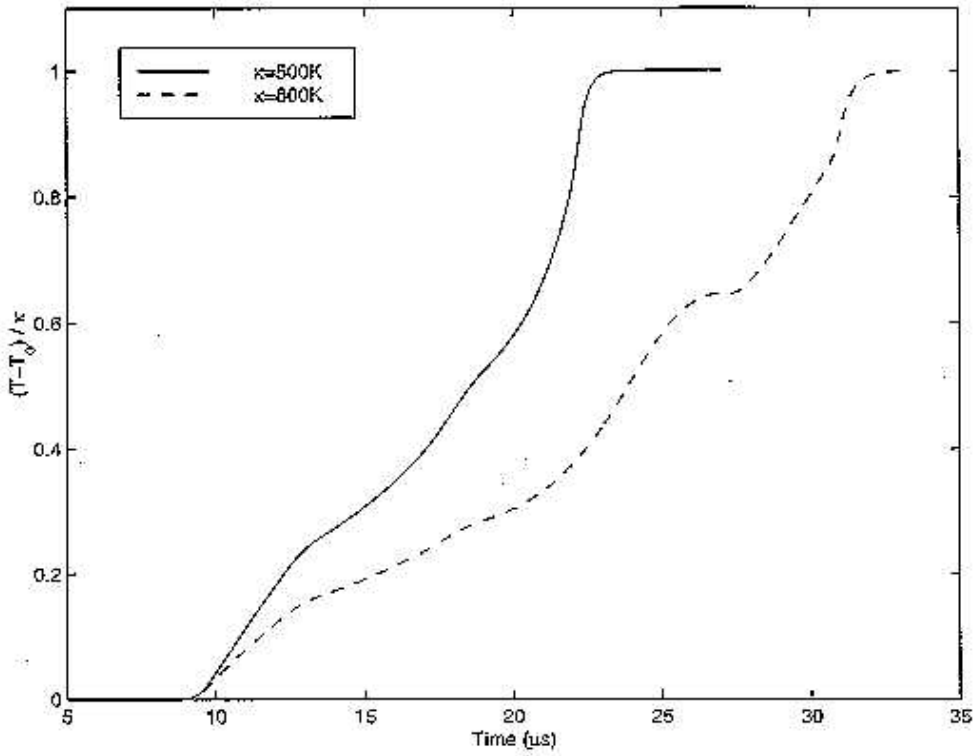

Figure 21d. Time history of non-dimensional temperature for element E (see Fig. 7b for its location).

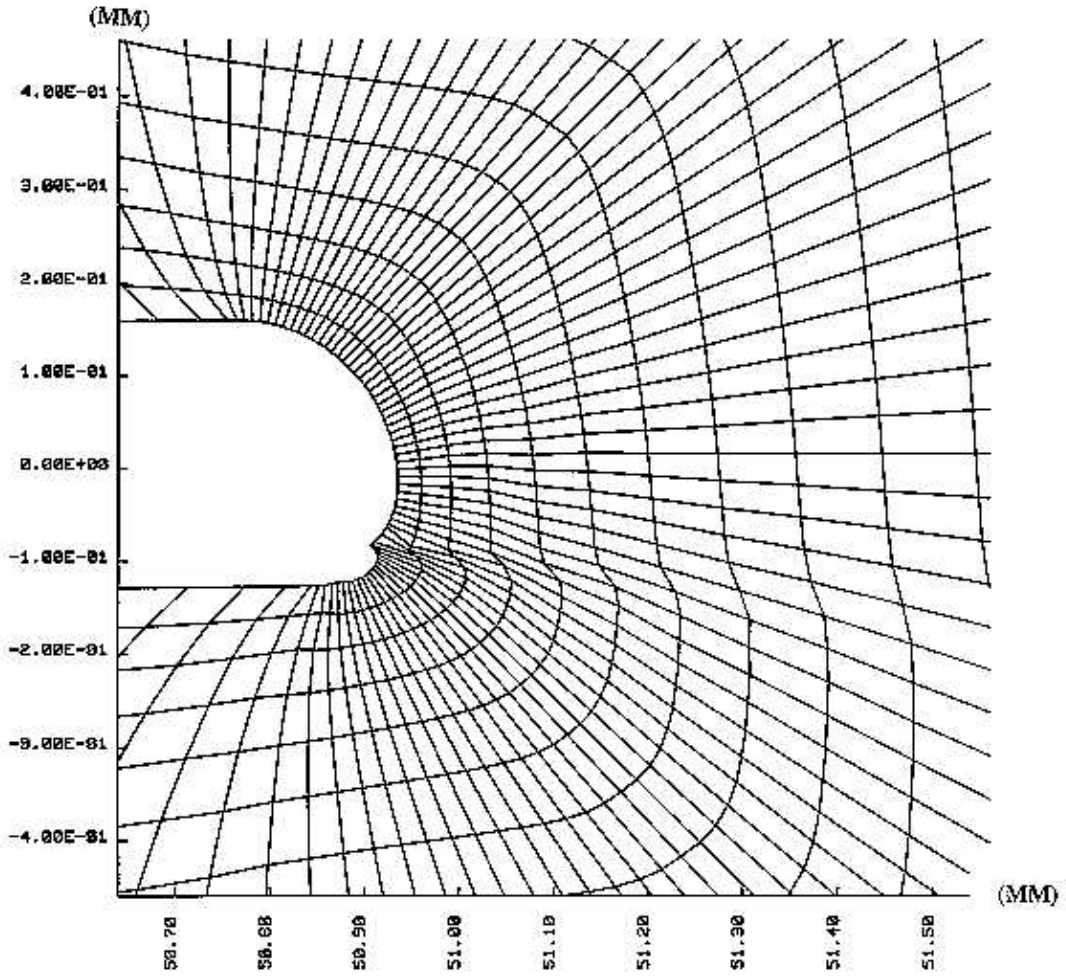

Figure 22a. The deformed mesh near the notch-tip for κ = 500 K at t=22.2 μs .

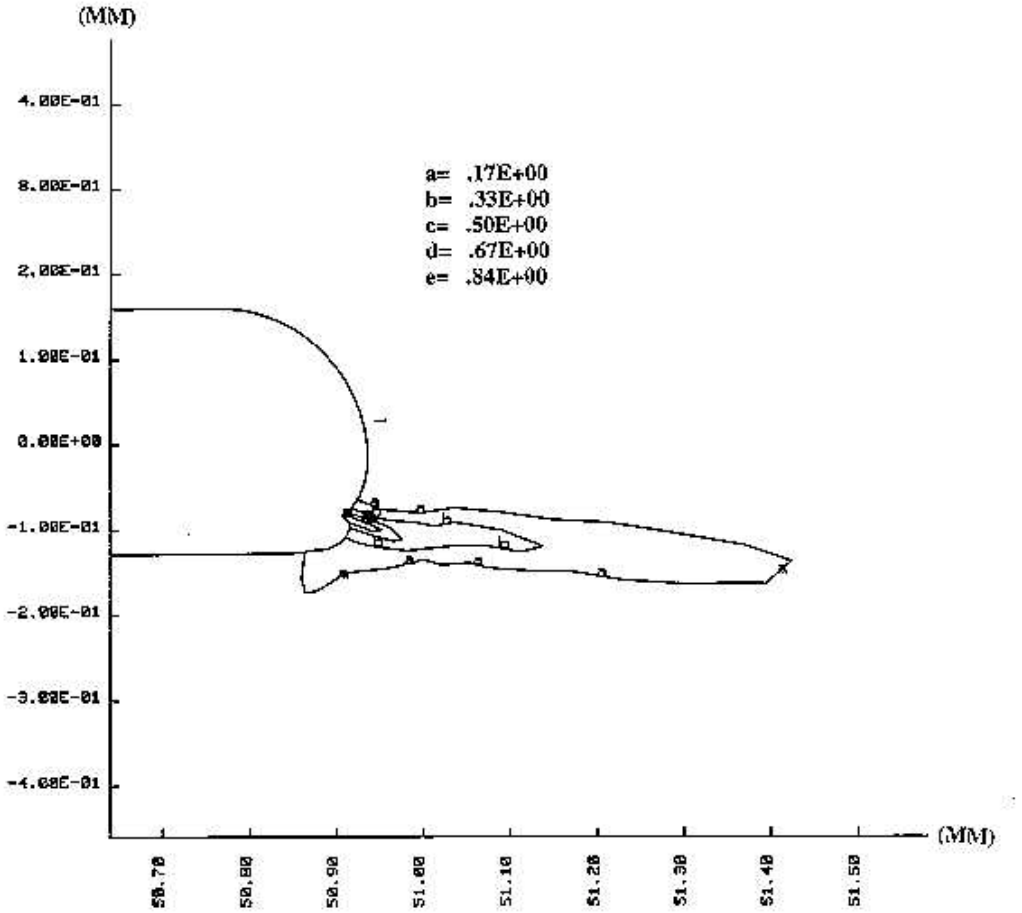

Figure 22b. Contours of the effective plastic strain near the notch-tip for κ = 500 K at t=22.2 μs .

Vita

Rakesh Gummalla was born in Hyderabad, India which is a city in the southern part of India. In June of 1991, he began his undergraduate work at Osmania University. In spring of 1996, he began pursuing his Master's Degree in the Department of Engineering Mechanics at Virginia Tech. After finishing the graduate degree, he accepted an offer as a development engineer with the Goodyear Tire & Rubber Co., where he is involved in doing predictive analysis of Tires using Finite Element Method.